Future visions:

Synergies between quantum field theories and numerical calculations with microscopic Hamiltonians

Talk online: sachdev.physics.harvard.edu

Future visions:

Synergies between quantum field theories and numerical calculations with microscopic Hamiltonians

Talk online: sachdev.physics.harvard.edu

Synergies between quantum field theories and numerical calculations with microscopic Hamiltonians

Talk online: sachdev.physics.harvard.edu

Yejin Huh

Matthias Punk

Max Metlitski

Erez Berg

PHYSICS

VE RI TAS

HARVARD

1. Dimerized antiferromagnets and the Wilson-Fisher CFT

2. J-Q model and deconfined criticality

3. Kagome lattice and Z_2 spin liquids

4. Spin liquids on the honeycomb lattice

5. Quantum critical points in metals: Fermi surface reconstruction

1. Dimerized antiferromagnets and the Wilson-Fisher CFT

2. J-Q model and deconfined criticality

3. Kagome lattice and Z_2 spin liquids

4. Spin liquids on the honeycomb lattice

5. Quantum critical points in metals: Fermi surface reconstruction

Two-dimensional Spin Dimer Models

Exploring quantum criticality in idealized 2D setups

SU(2) invariant exchange

$$\mathcal{H} = \sum_{\langle jj' \rangle} J_{jj'} \vec{S}_j \cdot \vec{S}_{j'}$$

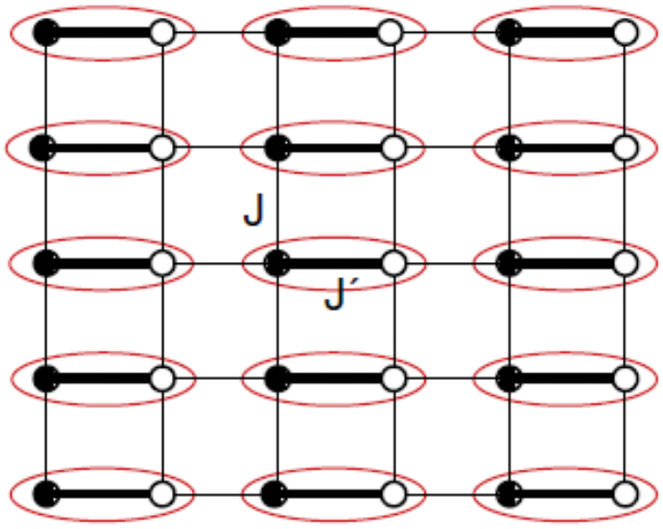

columnar

$(J'/J)_c$=1.90948(4)

(A.W. Sandvik AIP CP 2010)

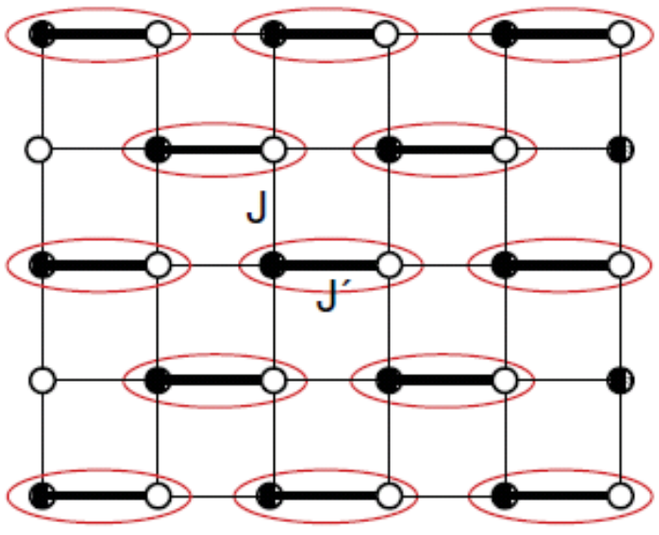

staggered

$(J'/J)_c$=2.5196(2)

(S. Wenzel et al. PRL 2008)

Various non-frustrated dimer arrangements have been considered

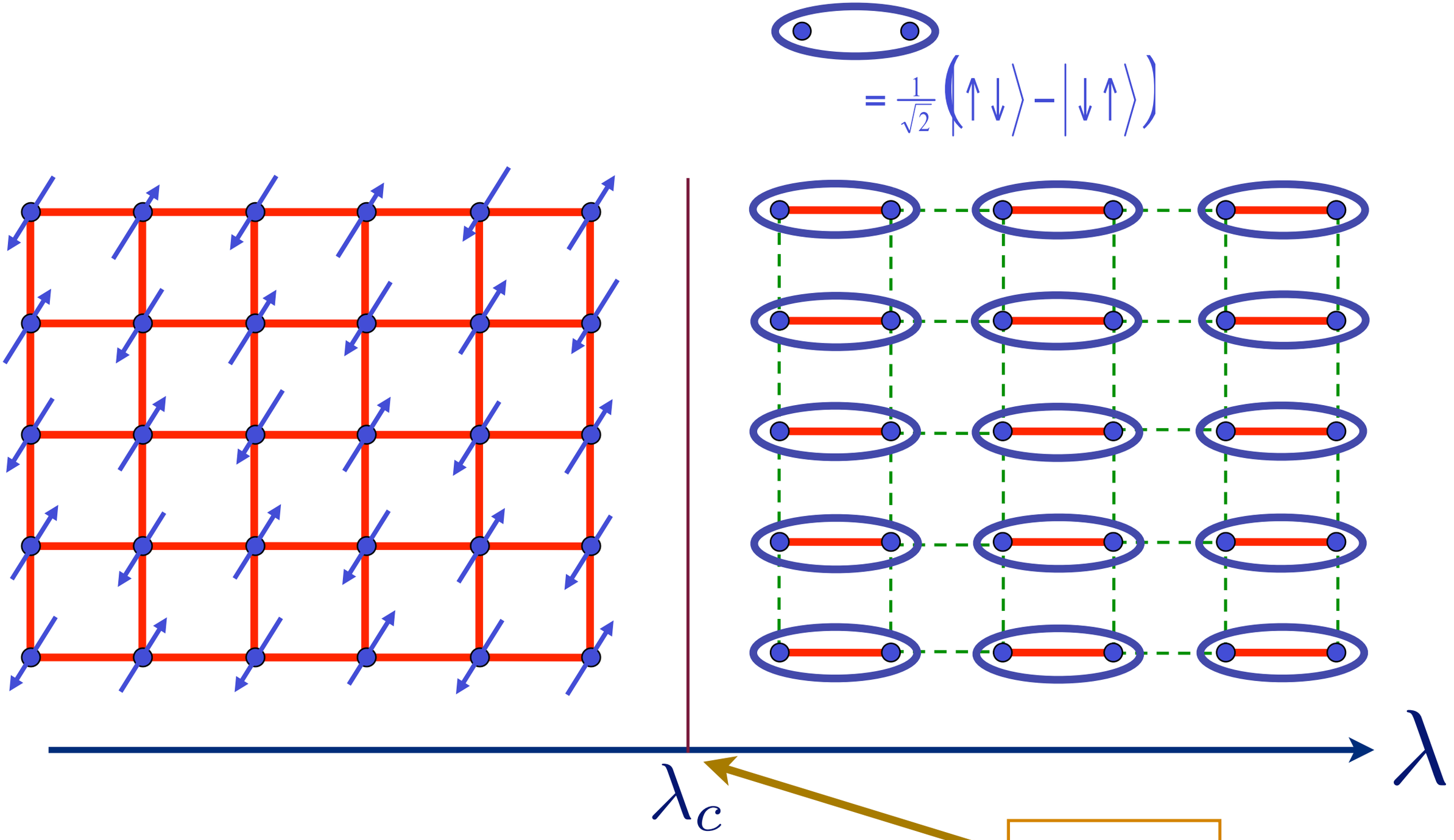

O(3) order parameter $\vec{\varphi}$

$$\mathcal{S} = \int d^2 r d\tau \left[(\partial_\tau \varphi)^2 + c^2 (\nabla_r \vec{\varphi})^2 + s\vec{\varphi}^2 + u\left(\vec{\varphi}^2\right)^2 \right]$$

Quantum Monte Carlo - critical exponents

Table IV: Fit results for the critical exponents ν, β/ν, and η. We summarize results including a variation of the critical point within its error bar. For the ladder model (top group of values) fit results and quality of fits are also given at the previous best estimate of α_c. The bottom group are results for the plaquette model. Numbers in [. . .] brackets denote the χ^2/d.o.f. For comparison relevant reference values for the 3D $O(3)$ universality class are given in the last line.

α_c	ν^a	β/ν^b	η^c
$1.9096 - \sigma$	0.712(4) [1.8]	0.516(2) [0.5]	0.026(2) [0.2]
1.9096	0.711(4) [1.8]	0.518(2) [1.1]	0.029(5) [0.8]
$1.9096 + \sigma$	0.710(4) [1.8]	0.519(3) [2.5]	0.032(7) [1.4]
1.9107^d	0.709(3) [1.7]	0.525(8) [15.3]	0.051(10) [12]
$1.8230 - \sigma$	0.708(4) [0.99]	0.515(2) [0.84]	0.025(4) [0.15]
1.8230	0.706(4) [1.04]	0.516(2) [0.40]	0.028(3) [0.31]
$1.8230 + \sigma$	0.706(4) [1.10]	0.517(2) [1.6]	0.031(5) [0.80]
Ref. 49	0.7112(5)	0.518(1)	0.0375(5)

[a] $L > 12$.
[b] $L > 16$.
[c] $L > 20$.
[d] Previous best estimate of Ref. 19.

S. Wenzel and W. Janke, arXiv:0808.1418

M. Troyer, M. Imada, and K. Ueda, *J. Phys. Soc. Japan* (1997)

Quantum Monte Carlo - critical exponents

Table IV: Fit results for the critical exponents ν, β/ν, and η. We summarize results including a variation of the critical point within its error bar. For the ladder model (top group of values) fit results and quality of fits are also given at the previous best estimate of α_c. The bottom group are results for the plaquette model. Numbers in [. . .] brackets denote the χ^2/d.o.f. For comparison relevant reference values for the 3D $O(3)$ universality class are given in the last line.

α_c	ν^a	β/ν^b	η^c
$1.9096 - \sigma$	0.712(4) [1.8]	0.516(2) [0.5]	0.026(2) [0.2]
1.9096	0.711(4) [1.8]	0.518(2) [1.1]	0.029(5) [0.8]
$1.9096 + \sigma$	0.710(4) [1.8]	0.519(3) [2.5]	0.032(7) [1.4]
1.9107^d	0.709(3) [1.7]	0.525(8) [15.3]	0.051(10) [12]
$1.8230 - \sigma$	0.708(4) [0.99]	0.515(2) [0.84]	0.025(4) [0.15]
1.8230	0.706(4) [1.04]	0.516(2) [0.40]	0.028(3) [0.31]
$1.8230 + \sigma$	0.706(4) [1.10]	0.517(2) [1.6]	0.031(5) [0.80]
Ref. 49	0.7112(5)	0.518(1)	0.0375(5)

[a] $L > 12$.
[b] $L > 16$.
[c] $L > 20$.
[d] Previous best estimate of Ref. 19.

Field-theoretic RG of CFT3 E. Vicari *et al.*

S. Wenzel and W. Janke, arXiv:0808.1418

M. Troyer, M. Imada, and K. Ueda, *J. Phys. Soc. Japan* (1997)

Staggered dimer model

Critical Field Theory

RWTH AACHEN UNIVERSITY

For the staggered dimer model the conventional φ^4 theory

$$\mathcal{S}_{24} = \frac{1}{2}\int d^2r\,d\tau\left[c_x^2(\partial_x\vec{\varphi})^2 + c_y^2(\partial_y\vec{\varphi})^2 + (\partial_\tau\vec{\varphi})^2 + m_0\vec{\varphi}^2\right]$$
$$+ \frac{u_0}{24}\int d^2r\,d\tau(\vec{\varphi}^2)^2$$

gets supplemented by the most relevant cubic term

$$\mathcal{S}_3 = i\gamma_0\int d^2r\,d\tau\;\vec{\varphi}\cdot(\partial_x\vec{\varphi}\times\partial_\tau\vec{\varphi})$$

What is the relevance of this cubic term?

Staggered dimer model

Classical Monte Carlo Analysis

RWTH AACHEN UNIVERSITY

MC data consistent with a fast algebraic decay of the correlators

$$C_{xy}(r) = \langle \mathcal{O}(r,0,0)\mathcal{O}(0) \rangle$$

$$C_z(r) = \langle \mathcal{O}(0,0,r)\mathcal{O}(0) \rangle$$

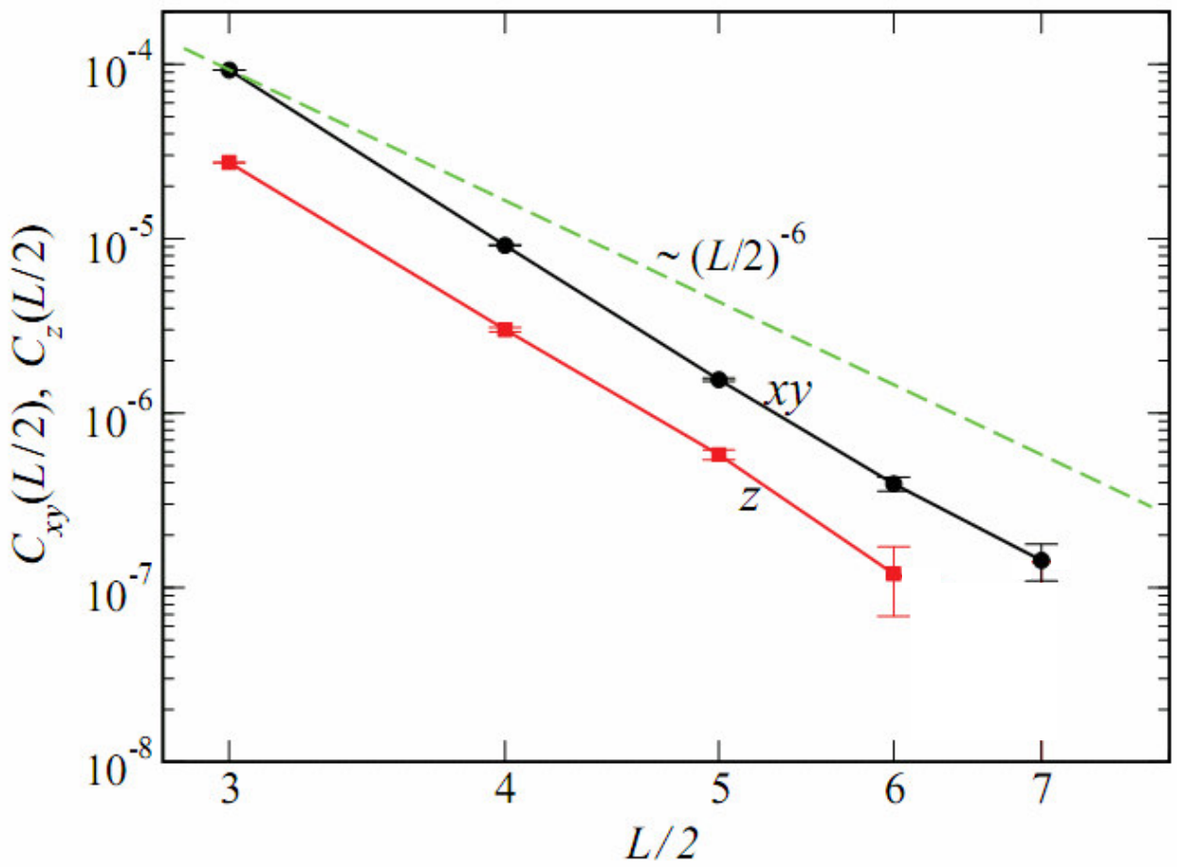

Overall fit results in

$$[\gamma_0]_{WF} = -0.4 \pm 0.2$$

Consistent with weak irrelevancy of the cubic operator at the Wilson-Fisher fixed point

1. Dimerized antiferromagnets and the Wilson-Fisher CFT

2. J-Q model and deconfined criticality

3. Kagome lattice and Z_2 spin liquids

4. Spin liquids on the honeycomb lattice

5. Quantum critical points in metals: Fermi surface reconstruction

1. Dimerized antiferromagnets and the Wilson-Fisher CFT

2. J-Q model and deconfined criticality

3. Kagome lattice and Z_2 spin liquids

4. Spin liquids on the honeycomb lattice

5. Quantum critical points in metals: Fermi surface reconstruction

Neel-VBS quantum transition

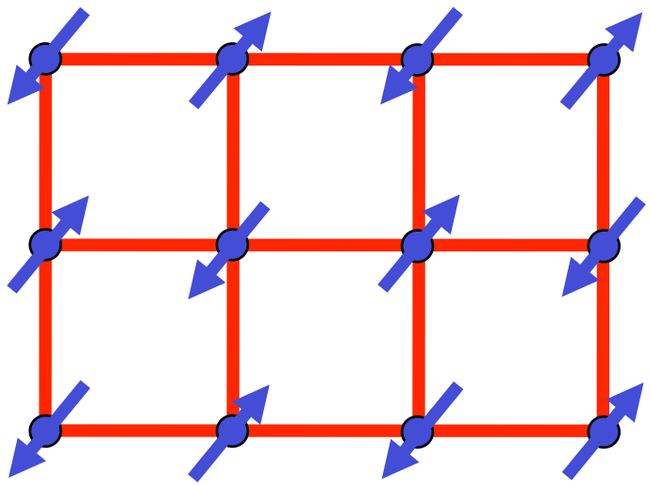

$\langle z_\alpha \rangle \neq 0$

Néel state

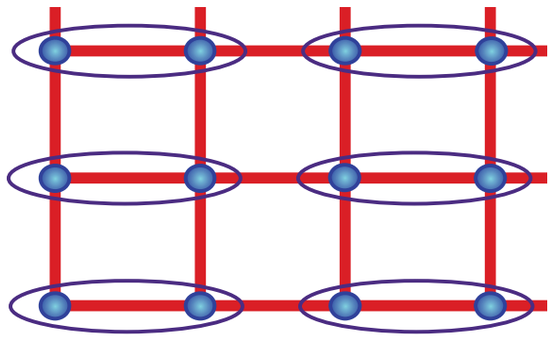

or

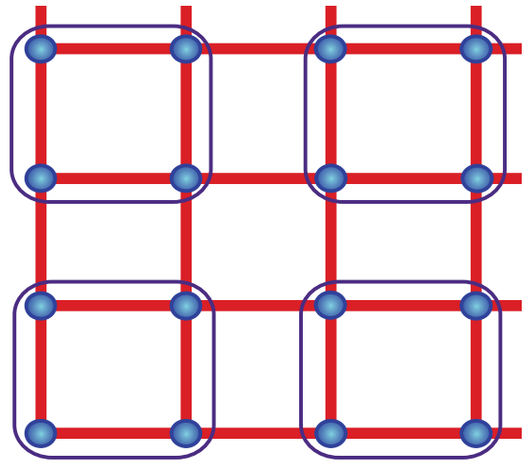

$\langle z_\alpha \rangle = 0$

VBS state with a nearly gapless photon

s_c

s

Critical theory for photons and deconfined spinons:

$$\mathcal{S}_z = \int d^2r d\tau \left[|(\partial_\mu - iA_\mu) z_\alpha|^2 + s|z_\alpha|^2 + u(|z_\alpha|^2)^2 + \frac{1}{2e_0^2}(\epsilon_{\mu\nu\lambda}\partial_\nu A_\lambda)^2 \right]$$

O.I. Motrunich and A. Vishwanath, *Phys. Rev. B* **70**, 075104 (2004).

T. Senthil, A. Vishwanath, L. Balents, S. Sachdev and M.P.A. Fisher, *Science* **303**, 1490 (2004).

SU(2) J-Q Model

A. W. Sandvik, PRL98, 227202 (2007)

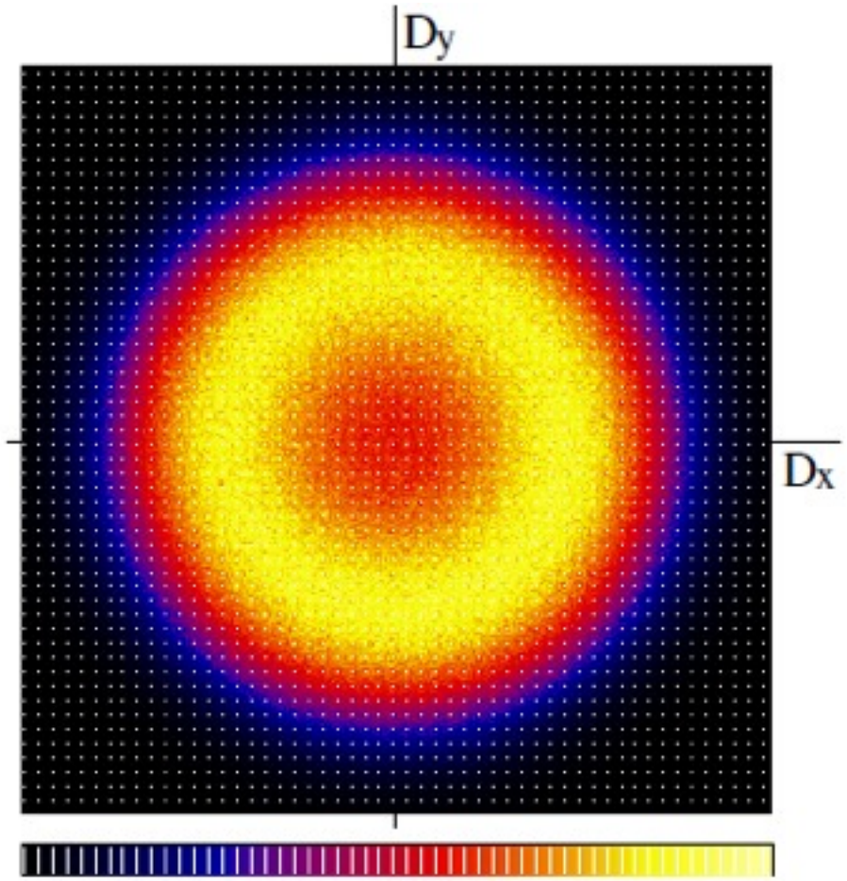

FIG. 5 (color online). Histogram of the dimer order parameter for an $L = 32$ system at $J/Q = 0$. The ring shape demonstrates an emergent $U(1)$ symmetry, i.e., irrelevance of the Z_4 anisotropy of the VBS order parameter.

U(1) Nature is confirmed at the critical point.

Monopole Scaling Dimension up to $O(N^{-1})$

$$\frac{\eta_D}{N} = \frac{2\Delta_1 - 1}{N} = 0.2492 - 0.32\frac{1}{N} + O\left(\frac{1}{N^2}\right)$$

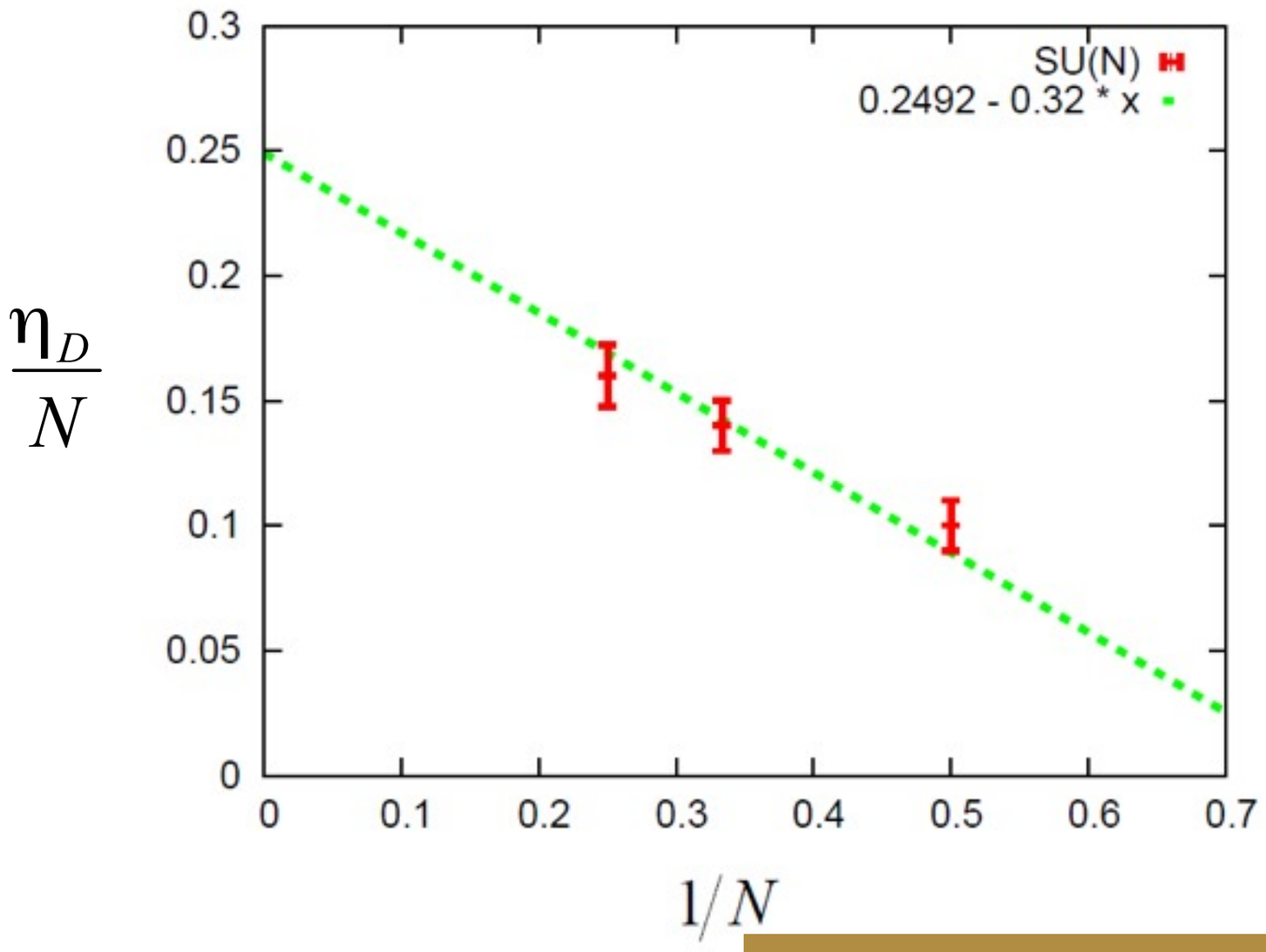

2D JQ-Model (Lou, Sandvik, N.K.)

Adding an impurity

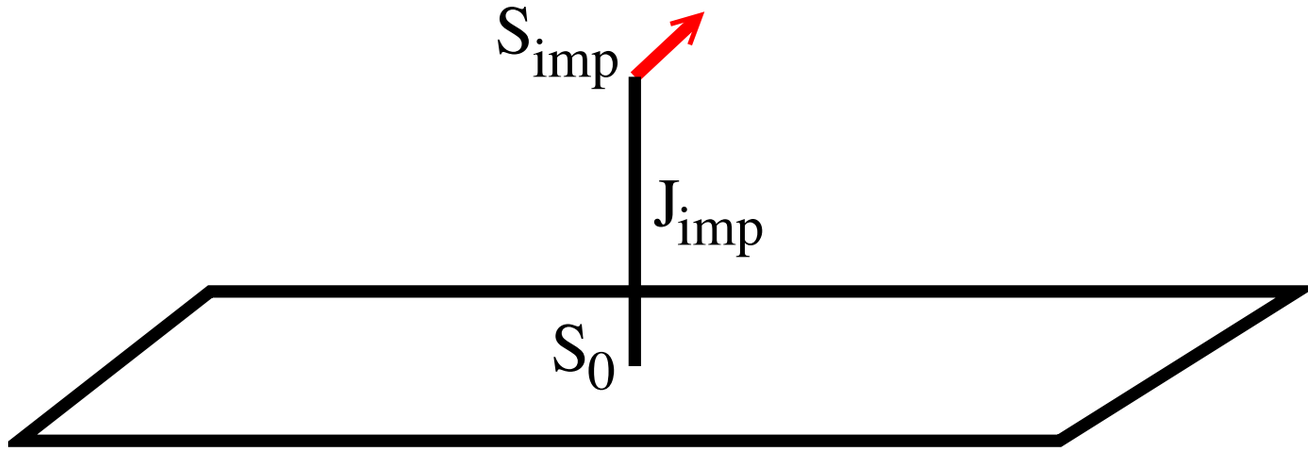

- $H_{JQ} + J_{\rm imp} \vec{S}_{\rm imp} \cdot \vec{S}_0$
- Is $J_{\rm imp}$ a 'relevant perturbation' at bulk transition?
- What effect does it have on the bulk?

$J_{\rm imp} = \infty$: Doping by non-magnetic ion to create missing-spin defect

---

- $SU(2)$ deconfined critical point seems to have some logarithmic violations of scaling
- $SU(3)$ JQ_2 model seems to obey impurity scaling at deconfined critical point. (Banerjee, KD & Alet PRB 2011)
  Not settled yet: Kaul (arXiv 2010) finds SU(3) behaves a lot like SU(2) (?)

Alet - properties of the Sutherland RVB state

See also Ying Tang, Anders Sandvik, and Chris Henley, arXiv:1010.6146

Critical dimer correlations

- Critical "dimer-dimer" four-point correlations

$$C^{ijkl} = \langle (\mathbf{S}_i \cdot \mathbf{S}_j)(\mathbf{S}_k \cdot \mathbf{S}_l) \rangle - \langle \mathbf{S}_i \cdot \mathbf{S}_j \rangle \langle \mathbf{S}_k \cdot \mathbf{S}_l \rangle$$

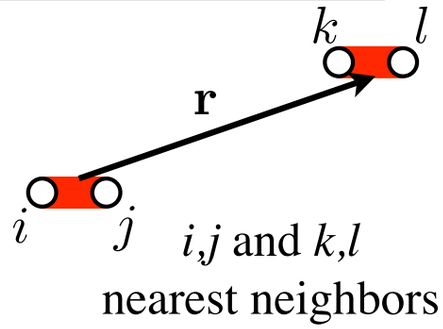

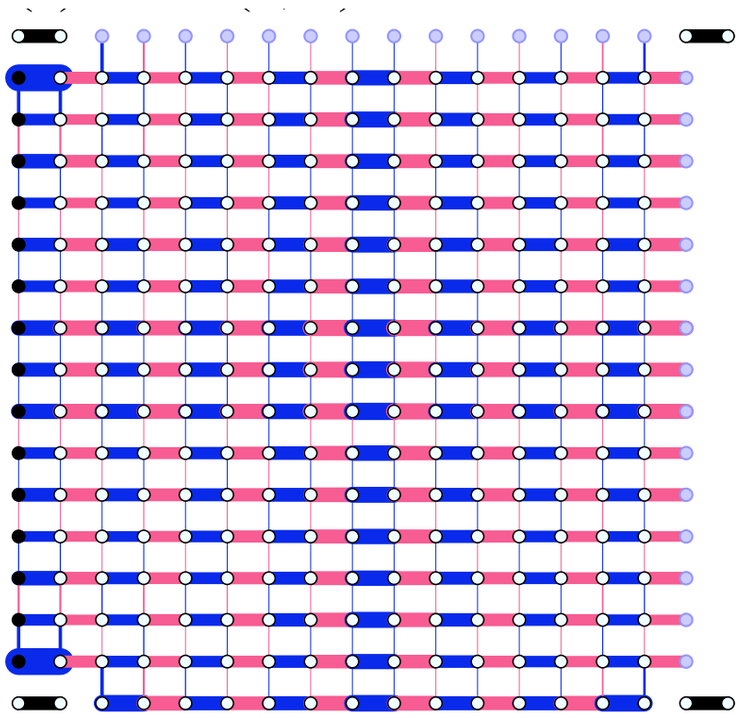

$C^{ijkl}(\mathbf{r})$ $|\mathbf{r}|$

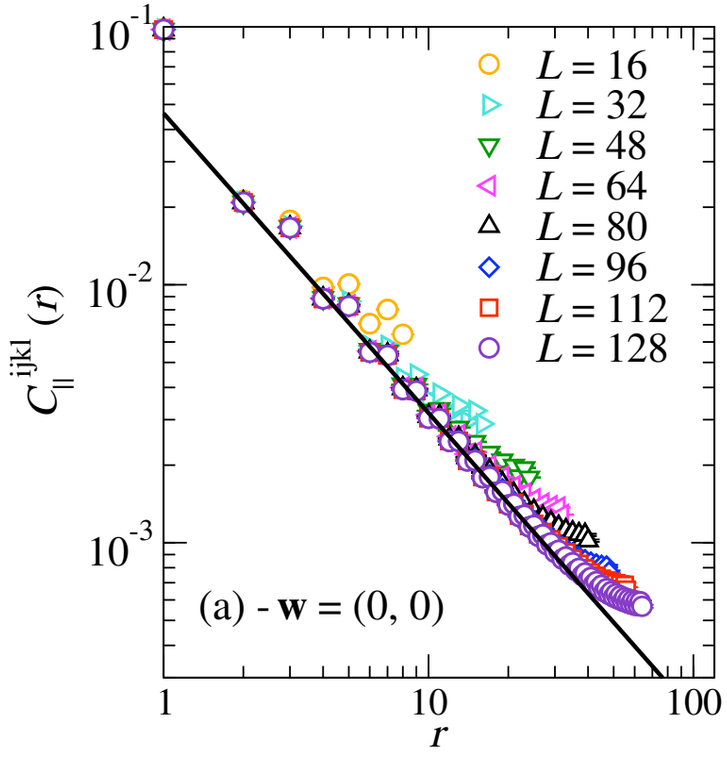

$C^{ijkl}(\mathbf{r}) \simeq 1/|\mathbf{r}|^{\alpha}$

$\alpha \simeq 1.16$

=2 for classical dimers

Gapless "photon" phase with all monopole operators tuned to zero?

1. Dimerized antiferromagnets and the Wilson-Fisher CFT

2. J-Q model and deconfined criticality

3. Kagome lattice and Z_2 spin liquids

4. Spin liquids on the honeycomb lattice

5. Quantum critical points in metals: Fermi surface reconstruction

1. Dimerized antiferromagnets and the Wilson-Fisher CFT

2. J-Q model and deconfined criticality

3. Kagome lattice and Z_2 spin liquids

4. Spin liquids on the honeycomb lattice

5. Quantum critical points in metals: Fermi surface reconstruction

Some more recent history

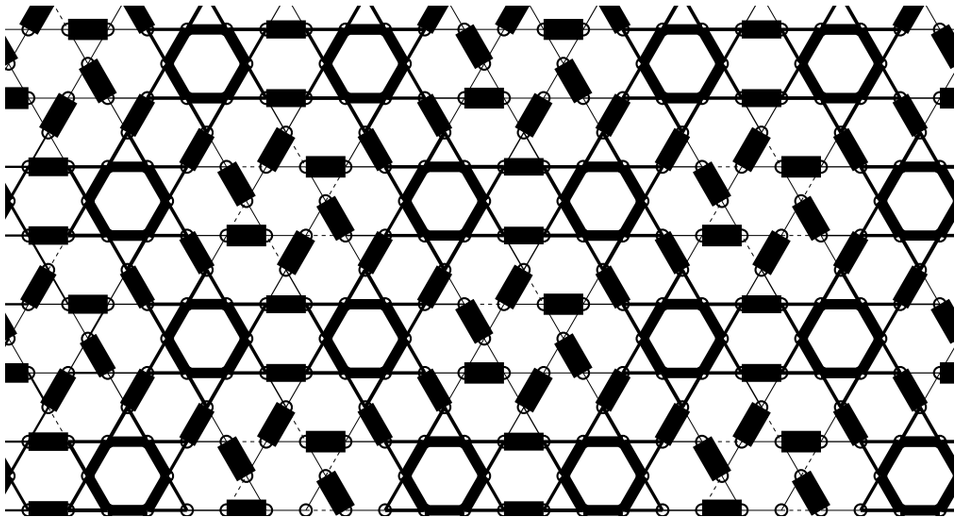

36 site unit cell valence bond crystal: honeycomb valence bond crystal (HVBC) (Marston and Zeng, originally)

- Key question: is it a valence bond crystal or a spin liquid? What kind of VBC or SL?
- Three key approaches support HVBC:
  - Series expansions, Singh and Huse (E=-0.433(1))
  - MERA, Evenbly and Vidal (E < -0.4322 exact bound!)
    - Multiscale entanglement renormalization ansatz, a tensor product relative of DMRG capable of infinite 2D
  - High order ffective Dimer Model, Poilblanc et al (but SL close by)

S. White, seminar at Harvard, March 2011

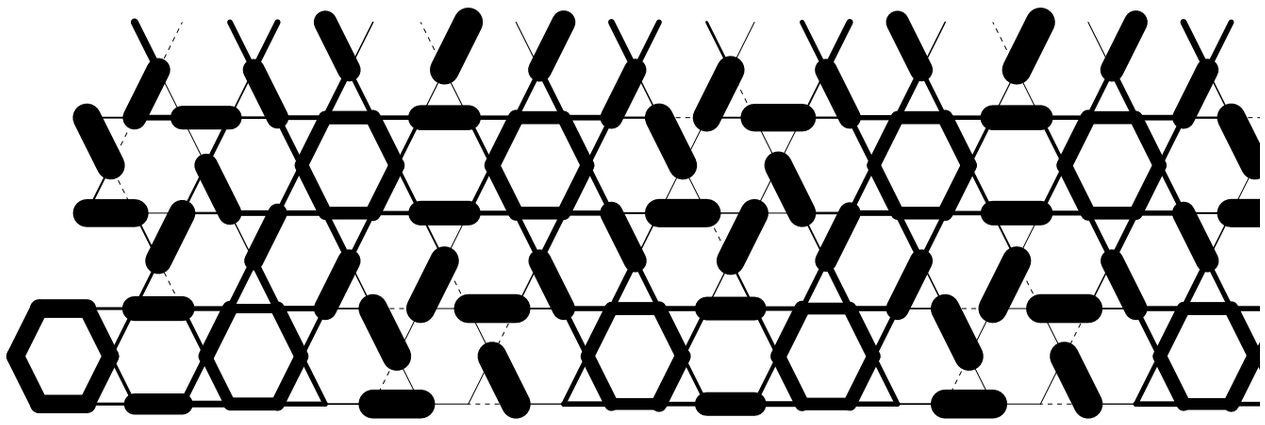

m=200
sweep 6

This run had special path and edges tuned to favor HVBC.

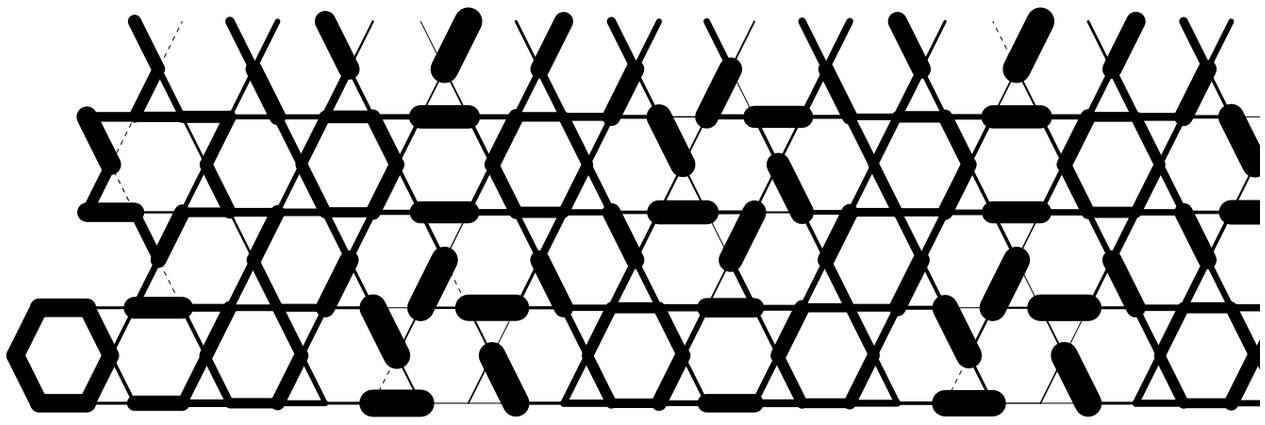

m=600
sweep 14

HVBC is metastable for small m, but for m ~ 2400 it transitions to the spin liquid

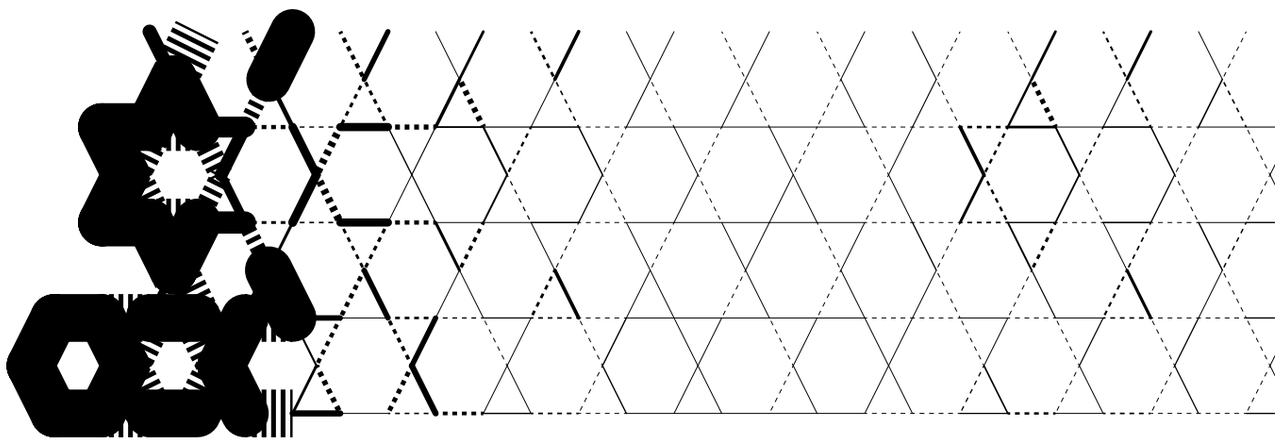

m=8000
sweep 34

With standard path HVBC is immediately unstable, m ~ 100

SL energy for this cylinder, bulk:
-0.43824(2) XC8

S. White, seminar at Harvard, March 2011

Singlet and Triplet Gaps

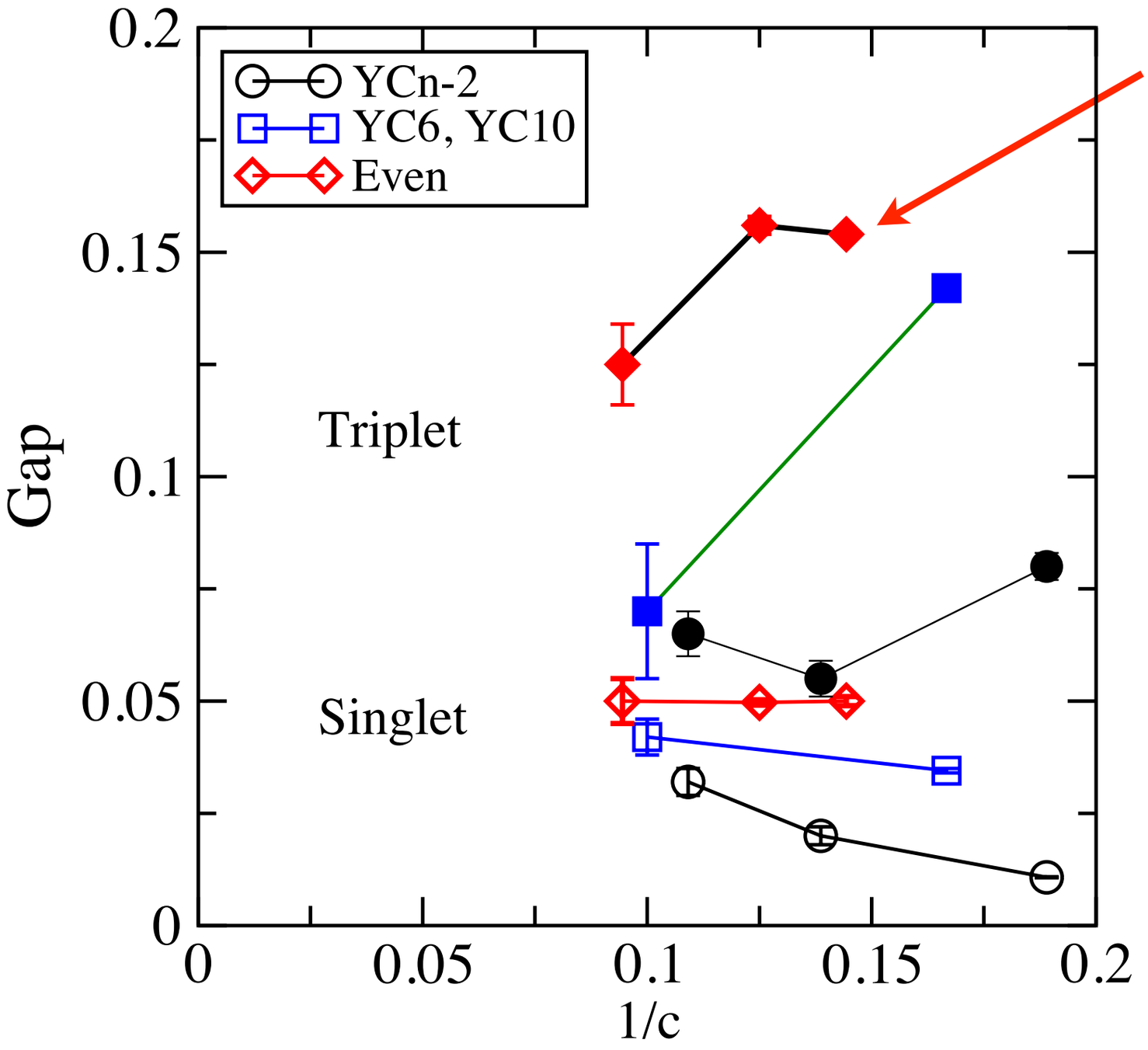

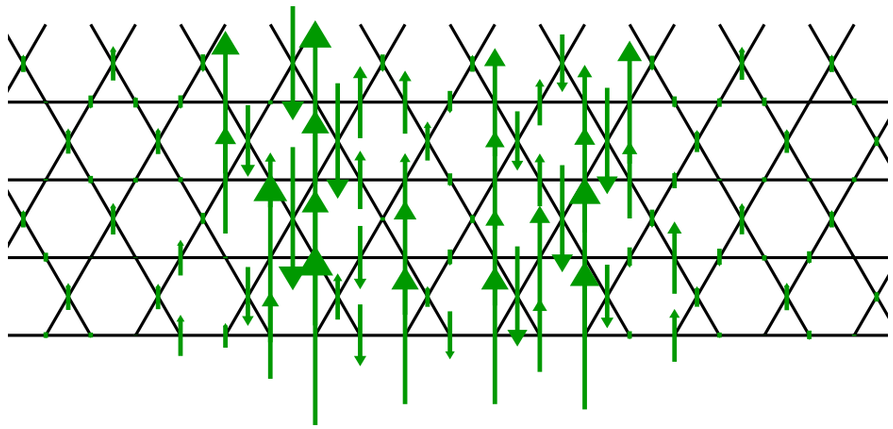

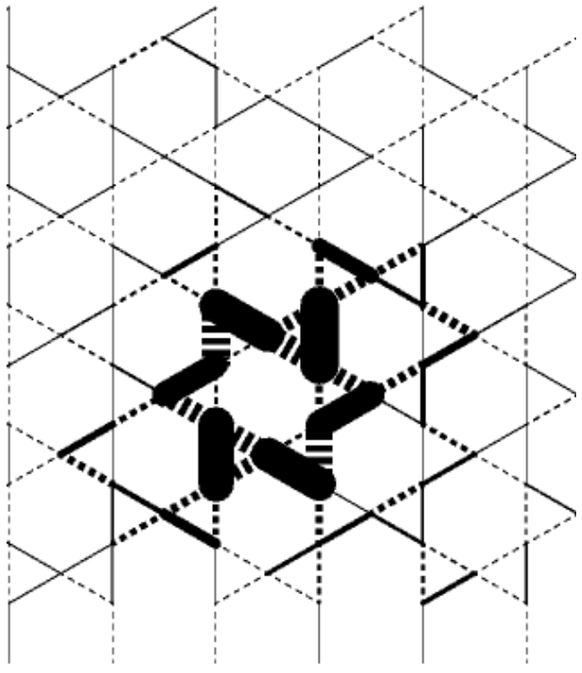

Singlet excitation
before delocalization

S. White, seminar at Harvard, March 2011

Parton construction of Z_2 spin liquids

$$\vec{S}_i = \frac{1}{2} b^\dagger_{i\alpha} \vec{\sigma}_{\alpha\beta} b_{i\beta},$$

$$\mathcal{H}_b = -\sum_{i<j} Q_{ij} \varepsilon_{\alpha\beta} b^\dagger_{i\alpha} b^\dagger_{j\beta} + \text{H.c.} + \lambda \sum_i b^\dagger_{i\alpha} b_{i\alpha},$$

$$E[\{Q_{ij}\}] = -\sum_{i<j} \left(\alpha |Q_{ij}|^2 + \frac{\beta}{2} |Q_{ij}|^4 \right) + K \prod_{\text{even loops}} Q_{ij} Q^*_{jk} \ldots Q^*_{\ell i}$$

N. Read and S. Sachdev, *Phys. Rev. Lett.* **66**, 1773 (1991)
X.-G. Wen, *Phys. Rev. B* **44**, 2664 (1991)

$$E[\{Q_{ij}\}] = -\sum_{i<j}\left(\alpha|Q_{ij}|^2 + \frac{\beta}{2}|Q_{ij}|^4\right)$$

$$+ K \prod_{\text{even loops}} Q_{ij}Q^*_{jk}\ldots Q^*_{\ell i}$$

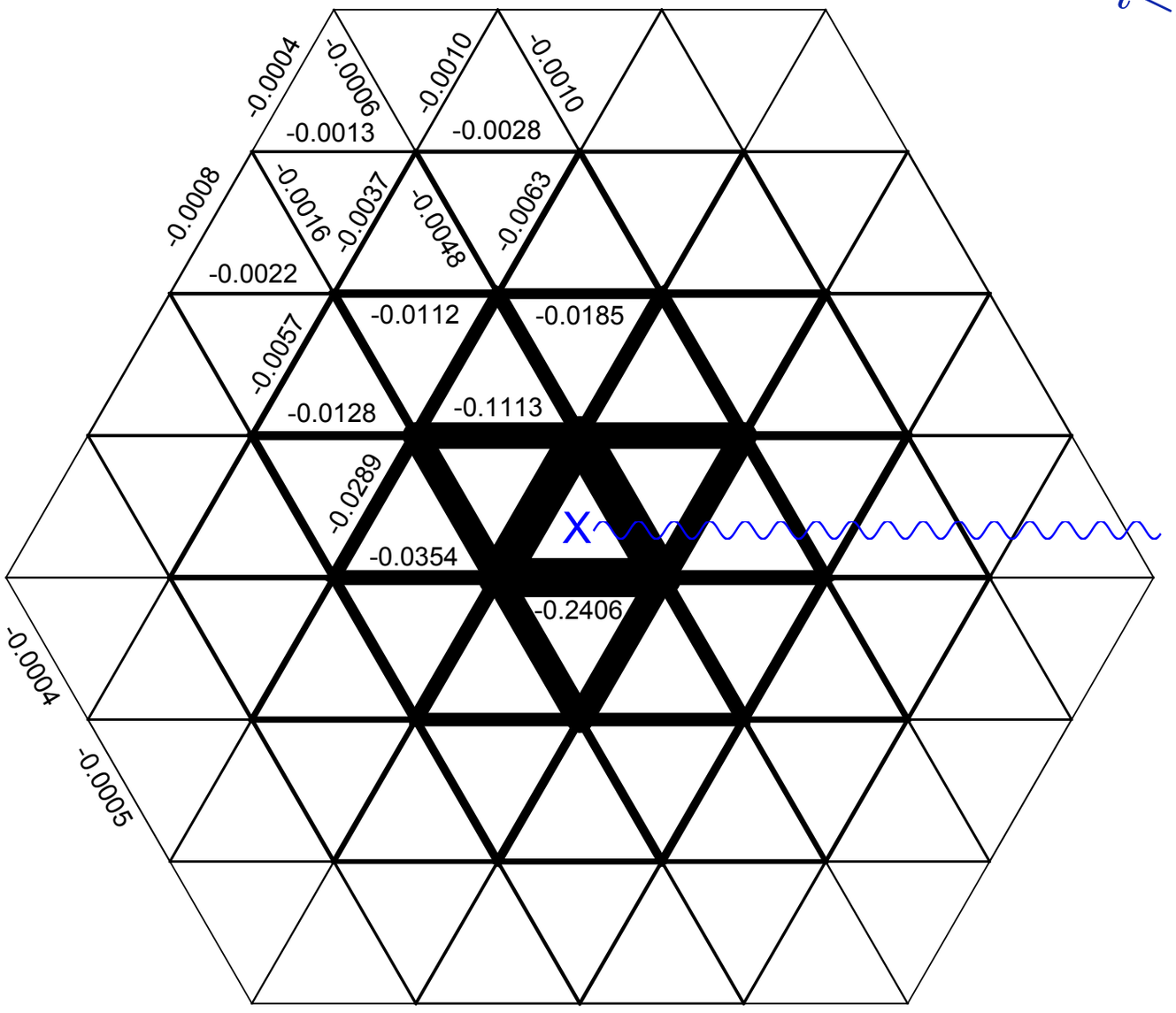

Y. Huh, M. Punk, and
S. Sachdev, arXiv:1106.3330

A vison on the triangular lattice. The center of the vison is marked by the X. The wavy line is the 'branch-cut' where we have $\mathrm{sgn}(Q^v_{ij}) = -\mathrm{sgn}(Q_{ij})$ only on the links crossed by the line. Plotted is the minimization result of $E[\{Q_{ij}\}]$

Parton construction of Z_2 spin liquids

Field theory near a magnetic ordering transition:
U(1) gauge theory with a charge 2 Higgs field:

$$\begin{aligned}\mathcal{L} &= |(\partial_\mu - 2iA_\mu)\Phi|^2 + s|\Phi|^2 + u|\Phi|^4 \\ &+ |(\partial_\mu - iA_\mu)z_\alpha|^2 + \widetilde{s}|z_\alpha|^2 + \widetilde{u}|z_\alpha|^4 \\ &+ \lambda\Phi^* \varepsilon_{\alpha\beta} z_\alpha \nabla z_\beta + \text{H.c.}\end{aligned}$$

This field theory has vortex solutions, with flux π, which are analogs of Abrikosov vortices in the BCS theory of superconductivity. However, here the gauge field is compact, and so $\pm\pi$ vortices are the same: these are Z_2 vortices or 'visons'.

N. Read and S. Sachdev, *Phys. Rev. Lett.* **66**, 1773 (1991)

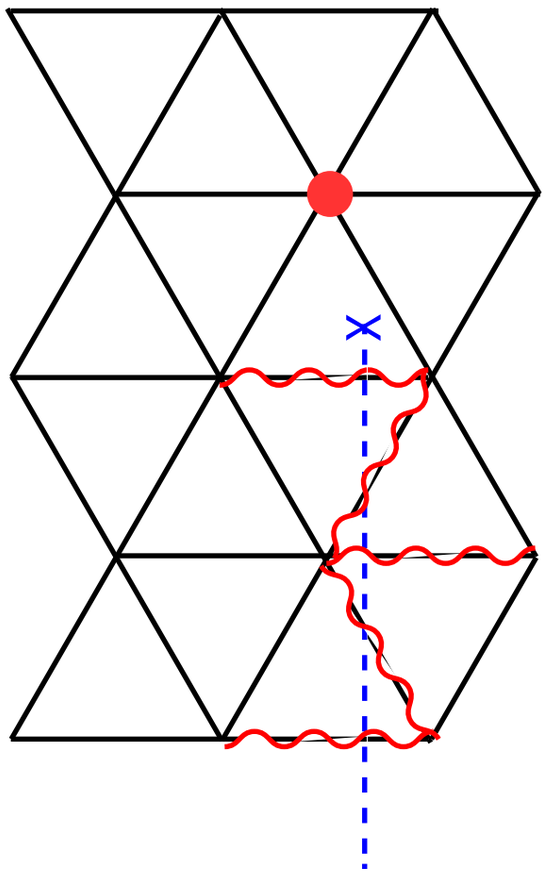

Periodic motion of a vison around the single site marked by the filled circle.

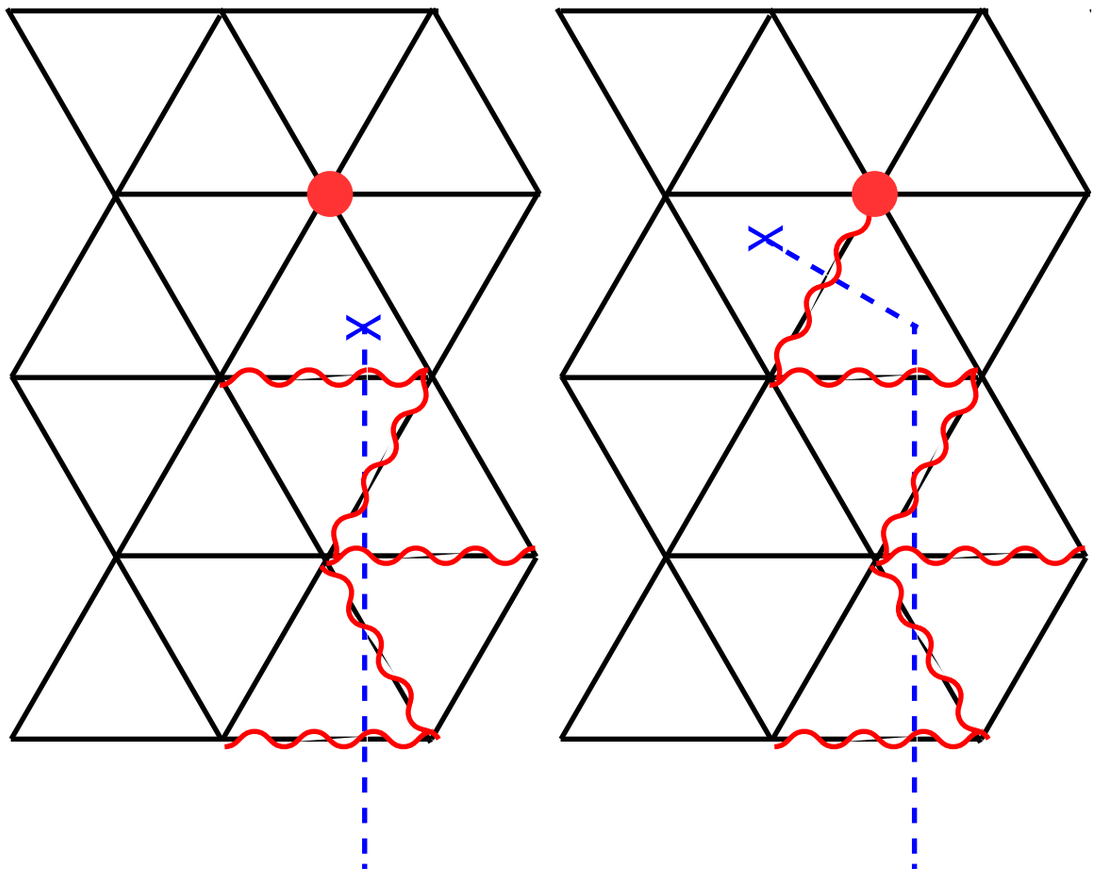

Periodic motion of a vison around the single site marked by the filled circle.

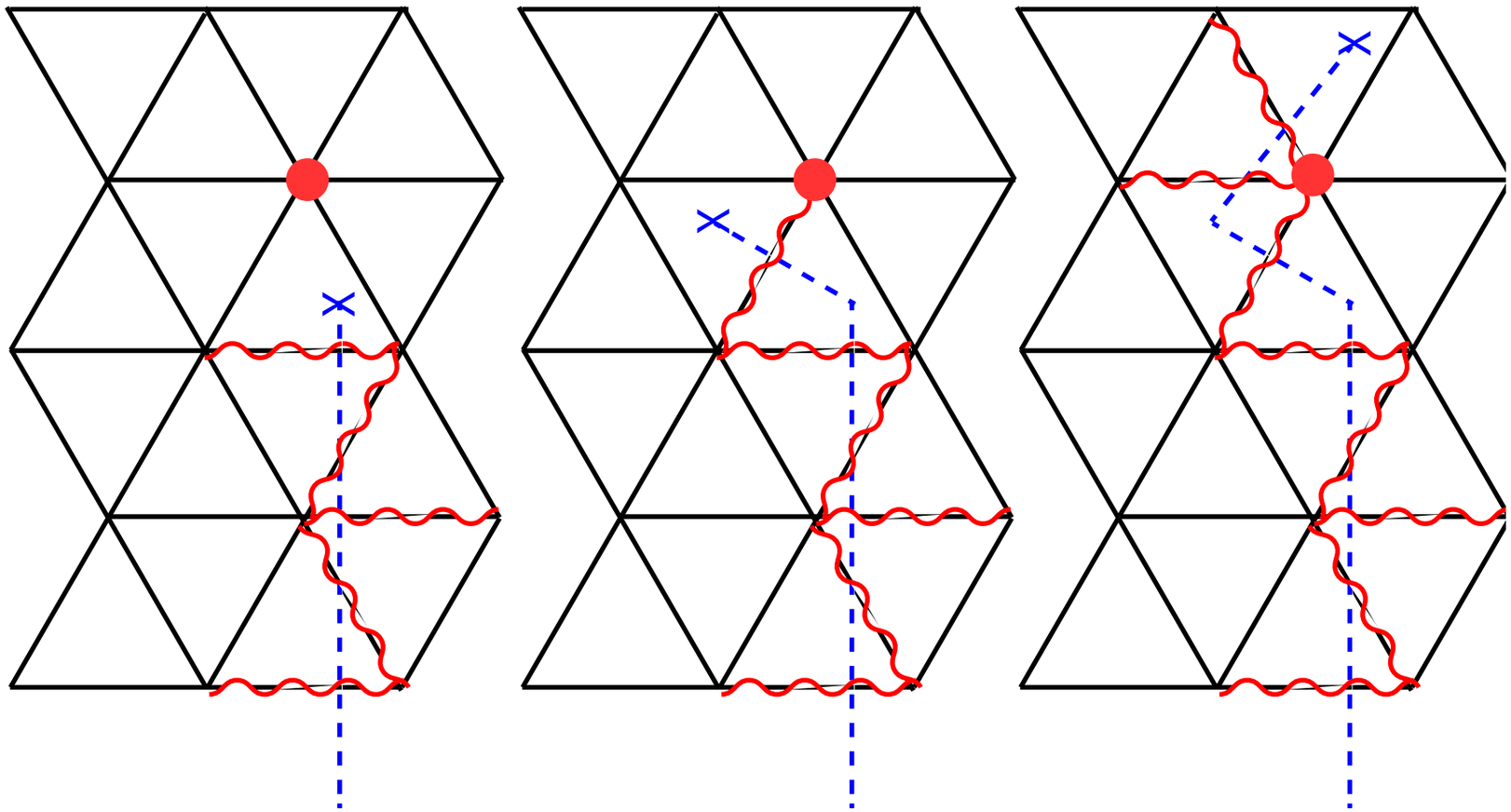

Periodic motion of a vison around the single site marked by the filled circle.

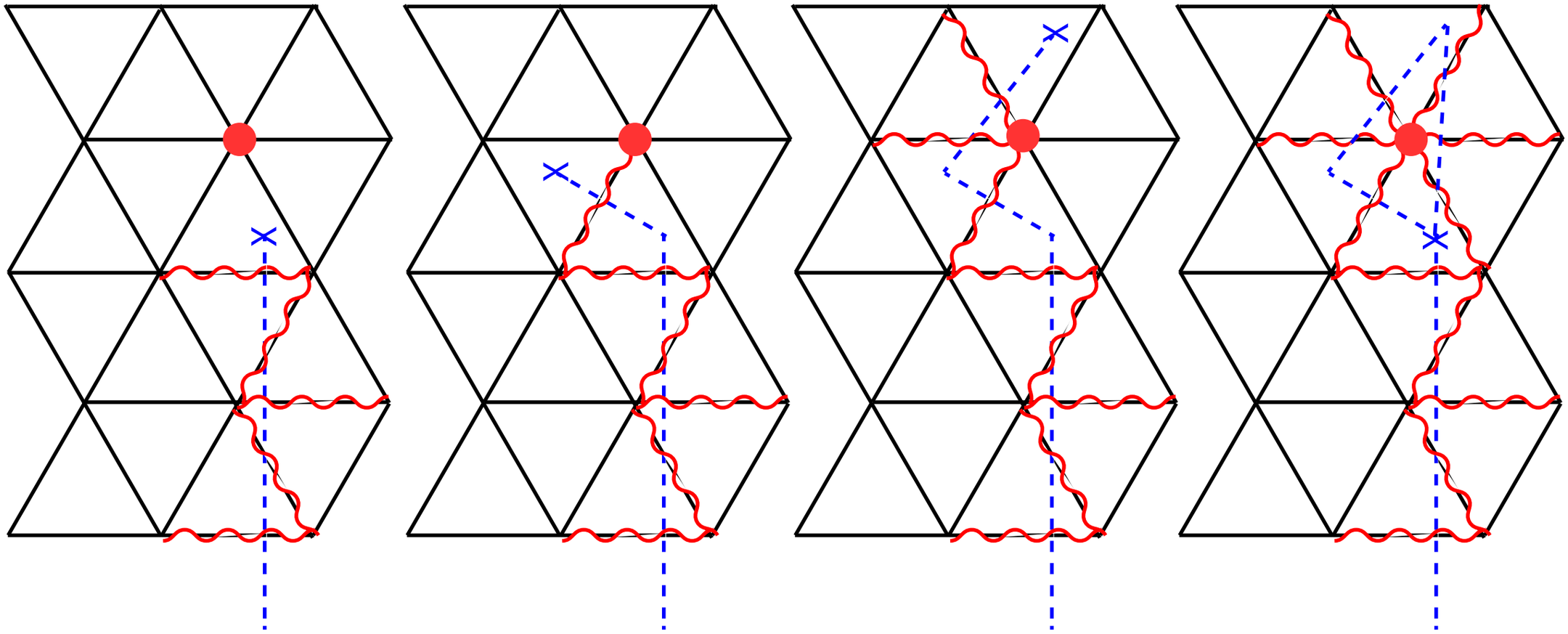

Periodic motion of a vison around the single site marked by the filled circle. The right state is gauge-equivalent to the left state, after the gauge transformation $b_{i\alpha} \to -b_{i\alpha}$ only for the site i marked by the filled circle.

$\Rightarrow$ Vison has a Berry phase of π upon encircling a site.

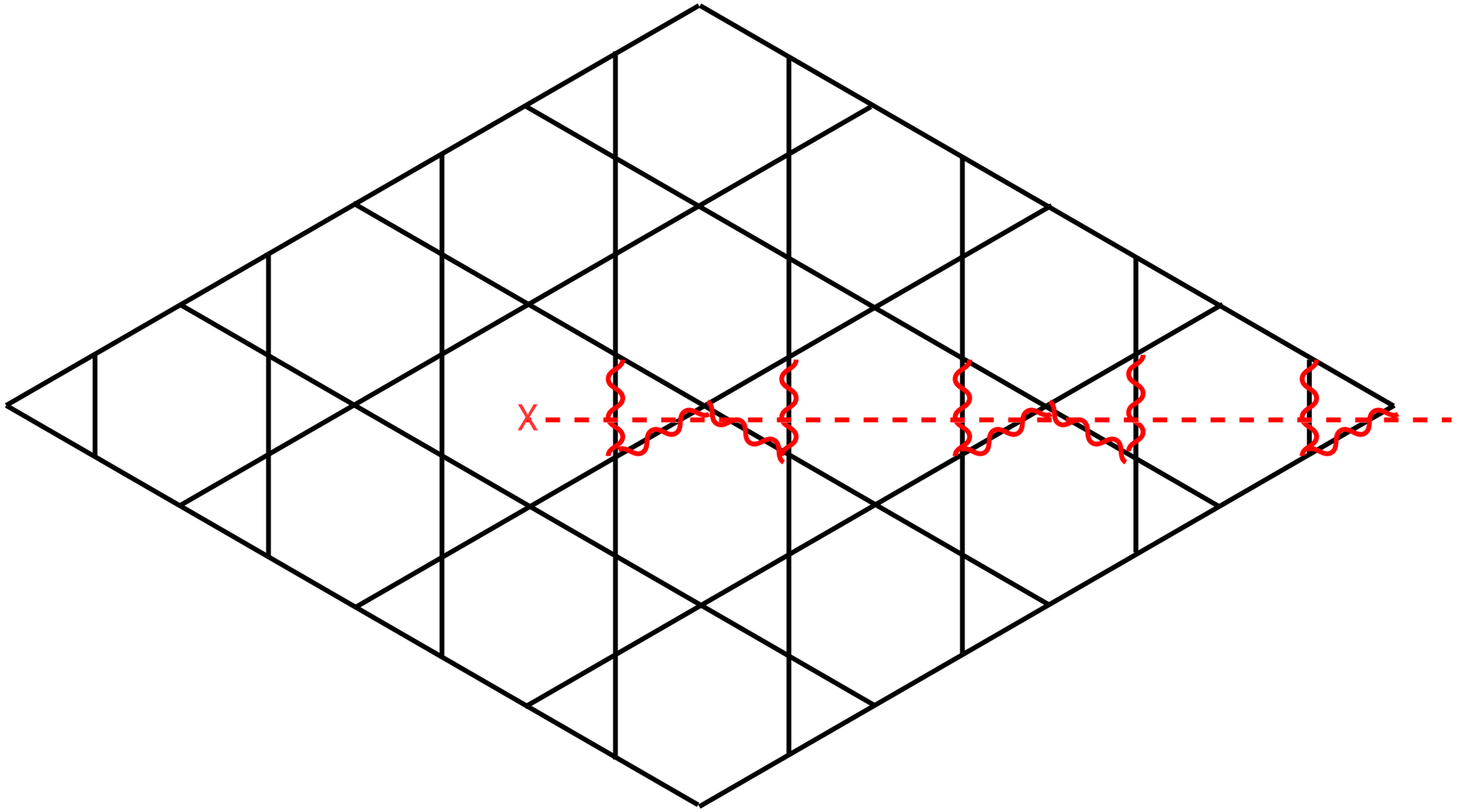

Vison on the kagome lattice

PSG of vison states

The simplest case on the kagome has the visons transforming under the 48 element group GL(2,Z_3): the group of invertible 2×2 matrices which elements belonging to the field Z_3. This is *not* isomorphic to any previously studied point group in solid state physics (or in any other field of physics, as far as we know).

The low energy vison states are described by the excitations of the following field theory of a 4-component real field ψ_n

$$\begin{aligned}\mathcal{L} \;=\; & \sum_{n=1\ldots4} \left((\nabla\psi_n)^2 + (\partial_\tau\psi_n)^2 + r\psi_n^2 + u\psi_n^4\right) + a\sum_{n<m}\psi_n^2\psi_m^2 \\ & + b\big[\psi_1^2(\psi_2\psi_3 - \psi_2\psi_4 + \psi_3\psi_4) + \psi_2^2(\psi_1\psi_3 + \psi_1\psi_4 - \psi_3\psi_4) \\ & \quad + \psi_3^2(\psi_1\psi_2 - \psi_1\psi_4 + \psi_2\psi_4) - \psi_4^2(\psi_1\psi_2 + \psi_1\psi_3 + \psi_2\psi_3)\big].\end{aligned}$$

Y. Huh, M. Punk, and
S. Sachdev, arXiv:1106.3330

Confinement transition from a Z_2 spin liquid to a VBS state

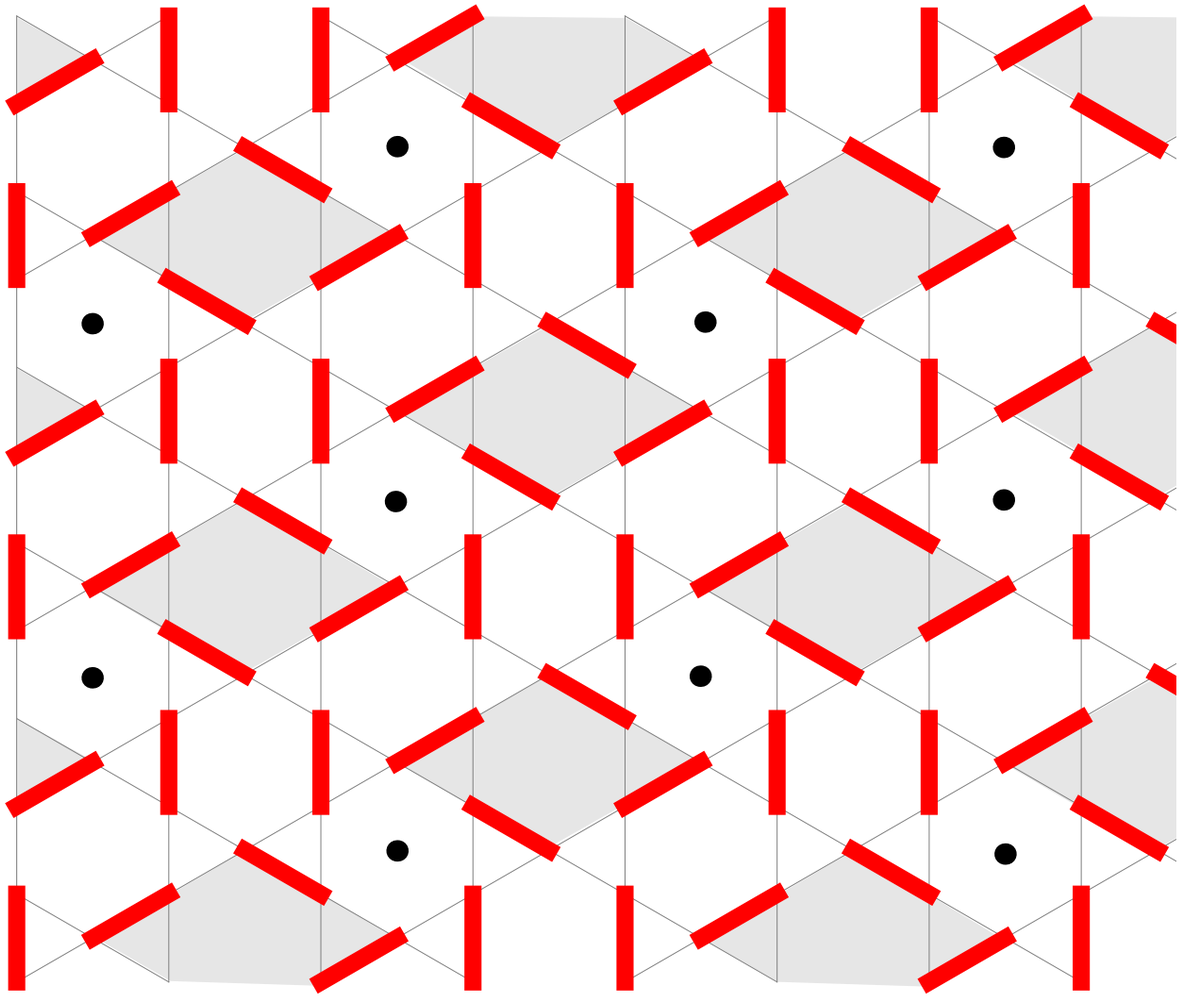

The diamond pattern VBC

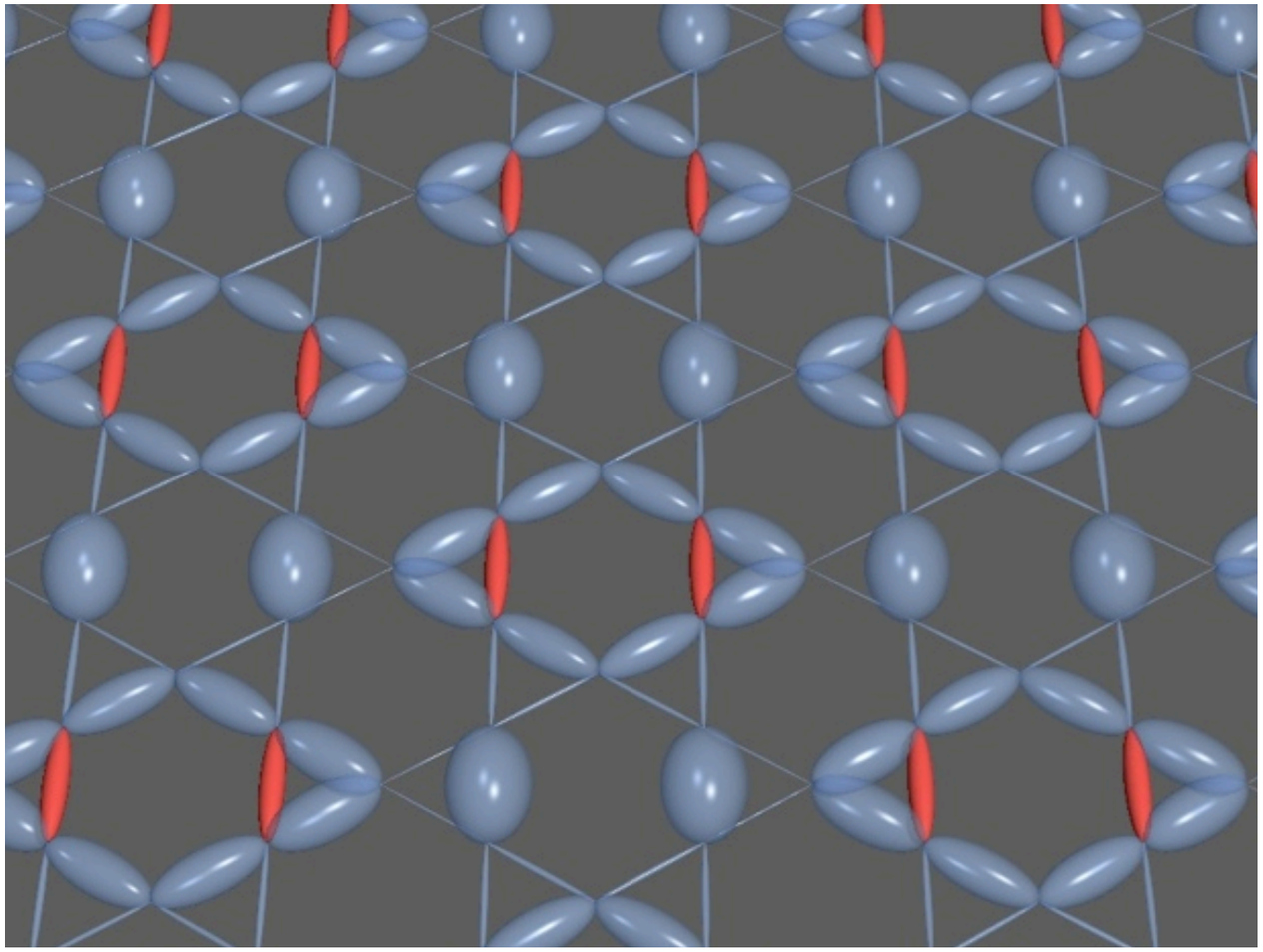

Condensation of vison with GL(2,Z_3) PSG leads to a VBS pattern similar to the "diamond" pattern favored by the DMRG studies of Steve White and collaborators.

Energy Vs Gauge Breaking parameter plots

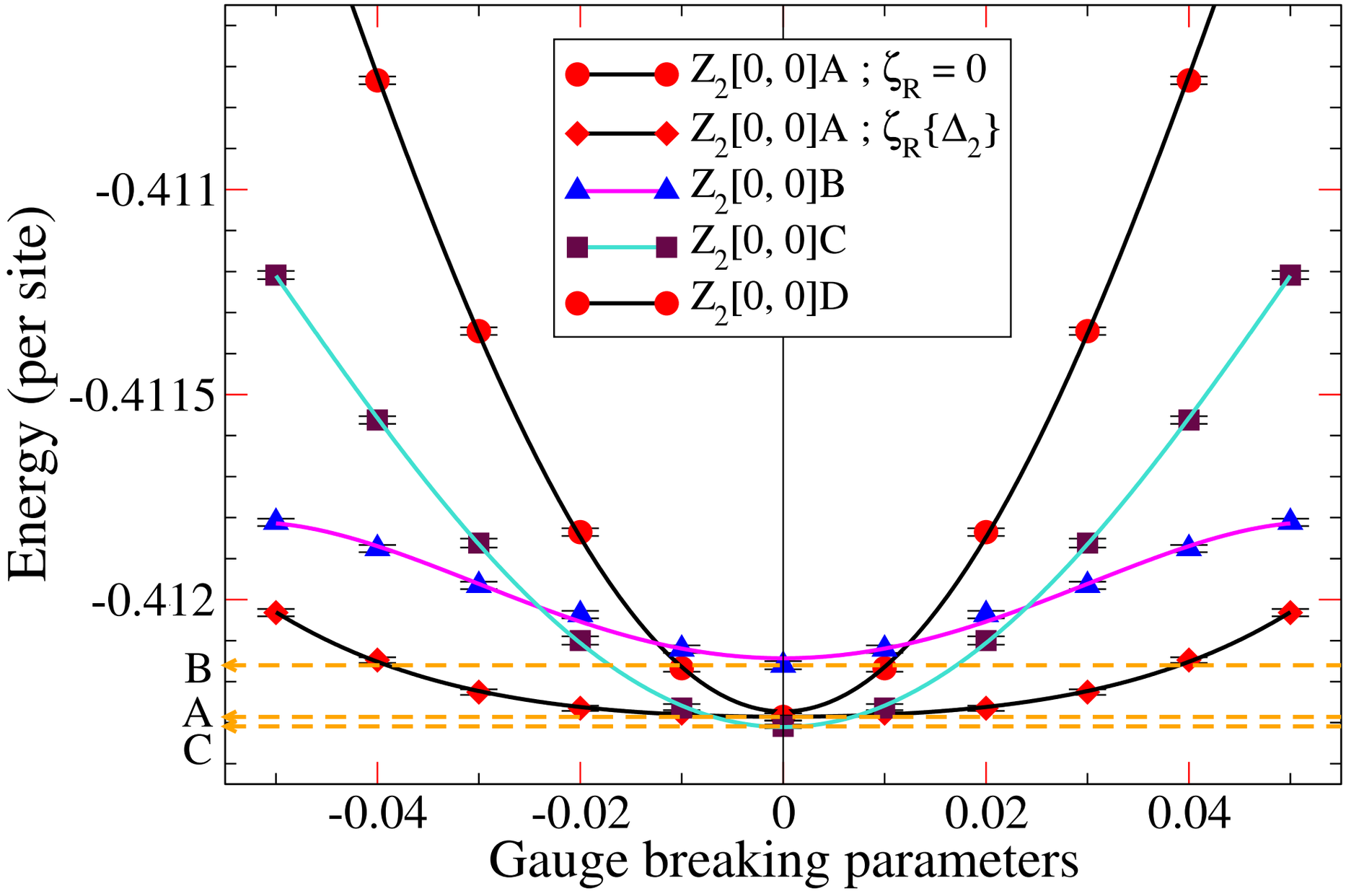

Variational wavefunctions for U(1) and Z_2 spin liquids

Y. Iqbal, F. Becca, and D. Poilblanc

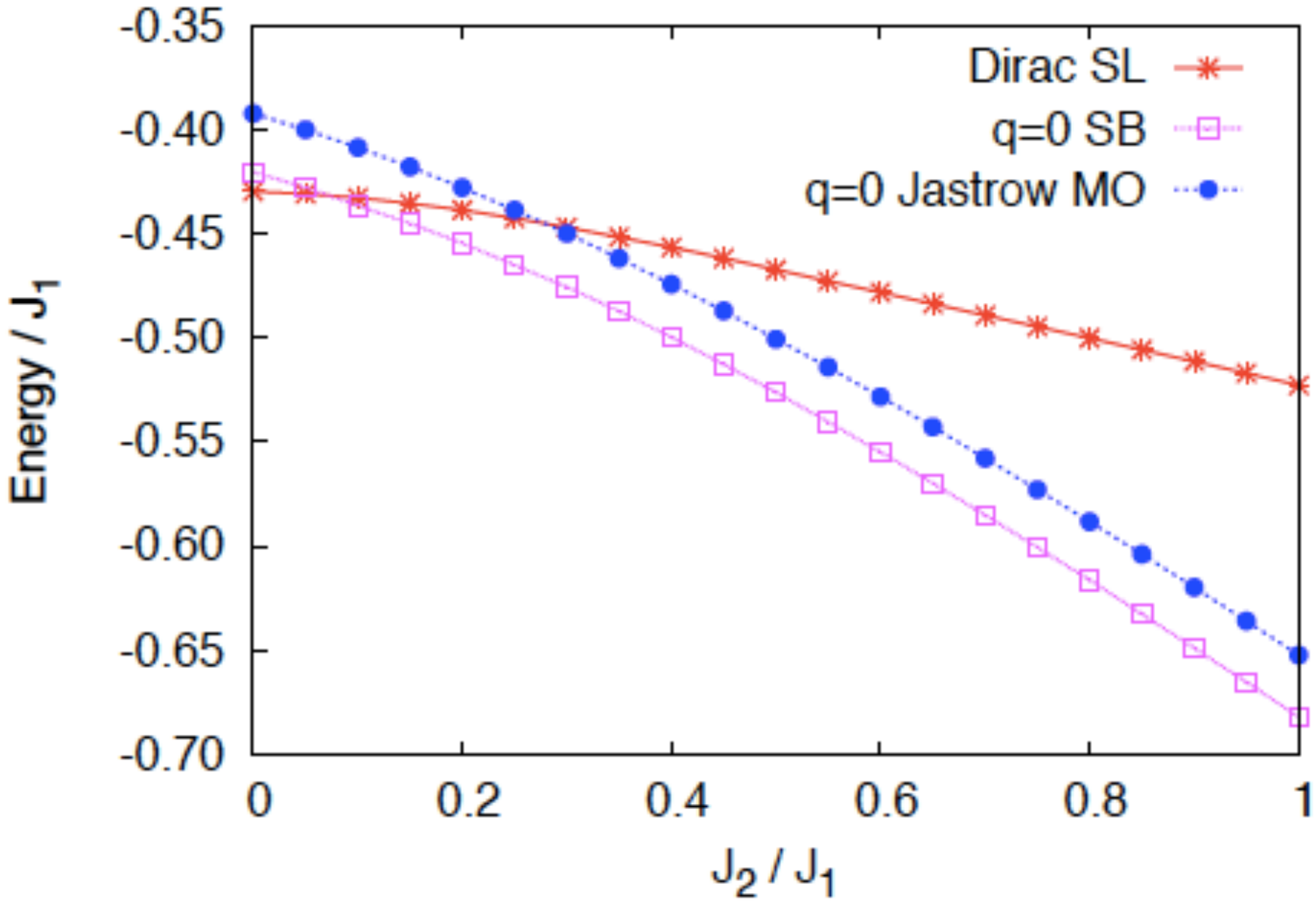

FIG. 4: Comparison of trial energies per site for Dirac SL, $\mathbf{q} = \mathbf{0}$ SB wave function, and $\mathbf{q} = \mathbf{0}$ Jastrow-type magnetically ordered (MO) state. The SB state has poorer energy than Dirac SL for $J_2/J_1 \lesssim 0.08$, but performs better for larger J_2 and better than the Jastrow-type MO for all J_2.

Tiamhock Tay and Olexei I. Motrunich

1. Dimerized antiferromagnets and the Wilson-Fisher CFT

2. J-Q model and deconfined criticality

3. Kagome lattice and Z_2 spin liquids

4. Spin liquids on the honeycomb lattice

5. Quantum critical points in metals: Fermi surface reconstruction

1. Dimerized antiferromagnets and the Wilson-Fisher CFT

2. J-Q model and deconfined criticality

3. Kagome lattice and Z_2 spin liquids

4. Spin liquids on the honeycomb lattice

5. Quantum critical points in metals: Fermi surface reconstruction

The Mott transition

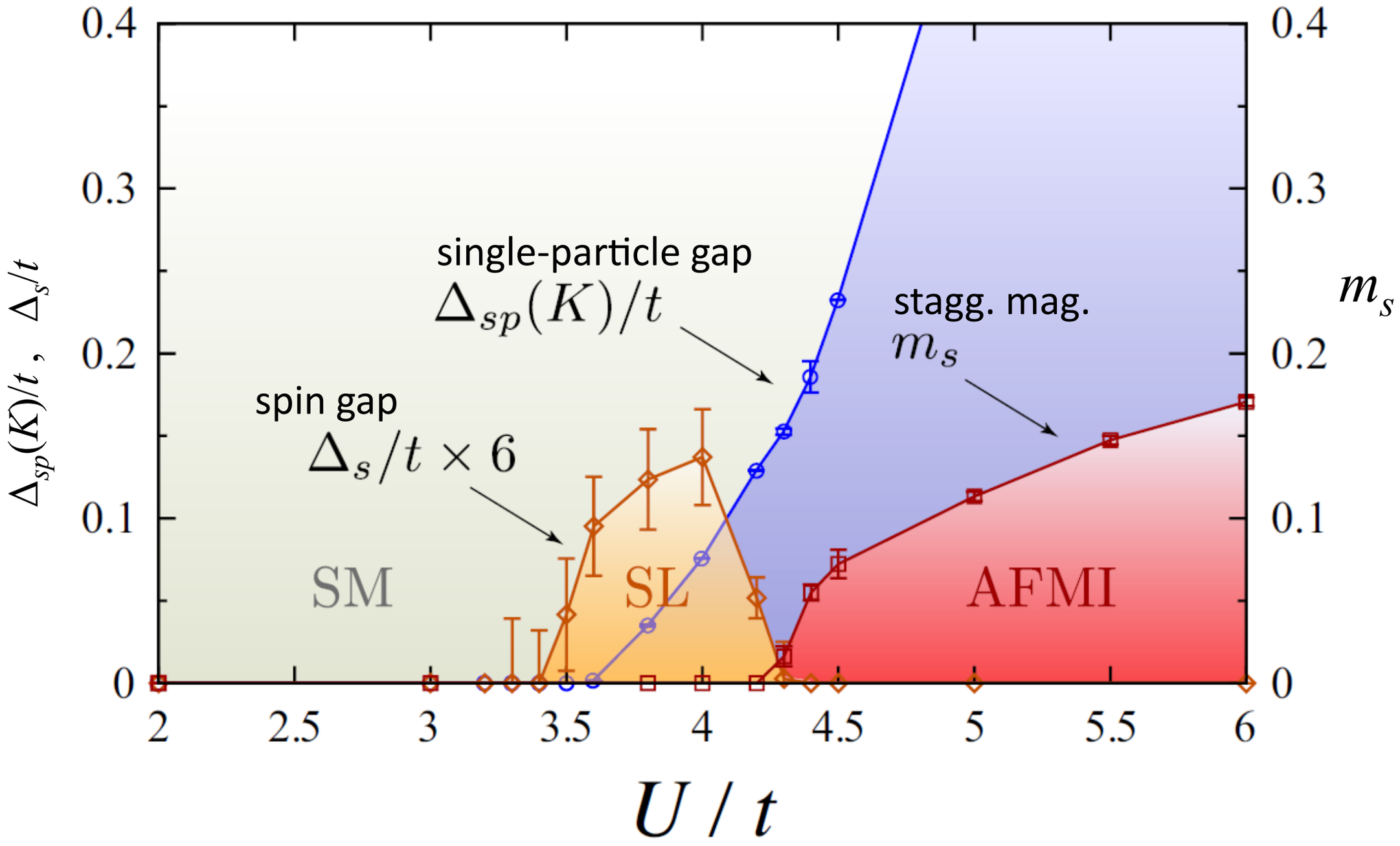

Intermediate state: finite spin gap, finite single-particle gap.

No broken symmetries. Not adiabatically connected to a band insulating state.

Sublattice Pairing State

We find only one natural candidate spin liquid state in Schwinger-fermion representation:

Sublattice Pairing State

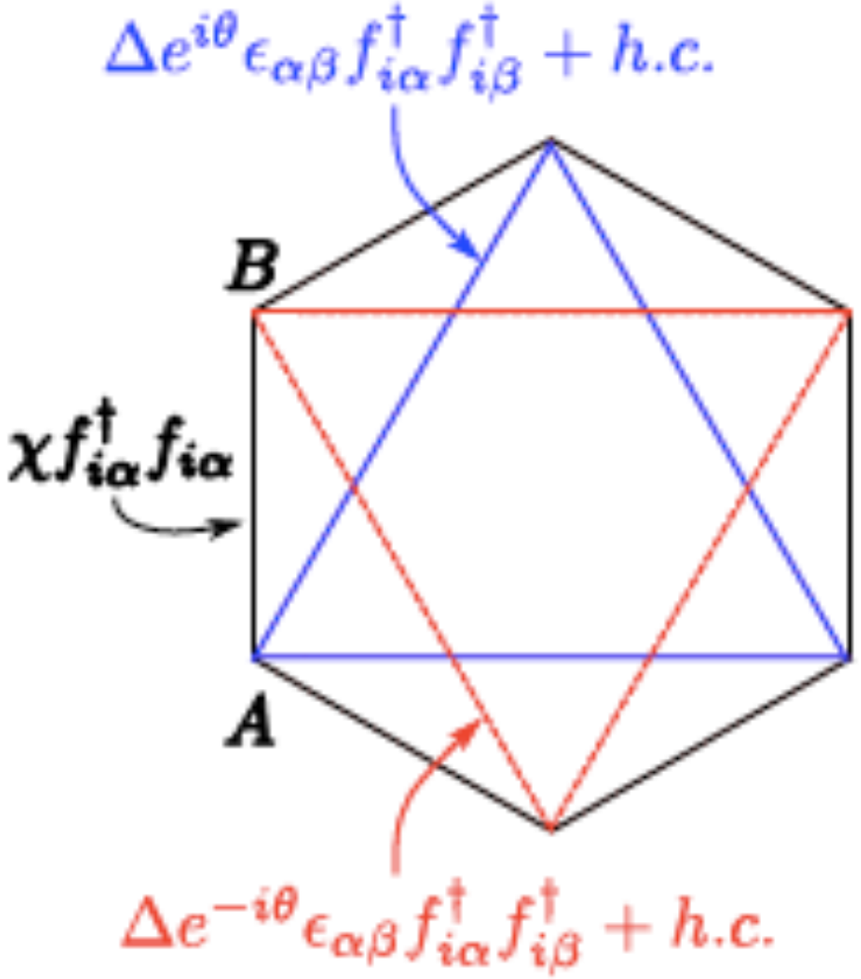

Low energy excitations:
fermionic spinons and visons (π-fluxes of Z_2 gauge field)

Yuan-Ming Lu and Ying Ran

We now understand at a microscopic level what makes a good wave function for a spin liquid on a bipartite lattice!

"Obeys" the Marshall Sign Rule + AA Singlets

We expect then that our wave function Gapped(Δ, θ) (i.e. SPS) is better then Gapless for some values of Δ and θ.

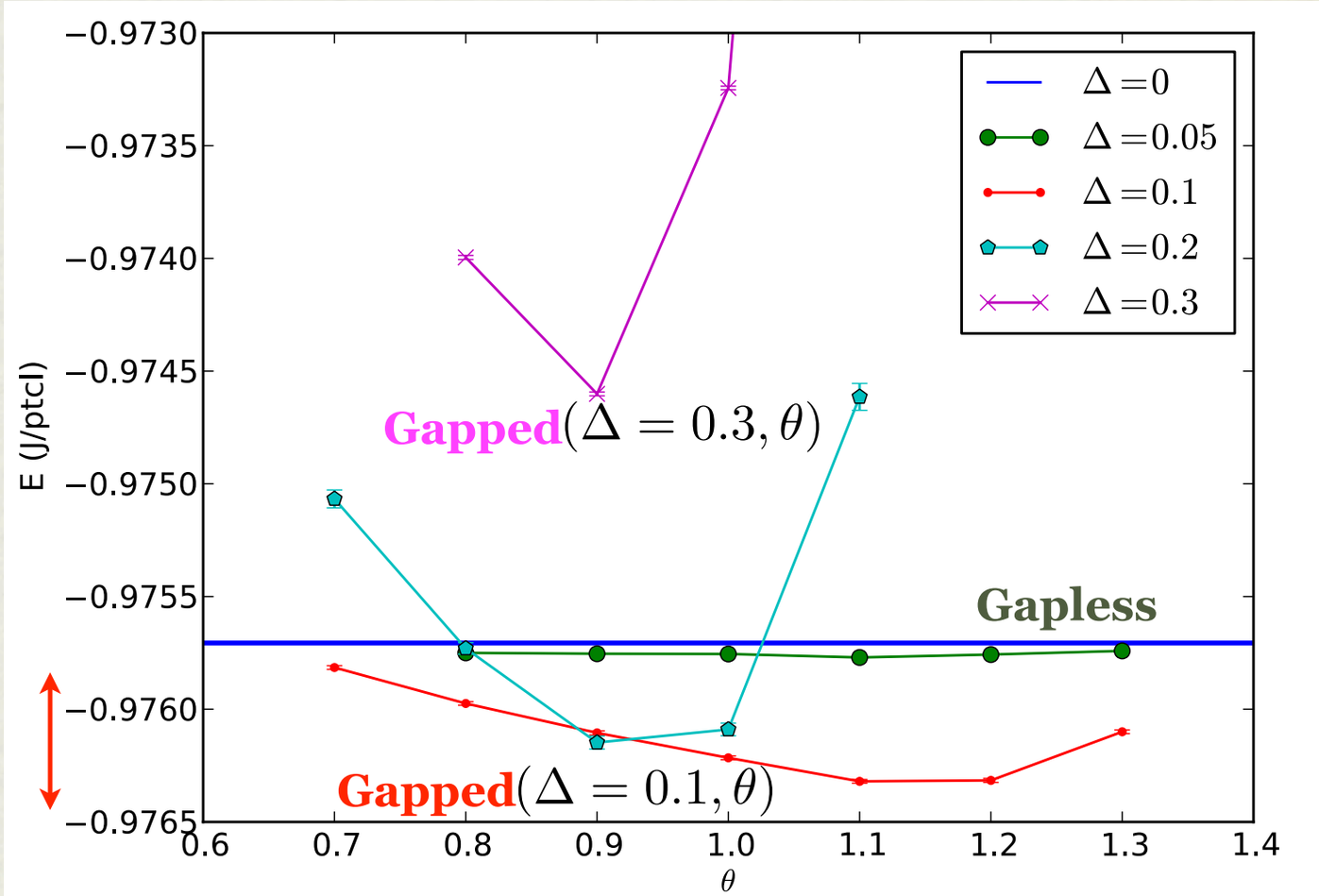

We have computed energetics over a huge manifold of possible spin liquids (including these). We find this one wins (for the qualitative reasons we discussed).

B. Clark, D. Abanin, S. Sondhi

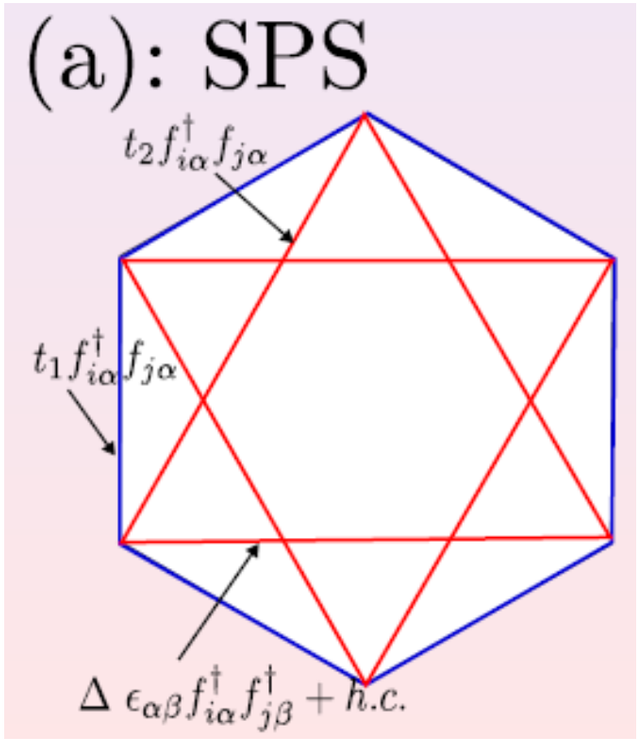

=

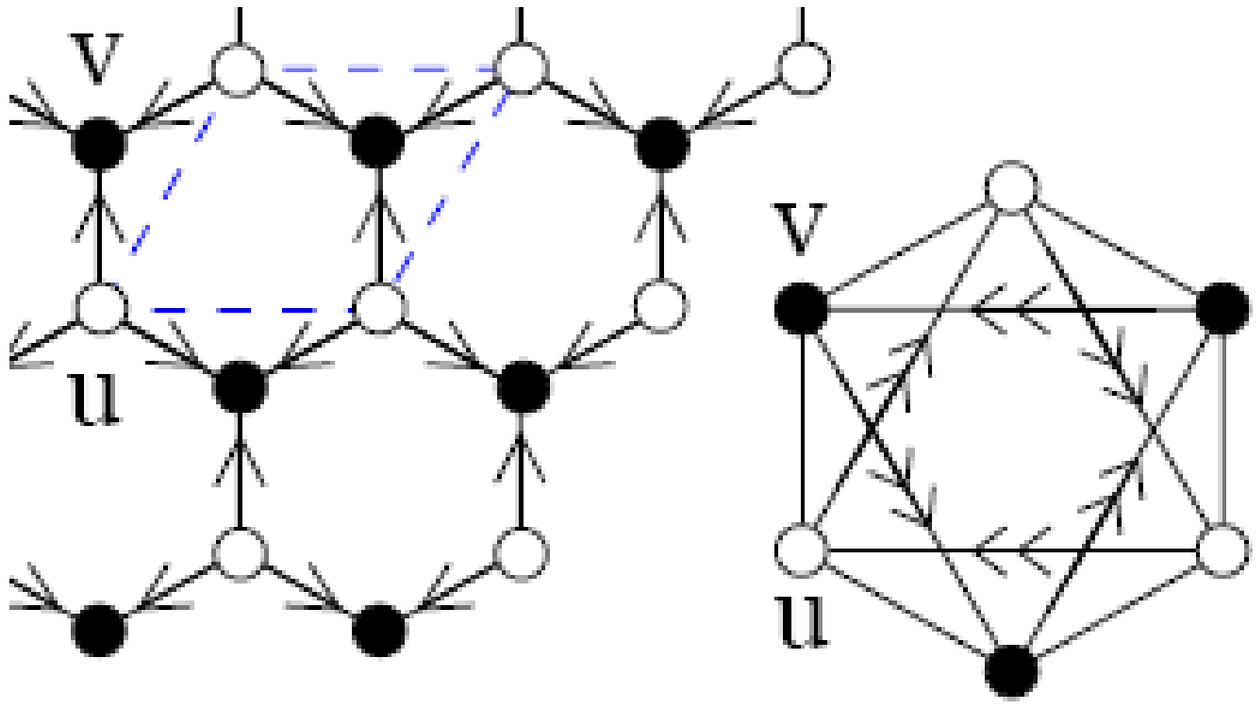

SPS

Schwinger-fermion rep.

f-spinon(fermion)+Z2 gauge field

Schwinger fermions

0-flux state

Schwinger-boson rep.

z-spinon(boson)+ Z2 gauge field

Schwinger bosons (Fa Wang)

Yuan-Ming Lu and Ying Ran

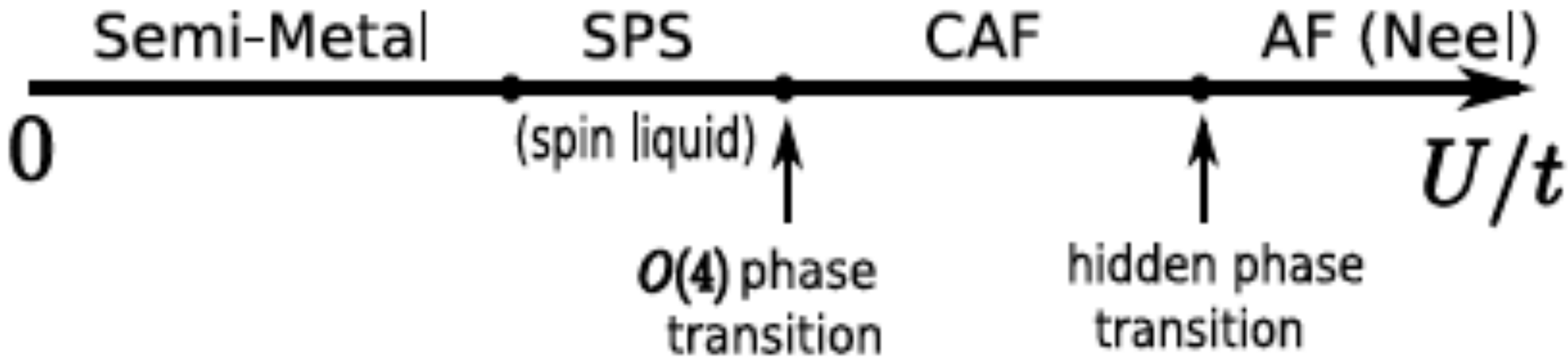

Yuan-Ming Lu and Ying Ran

Detecting the CAF phase in numerics

Two order parameters: (breaks SU(2) completely, 3 Goldstone modes)

- Vector Spin Chirality:

$$\vec{n} = \vec{S}_1 \times \vec{S}_2 + \vec{S}_2 \times \vec{S}_3 + \vec{S}_3 \times \vec{S}_1 + \vec{S}_4 \times \vec{S}_5 + \vec{S}_5 \times \vec{S}_6 + \vec{S}_6 \times \vec{S}_4$$

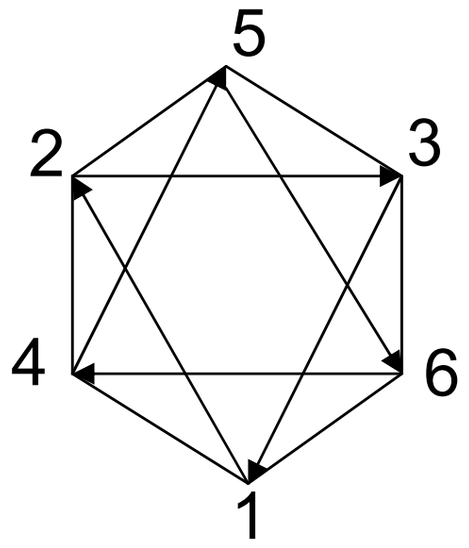

- Neel Order: $\vec{N}$

- Two orders satisfy: $\vec{n} \perp \vec{N}$

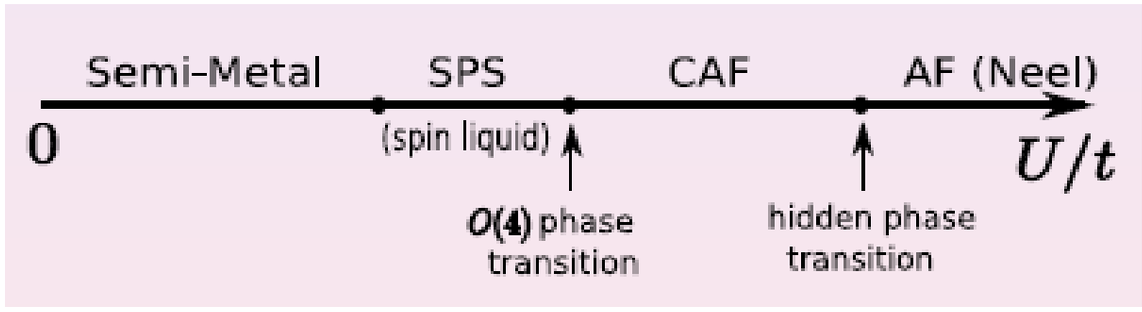

- Magnetic order is still collinear: $TR \circ C_6$ is a symmetry.

Yuan-Ming Lu and Ying Ran

Kitaev Model

$$H = J_1 \sum_{x-link} \sigma_n^x \sigma_m^x + J_2 \sum_{y-link} \sigma_n^y \sigma_m^y + J_3 \sum_{z-link} \sigma_n^z \sigma_m^z$$

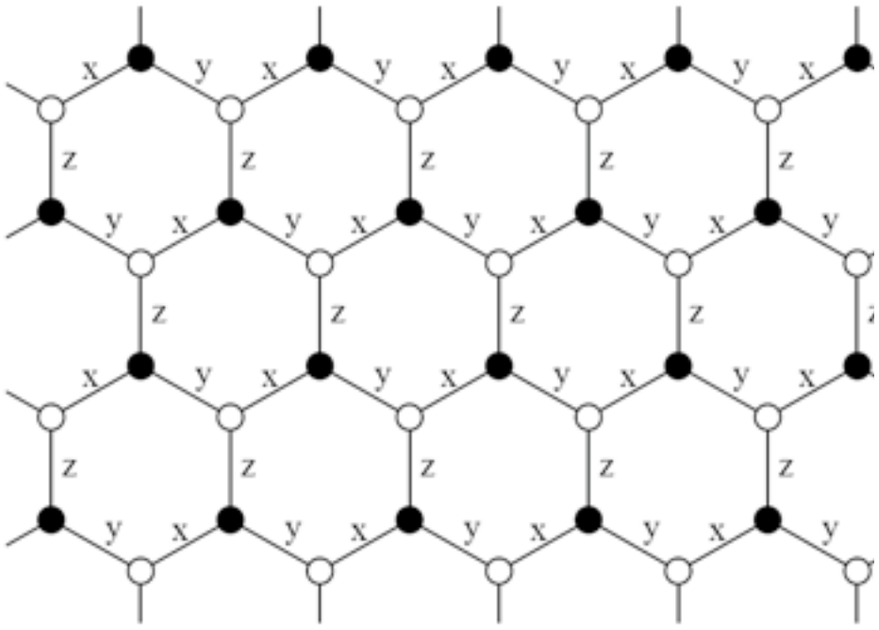

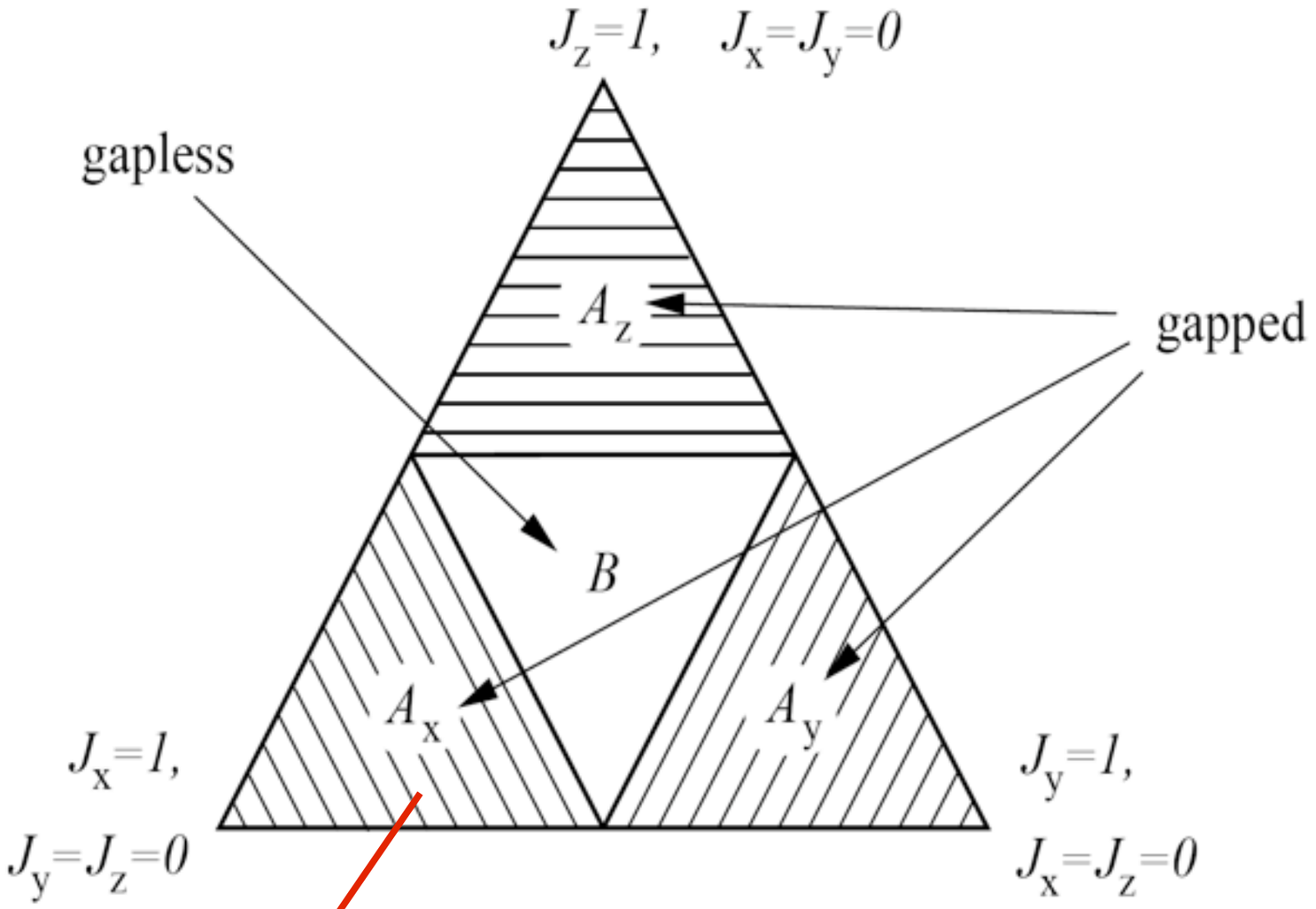

Z_2 spin liquids

Kitaev Model

$$H = J_1 \sum_{x-link} \sigma_n^x \sigma_m^x + J_2 \sum_{y-link} \sigma_n^y \sigma_m^y + J_3 \sum_{z-link} \sigma_n^z \sigma_m^z$$

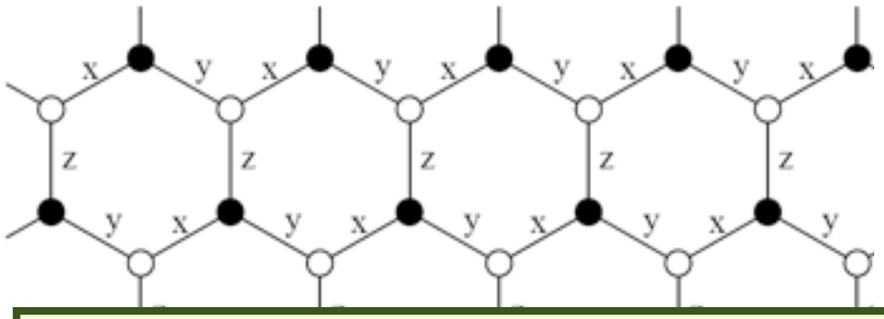

Exact solution includes both spinons and visons as Majorana fermions. Many extensions found on other lattices, including recent cases with both SU(2) symmetry and Fermi surfaces

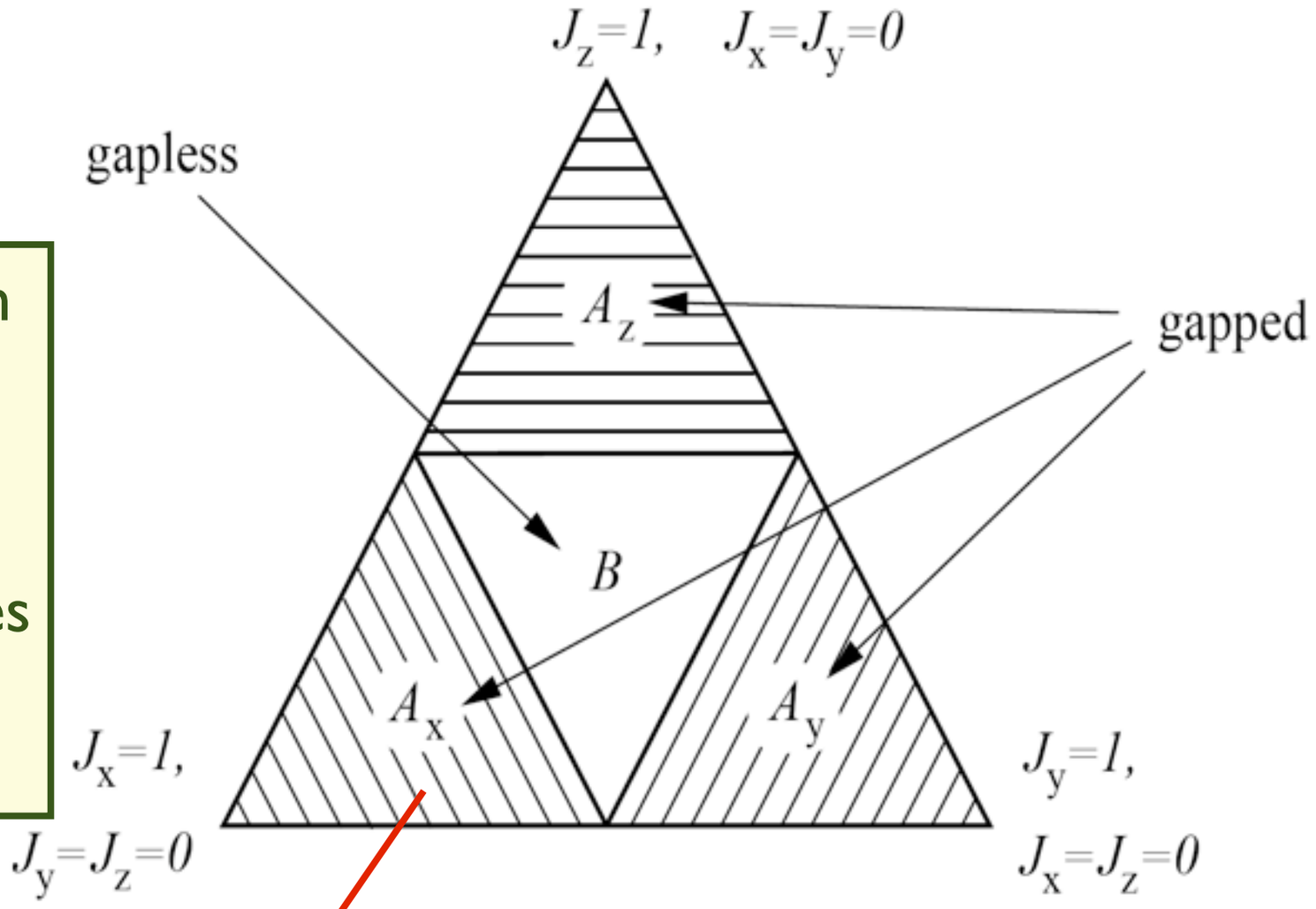

Z_2 spin liquids

1. Dimerized antiferromagnets and the Wilson-Fisher CFT

2. J-Q model and deconfined criticality

3. Kagome lattice and Z_2 spin liquids

4. Spin liquids on the honeycomb lattice

5. Quantum critical points in metals: Fermi surface reconstruction

1. Dimerized antiferromagnets and the Wilson-Fisher CFT

2. J-Q model and deconfined criticality

3. Kagome lattice and Z_2 spin liquids

4. Spin liquids on the honeycomb lattice

5. Quantum critical points in metals: Fermi surface reconstruction

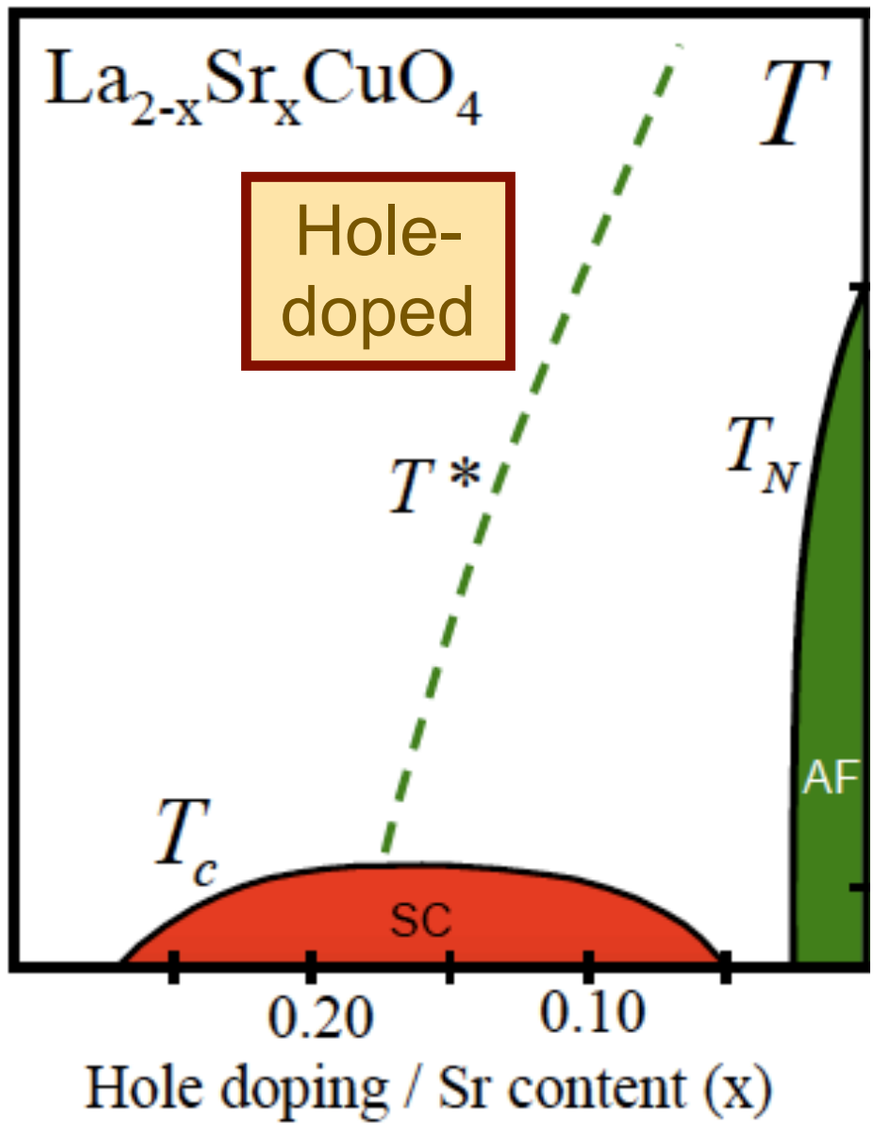
$La_{2-x}Sr_xCuO_4$
T
Hole-doped
T^*
T_N
AF
T_c
SC
0.20
0.10
Hole doping / Sr content (x)

Electron-doped cuprate superconductors

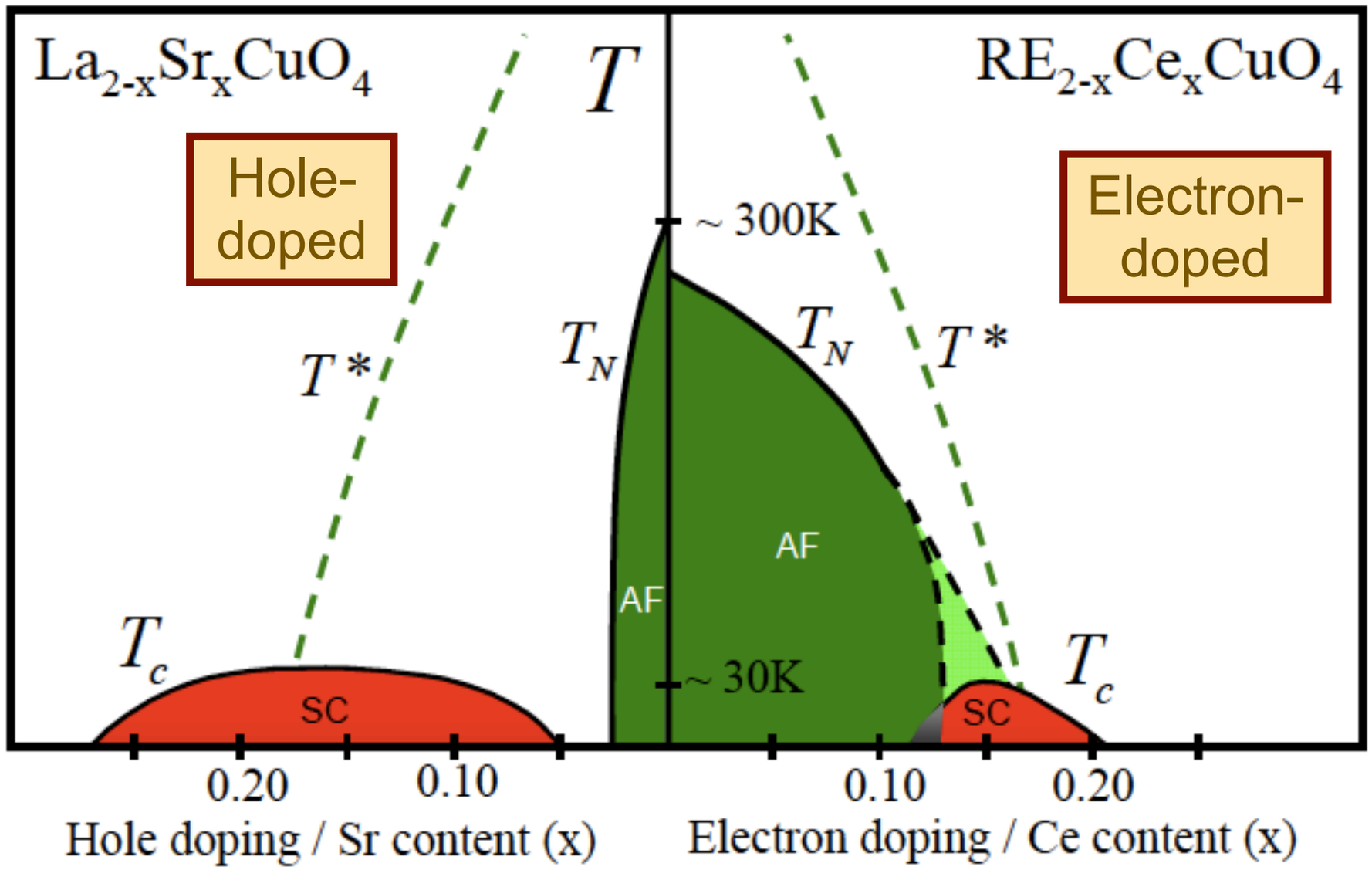

Electron-doped cuprate superconductors

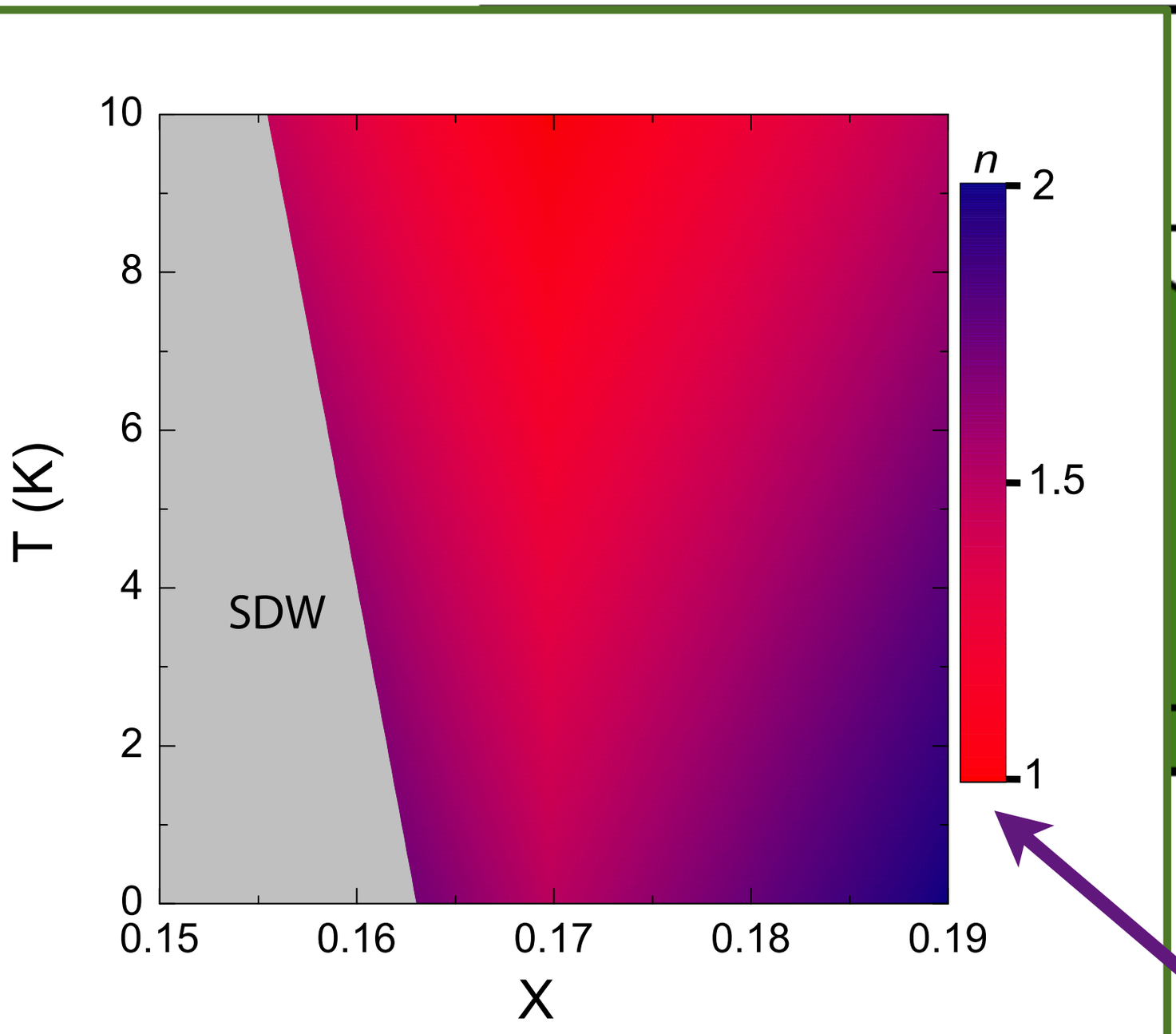

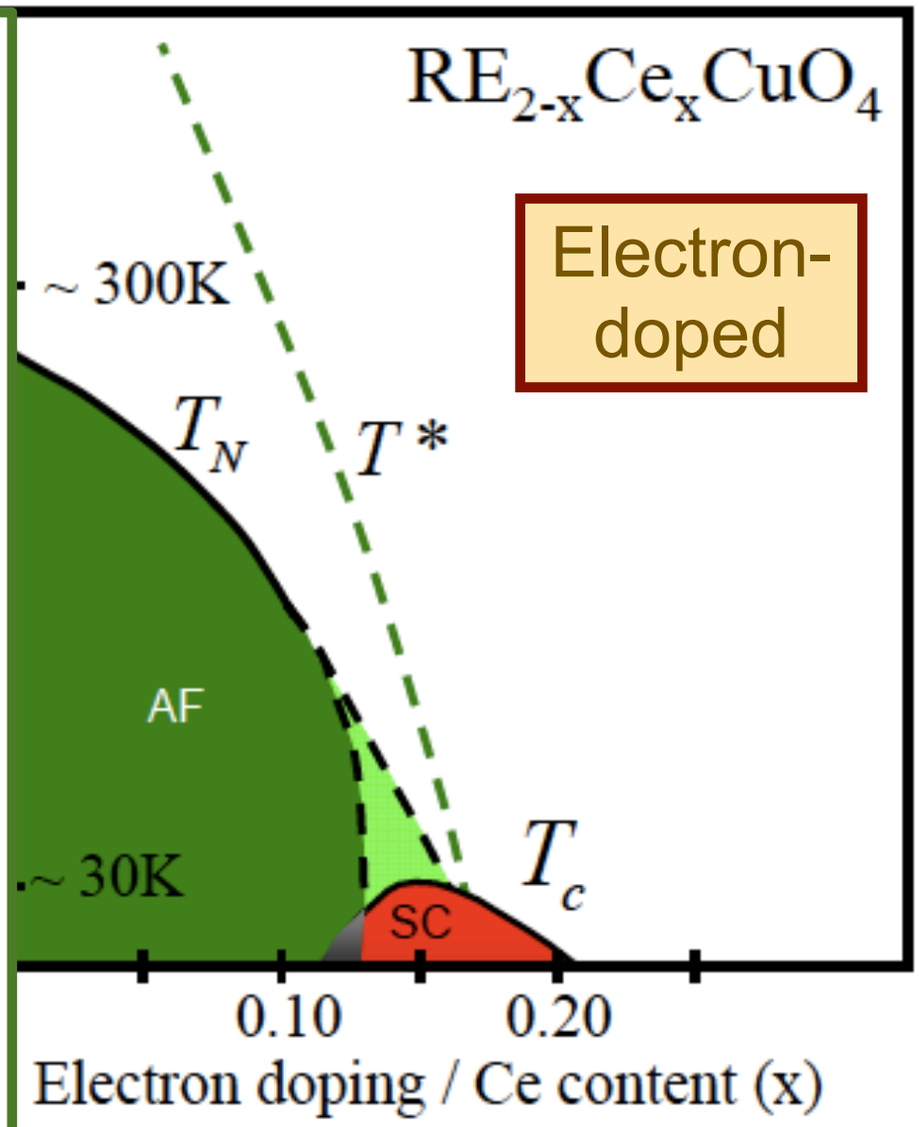

Figure prepared by K. Jin and and R. L. Greene based on N. P. Fournier, P. Armitage, and R. L. Greene, Rev. Mod. Phys. **82**, 2421 (2010).

Resistivity
$\sim \rho_0 + AT^n$

Electron-doped cuprate superconductors

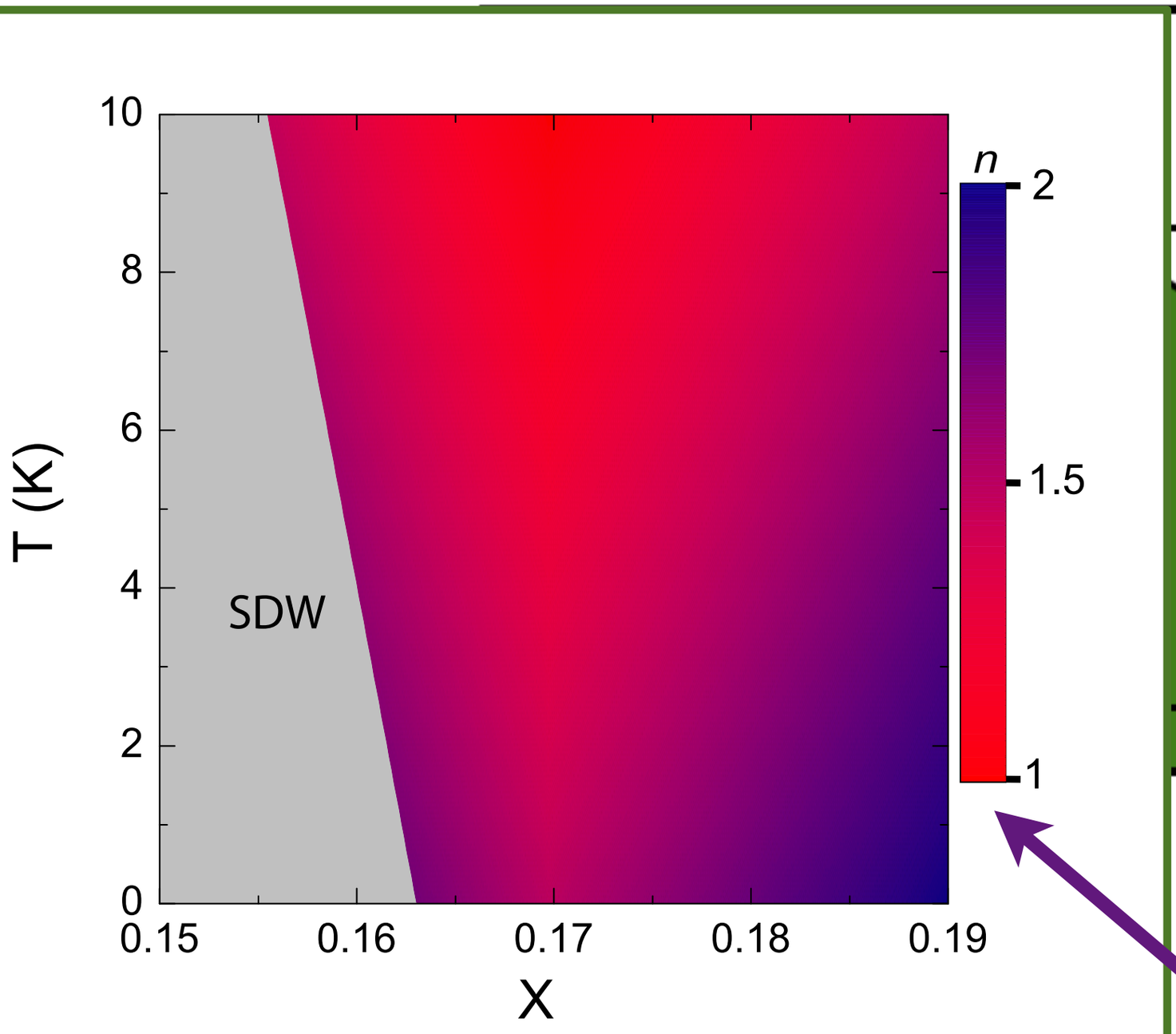

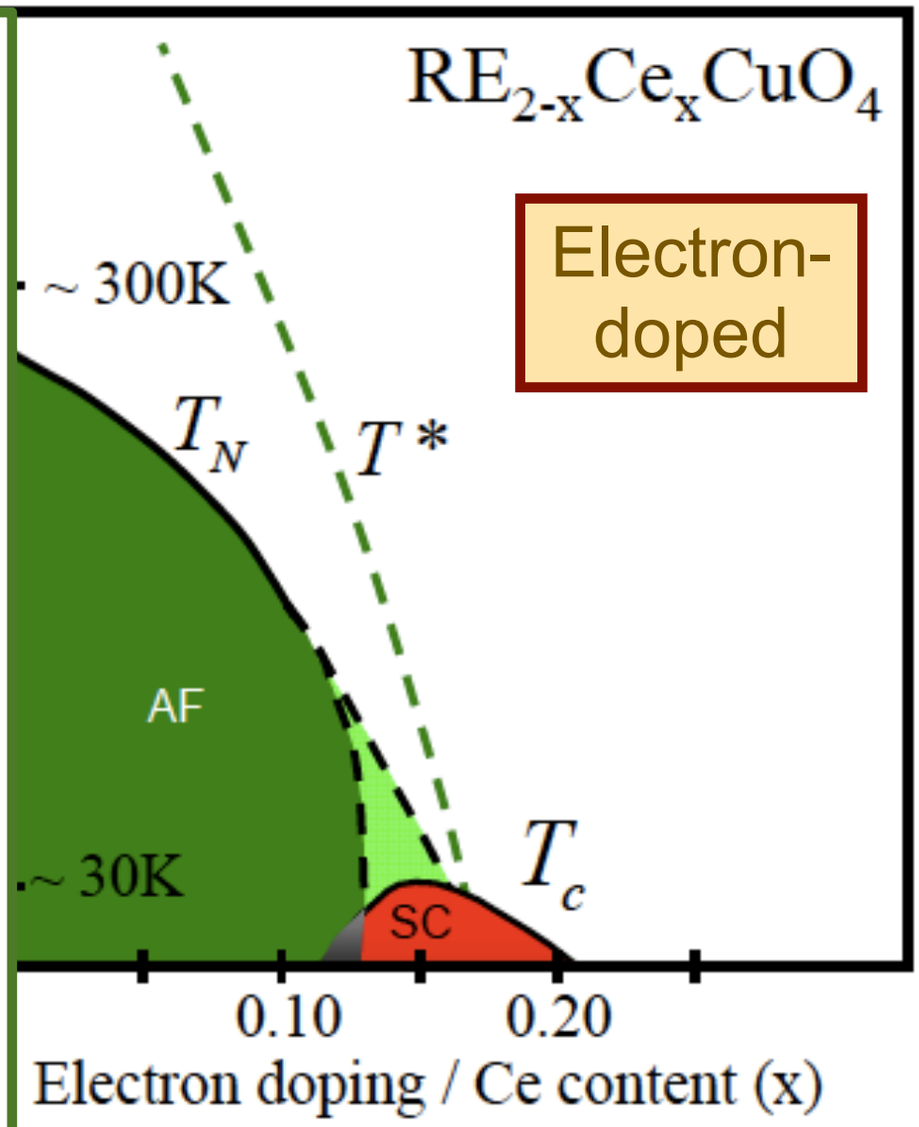

Figure prepared by K. Jin and and R. L. Greene based on N. P. Fournier, P. Armitage, and R. L. Greene, Rev. Mod. Phys. **82**, 2421 (2010).

Resistivity
$\sim \rho_0 + AT^n$

Electron-doped cuprate superconductors

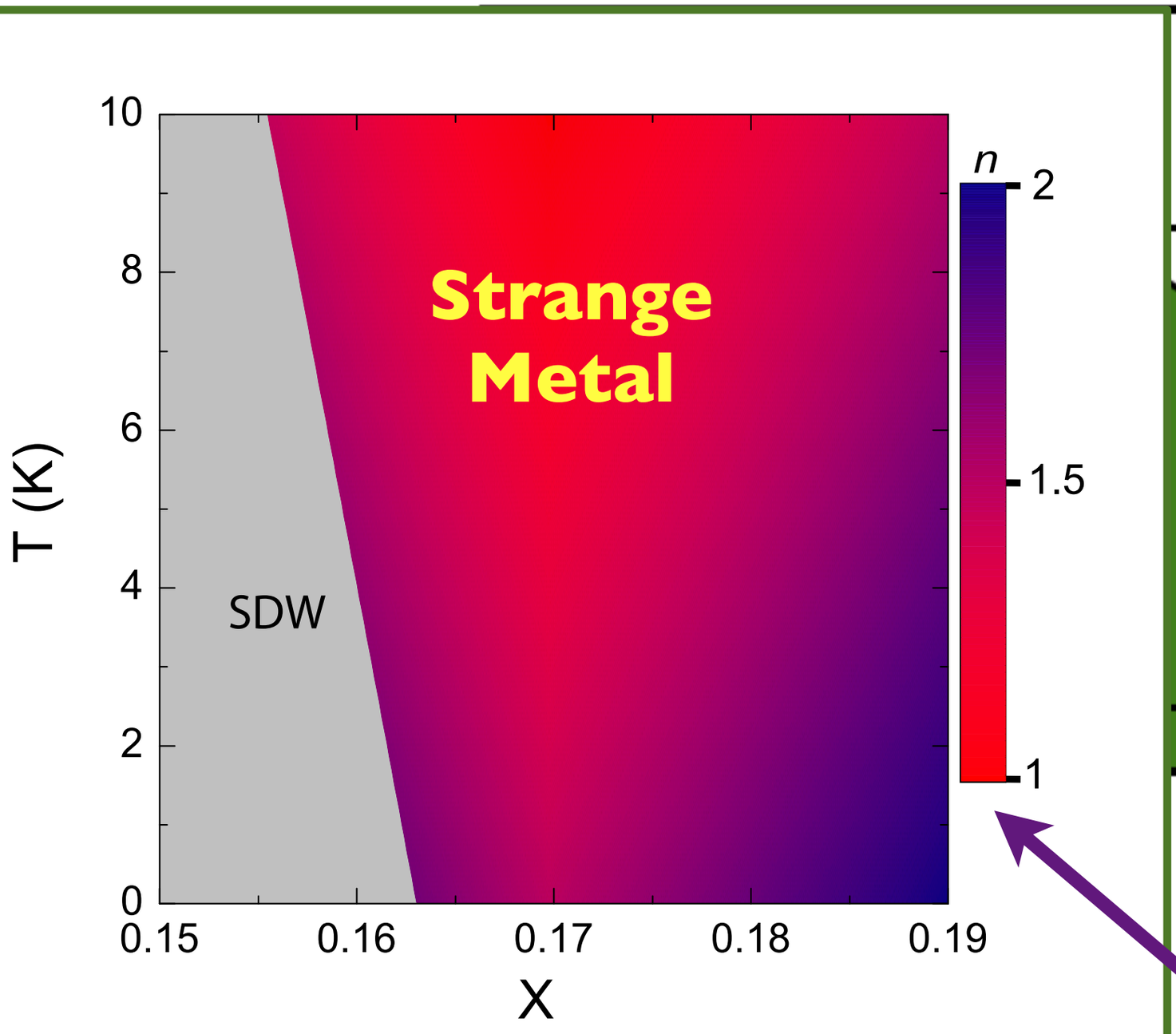

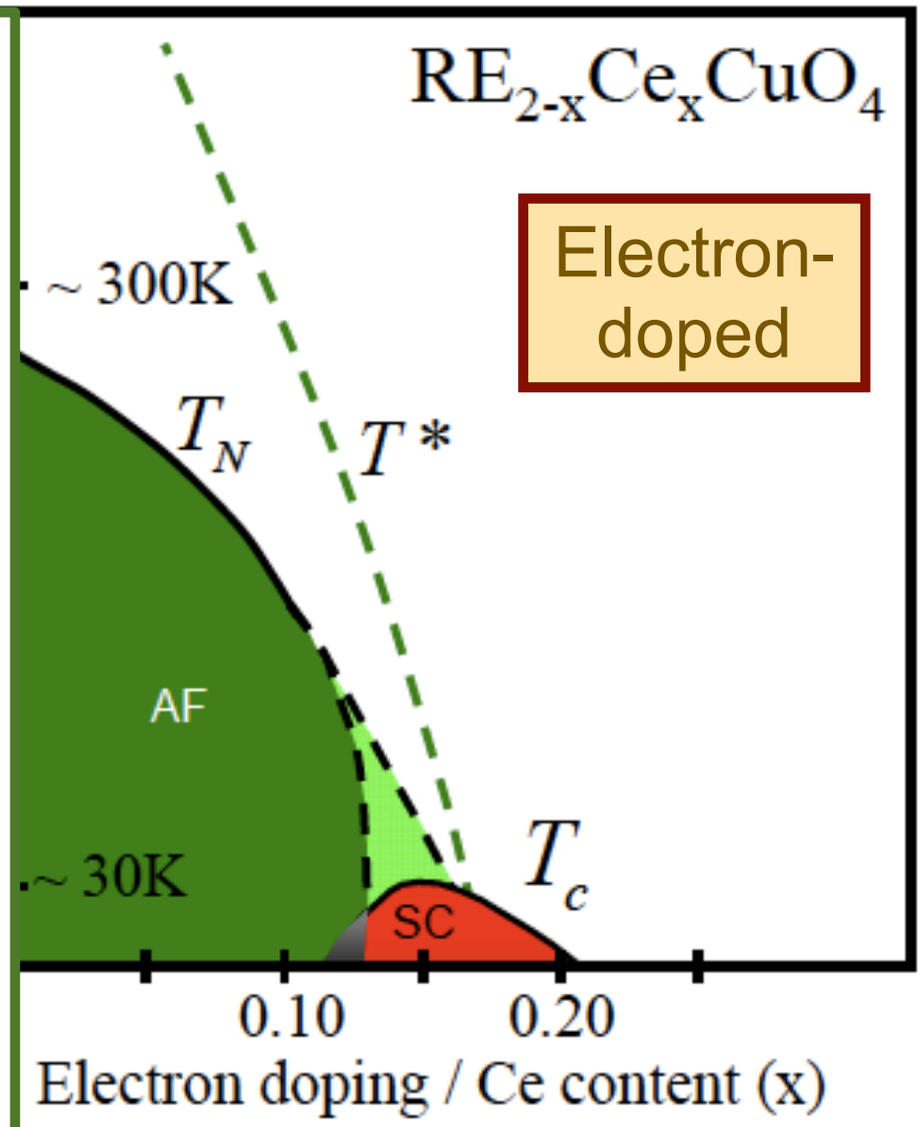

Figure prepared by K. Jin and and R. L. Greene based on N. P. Fournier, P. Armitage, and R. L. Greene, Rev. Mod. Phys. **82**, 2421 (2010).

Resistivity $\sim \rho_0 + AT^n$

Temperature-doping phase diagram of the iron pnictides:

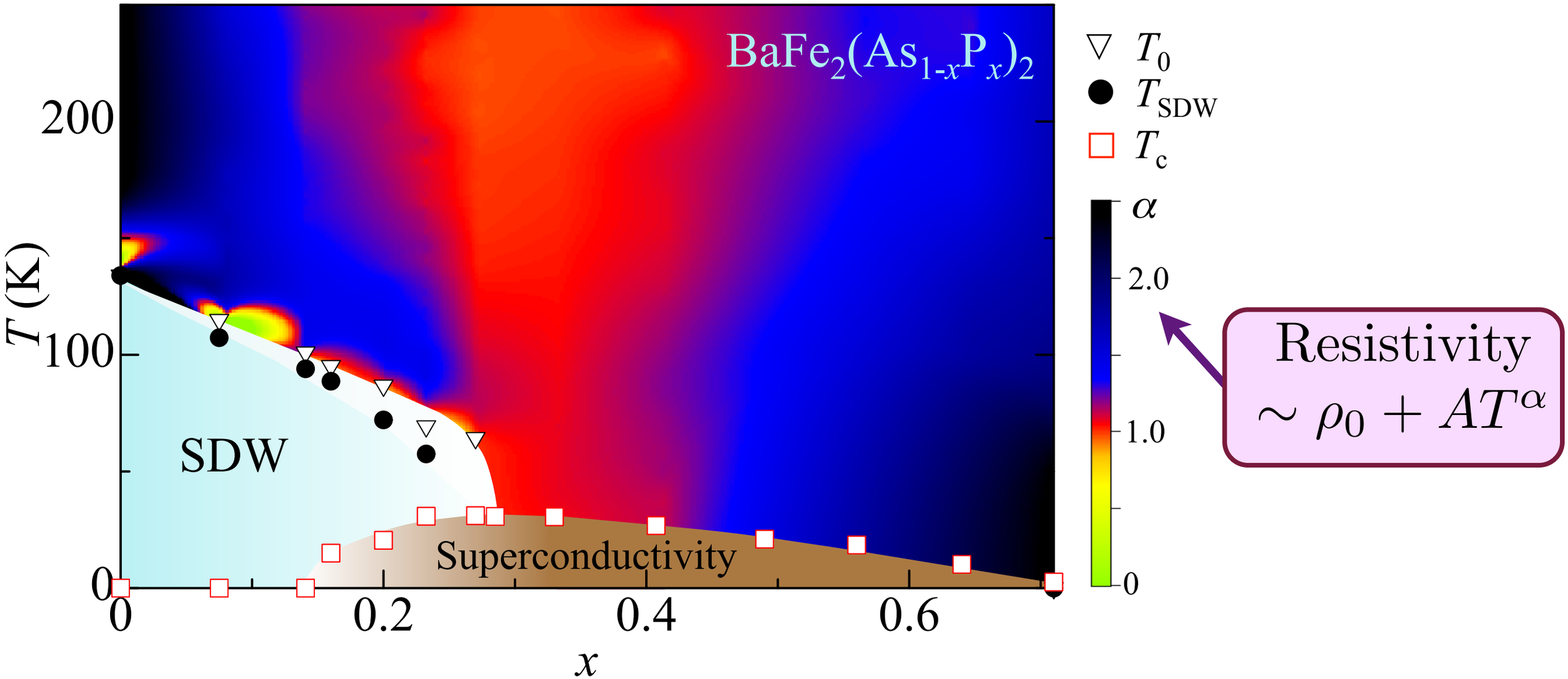

S. Kasahara, T. Shibauchi, K. Hashimoto, K. Ikada, S. Tonegawa, R. Okazaki, H. Shishido, H. Ikeda, H. Takeya, K. Hirata, T. Terashima, and Y. Matsuda,
Physical Review B **81**, 184519 (2010)

Temperature-doping phase diagram of the iron pnictides:

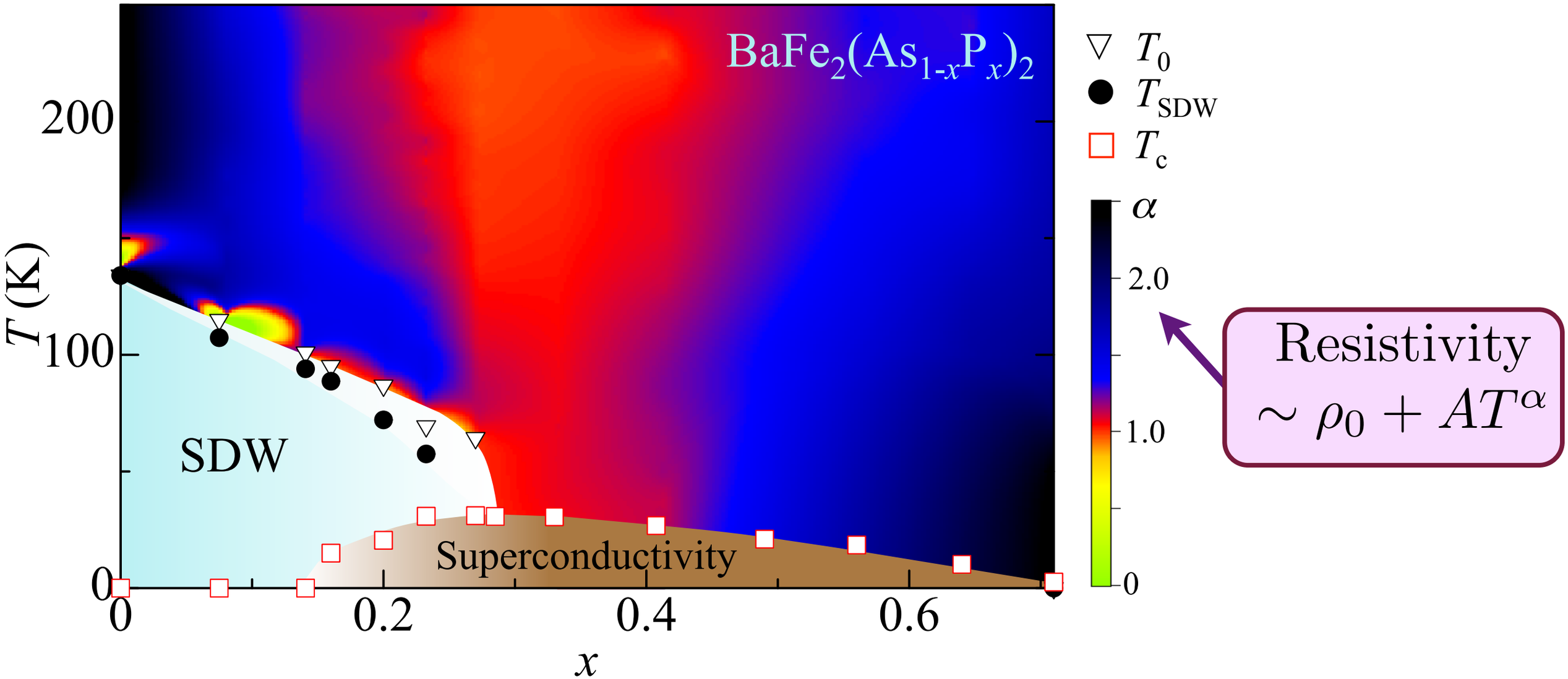

S. Kasahara, T. Shibauchi, K. Hashimoto, K. Ikada, S. Tonegawa, R. Okazaki, H. Shishido, H. Ikeda, H. Takeya, K. Hirata, T. Terashima, and Y. Matsuda,
Physical Review B **81**, 184519 (2010)

Temperature-doping phase diagram of the iron pnictides:

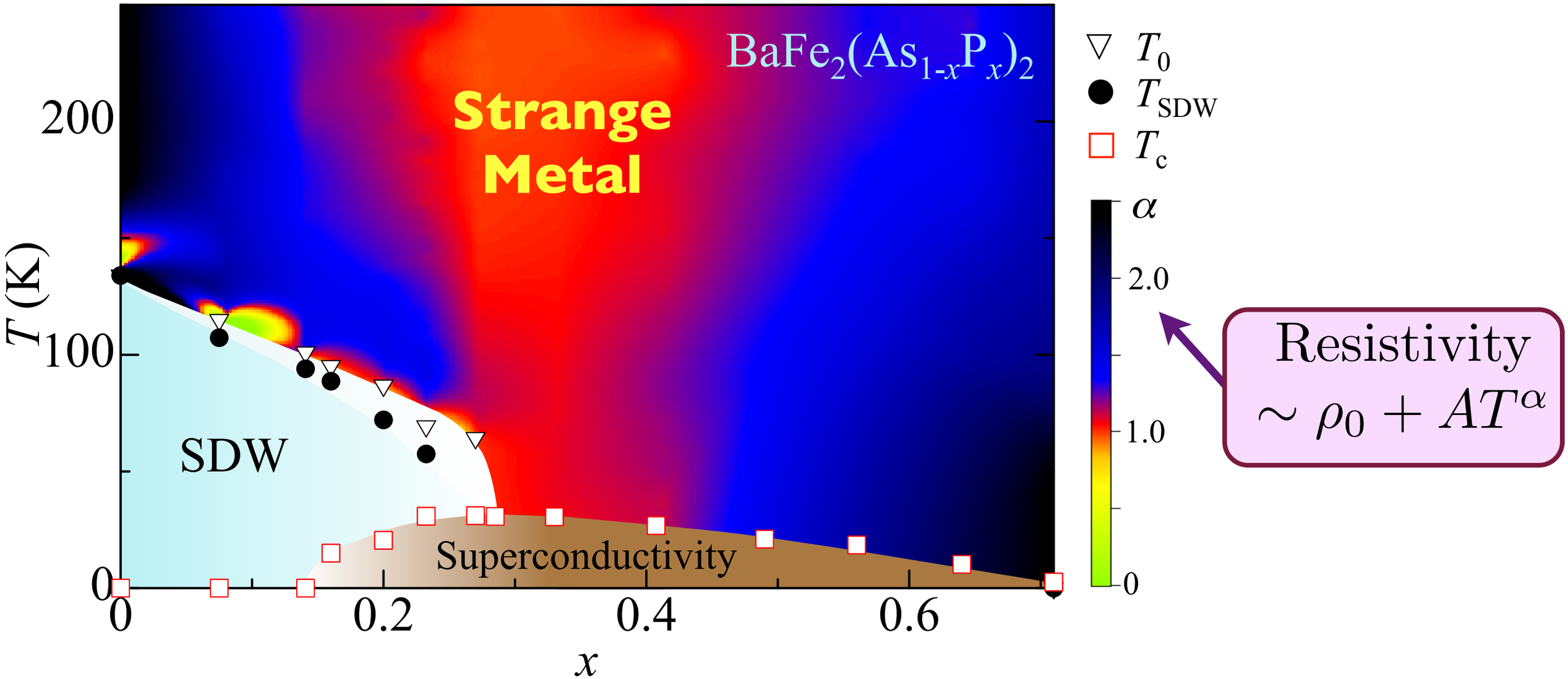

S. Kasahara, T. Shibauchi, K. Hashimoto, K. Ikada, S. Tonegawa, R. Okazaki, H. Shishido, H. Ikeda, H. Takeya, K. Hirata, T. Terashima, and Y. Matsuda,
Physical Review B **81**, 184519 (2010)

Temperature-pressure phase diagram of an organic superconductor

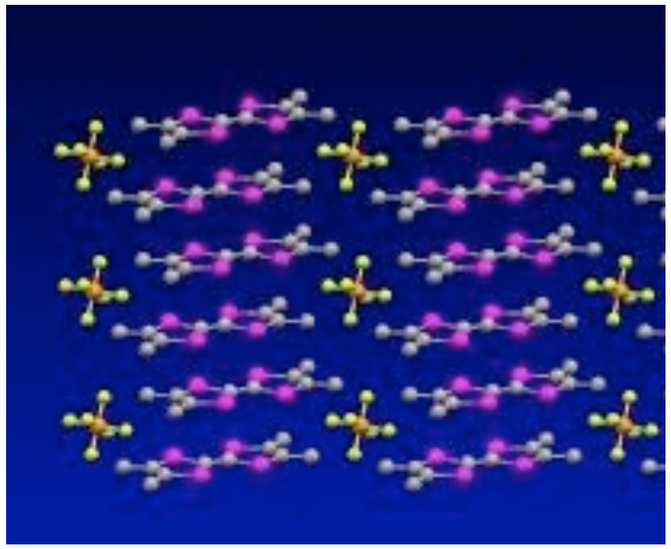

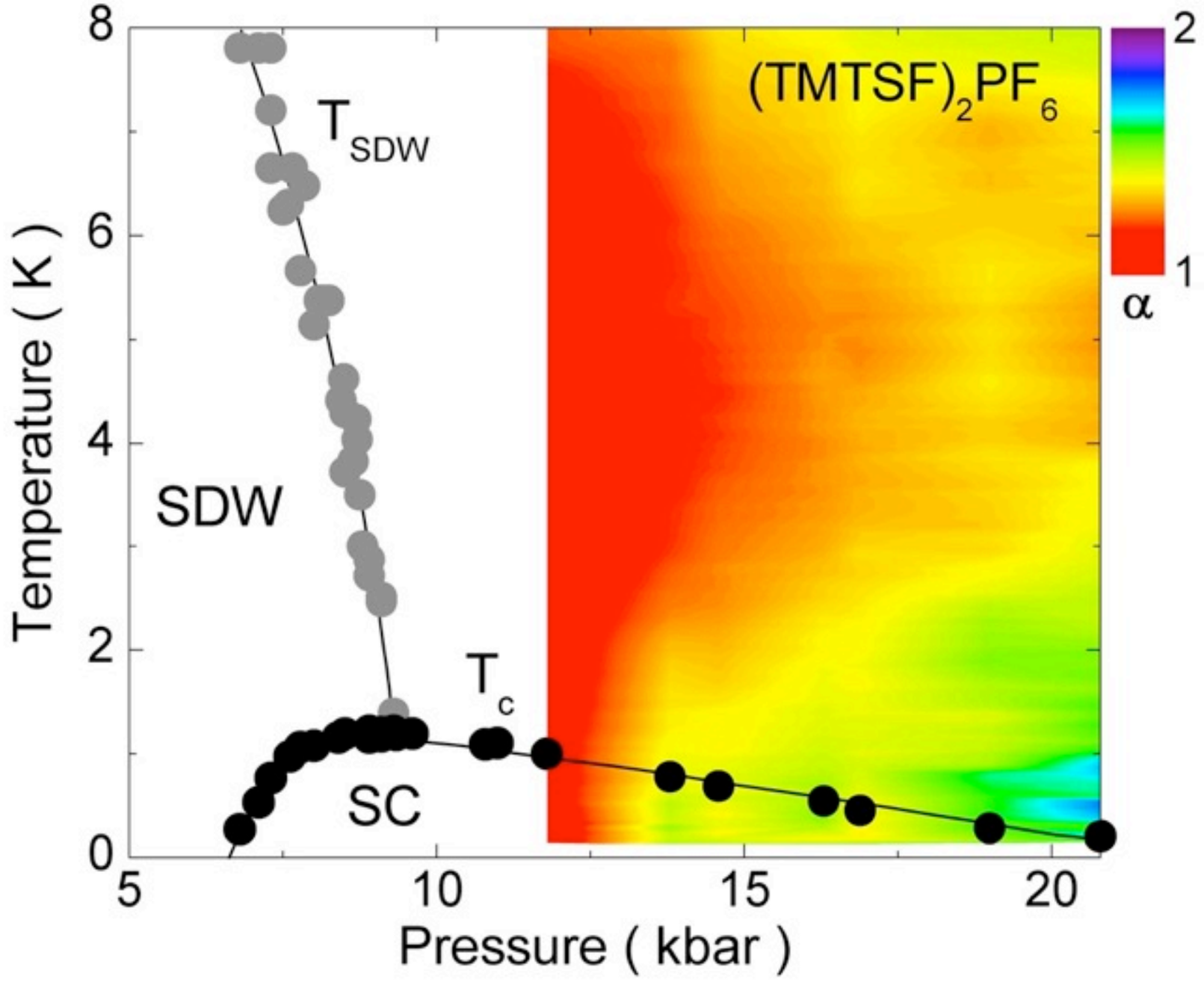

N. Doiron-Leyraud, P. Auban-Senzier, S. Rene de Cotret, A. Sedeki, C. Bourbonnais, D. Jerome, K. Bechgaard, and Louis Taillefer, Physical Review B 80, 214531 (2009)

Temperature-pressure phase diagram of an heavy-fermion superconductor

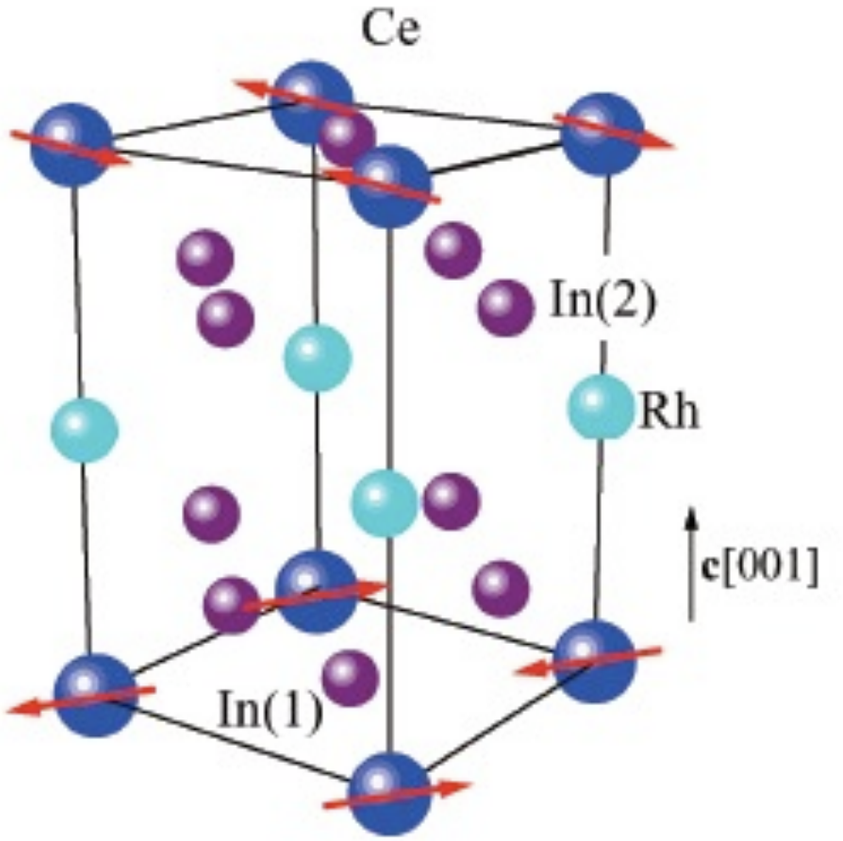

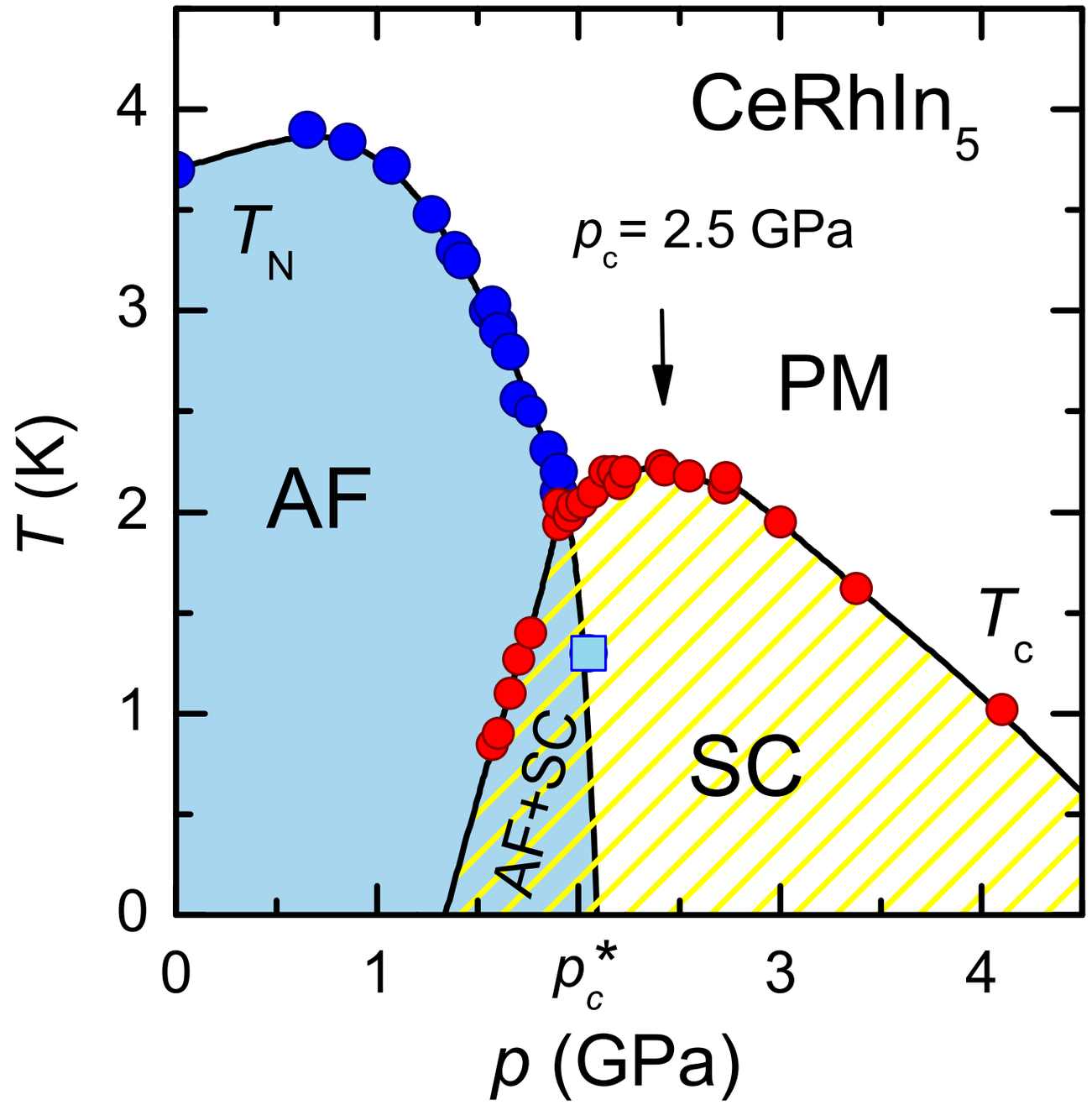

G. Knebel, D. Aoki, and J. Flouquet, arXiv:0911.5223.
Tuson Park, F. Ronning, H. Q. Yuan, M. B. Salamon, R. Movshovich, J. L. Sarrao, and J. D. Thompson, *Nature* **440**, 65 (2006)

Fermi surface

Metal with "large" Fermi surface

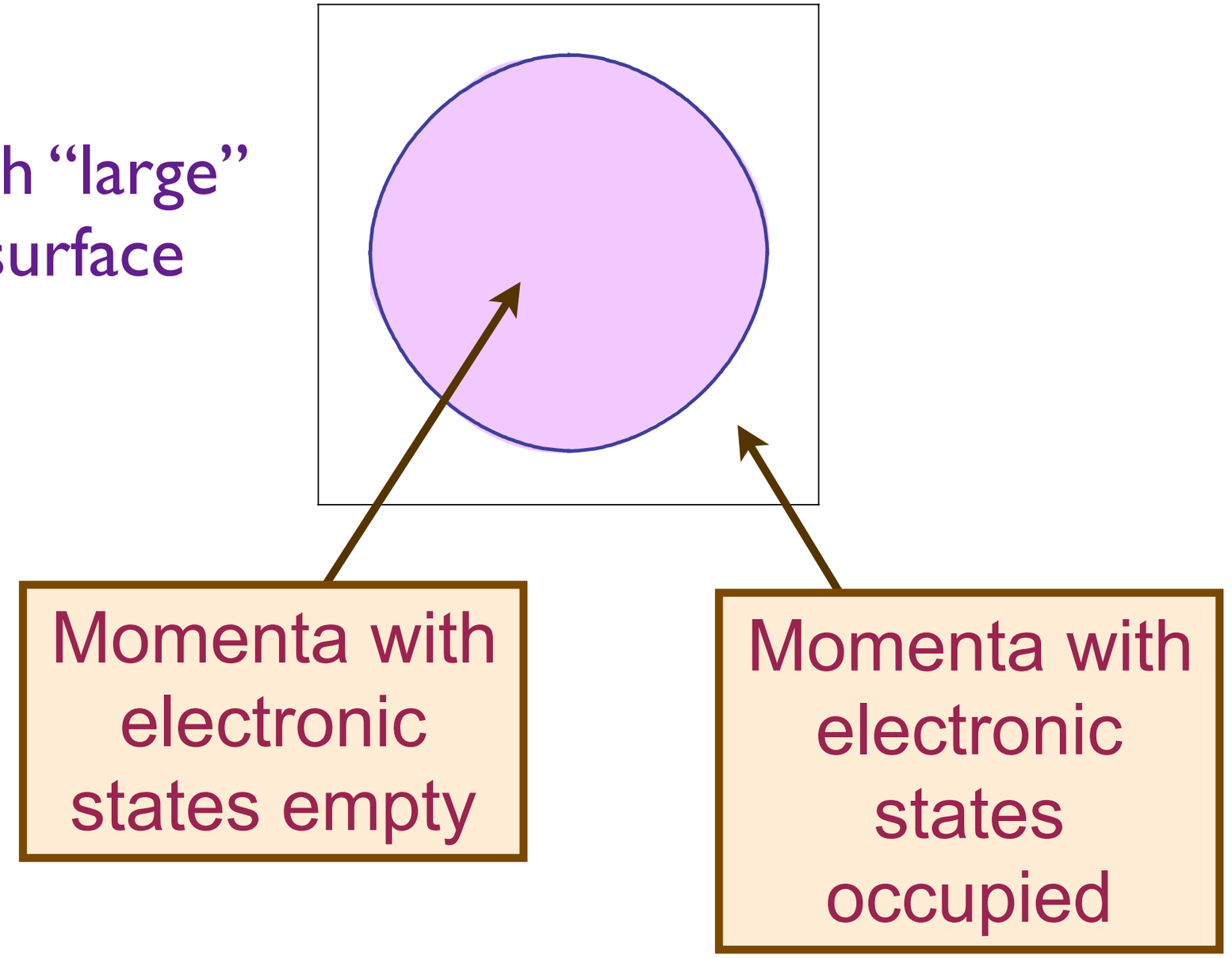

Fermi surface+antiferromagnetism

Metal with "large" Fermi surface

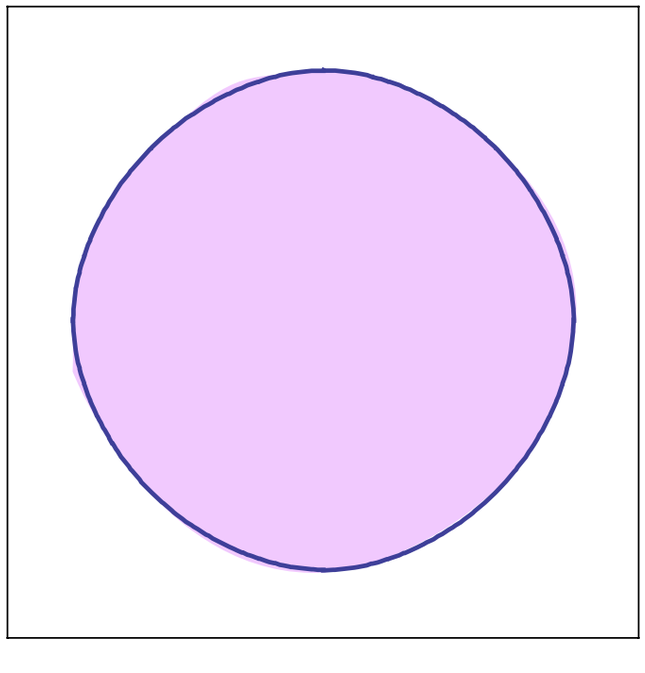

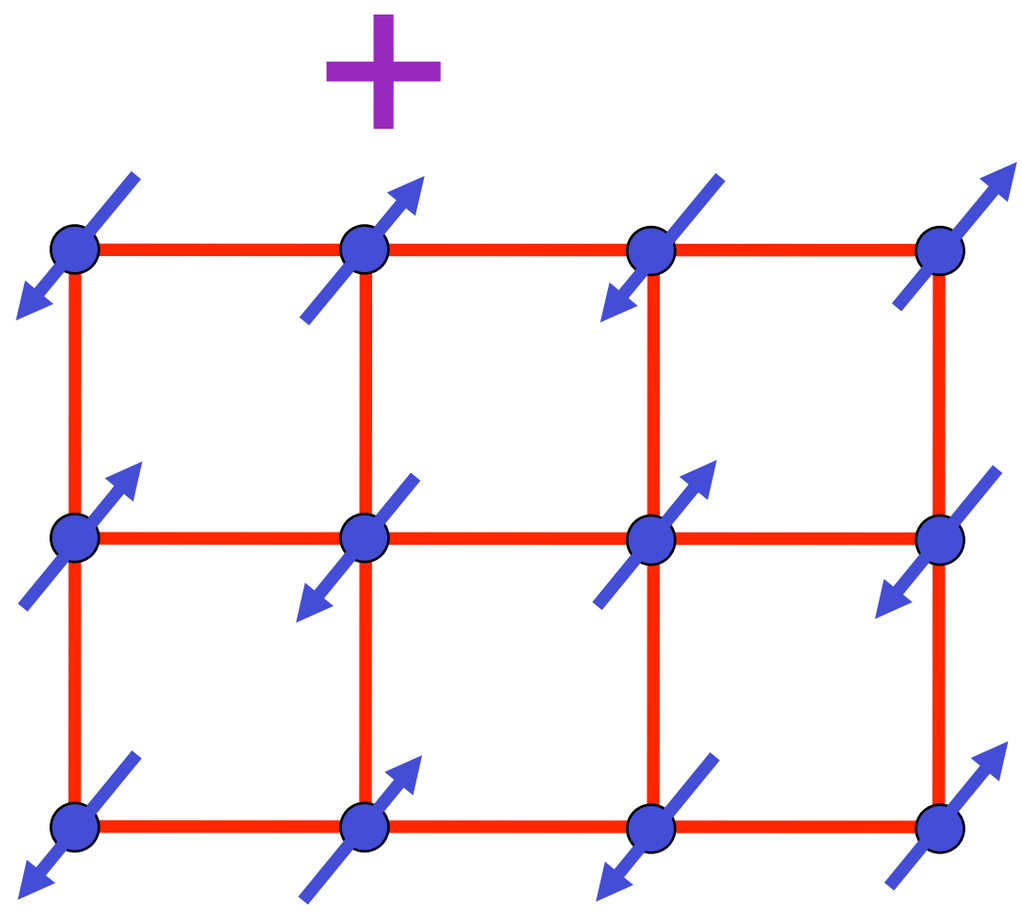

The electron spin polarization obeys

$$\left\langle \vec{S}(\mathbf{r},\tau) \right\rangle = \vec{\varphi}(\mathbf{r},\tau) e^{i\mathbf{K}\cdot\mathbf{r}}$$

where $\mathbf{K}$ is the ordering wavevector.

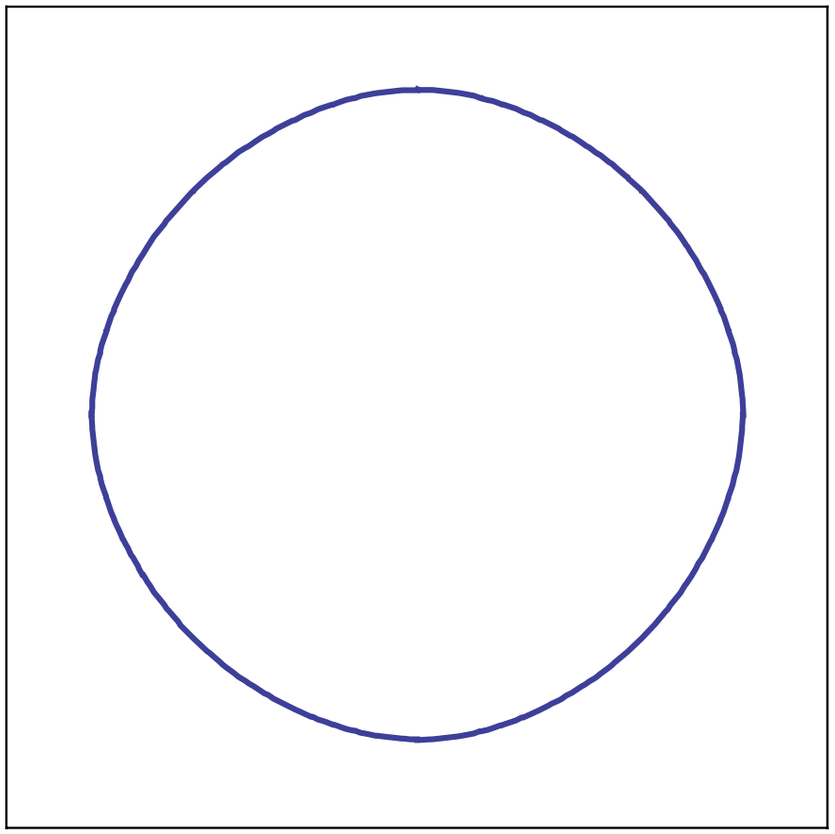

Metal with “large” Fermi surface

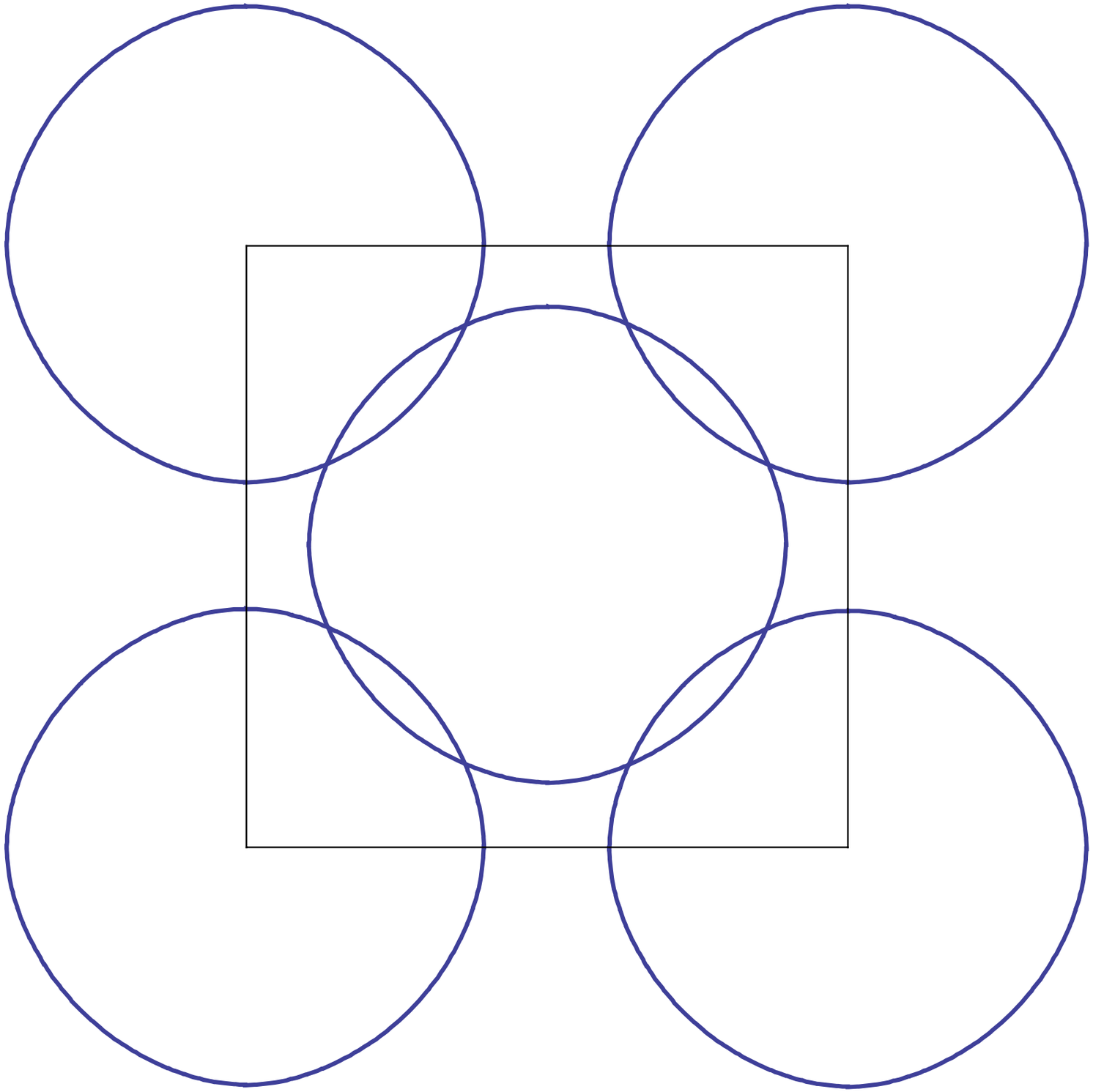

Fermi surfaces translated by $\mathbf{K} = (\pi, \pi)$.

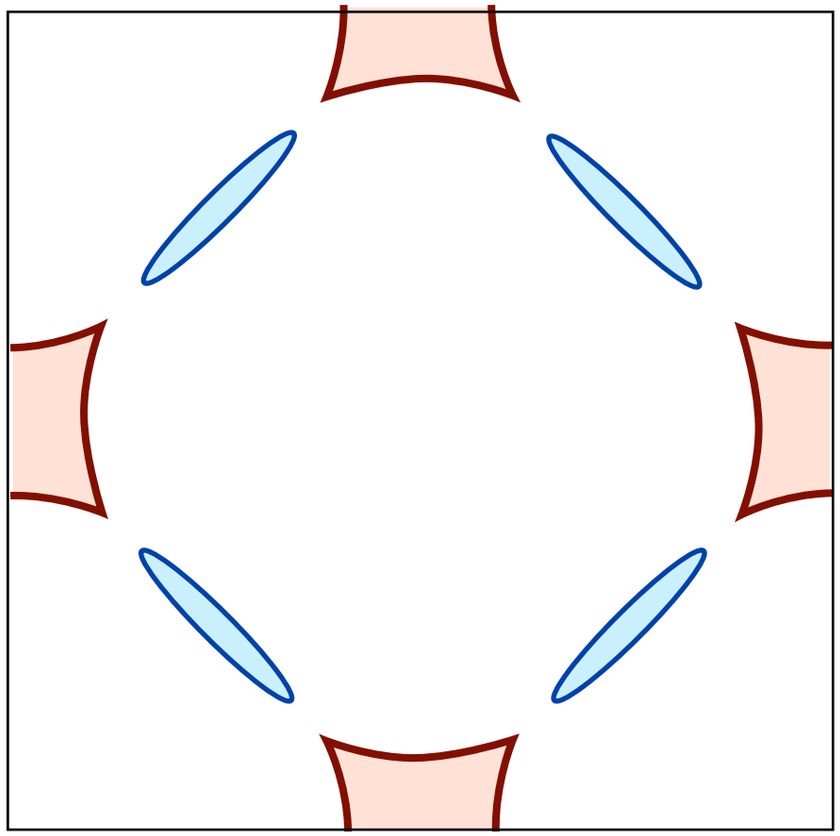

Electron and hole pockets in antiferromagnetic phase with $\langle \vec{\varphi} \rangle \neq 0$

Fermi surface+antiferromagnetism

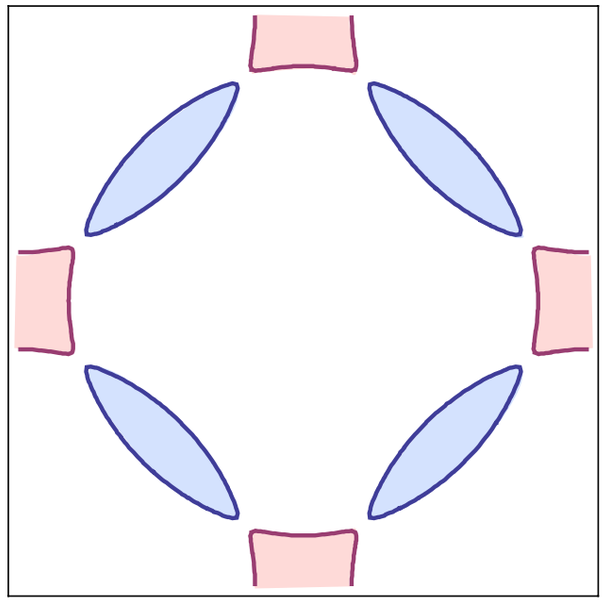

$\langle \vec{\varphi} \rangle \neq 0$

Metal with electron and hole pockets

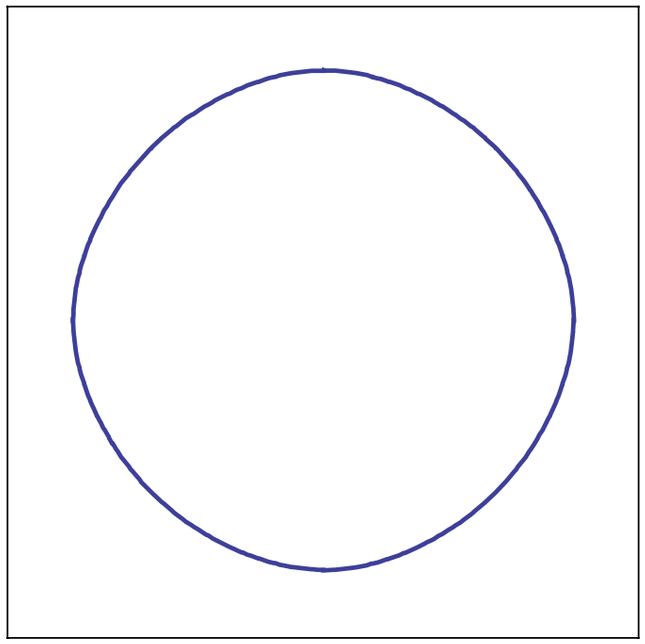

$\langle \vec{\varphi} \rangle = 0$

Metal with "large" Fermi surface

Increasing interaction

S. Sachdev, A.V. Chubukov, and A. Sokol, *Phys. Rev. B* **51**, 14874 (1995).
A.V. Chubukov and D. K. Morr, *Physics Reports* **288**, 355 (1997).

Quantum oscillations

$Nd_{2-x}Ce_xCuO_4$

T. Helm, M.V. Kartsovnik,
M. Bartkowiak, N. Bittner,
M. Lambacher, A. Erb, J. Wosnitza,
and R. Gross,
Phys. Rev. Lett. **103**, 157002 (2009).

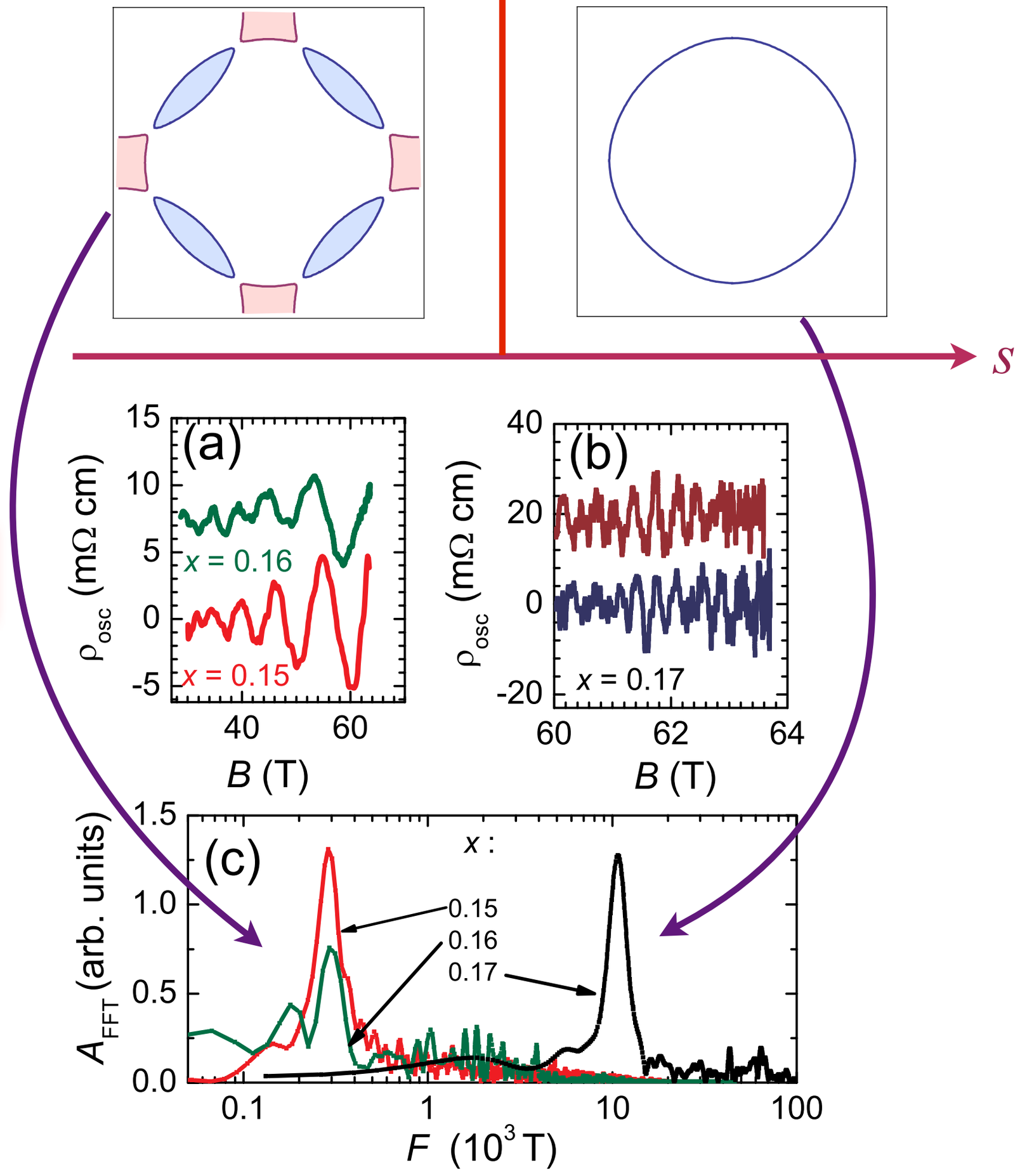

Photoemission in $Nd_{2-x}Ce_xCuO_4$

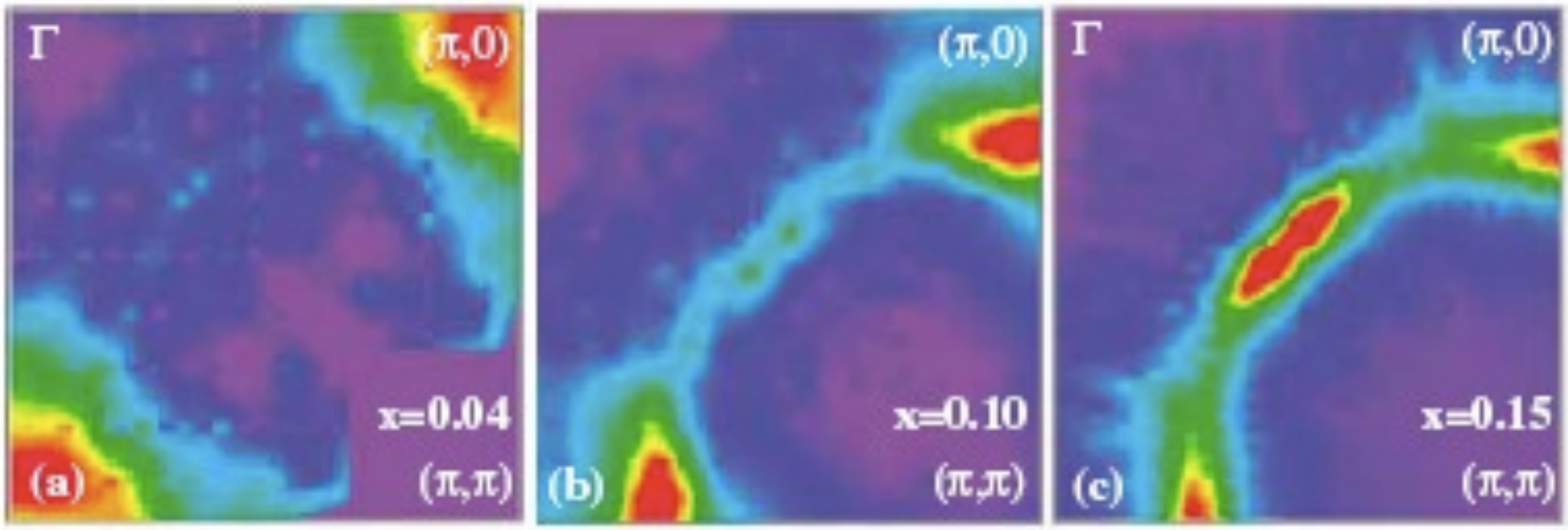

N. P. Armitage *et al.*, Phys. Rev. Lett. **88**, 257001 (2002).

Fermi surface+antiferromagnetism

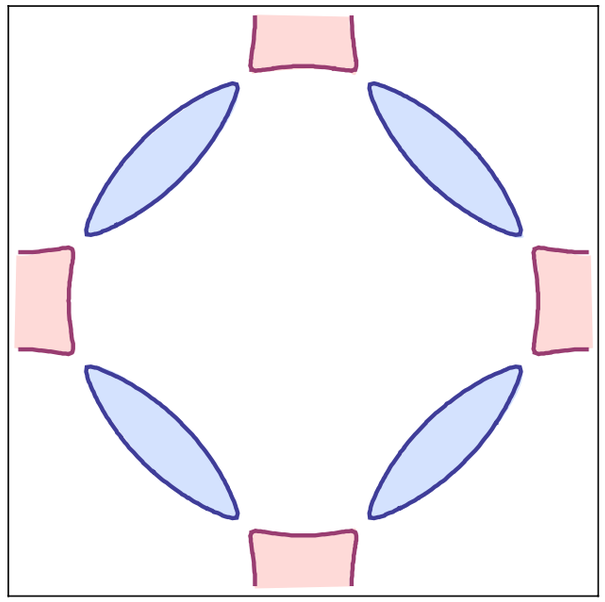

$\langle \vec{\varphi} \rangle \neq 0$

Metal with electron and hole pockets

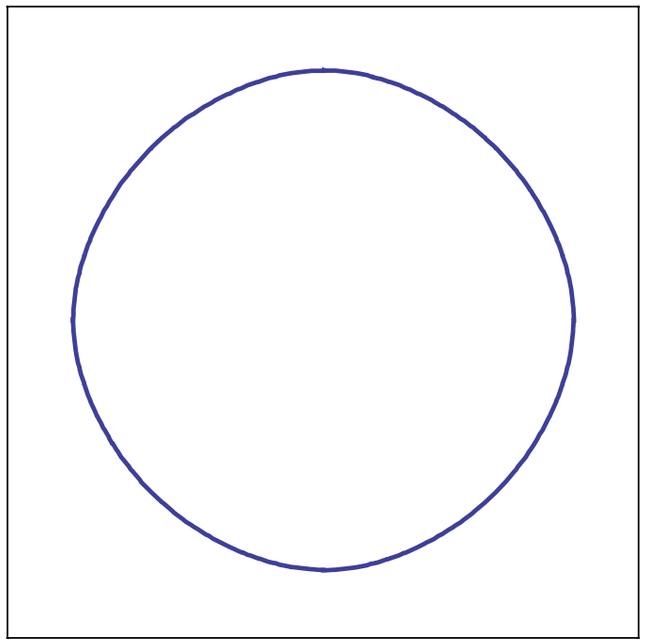

$\langle \vec{\varphi} \rangle = 0$

Metal with "large" Fermi surface

s

S. Sachdev, A.V. Chubukov, and A. Sokol, *Phys. Rev. B* **51**, 14874 (1995).
A.V. Chubukov and D. K. Morr, *Physics Reports* **288**, 355 (1997).

Spin-fermion model: Electrons with dispersion $\varepsilon_{\mathbf{k}}$ interacting with fluctuations of the antiferromagnetic order parameter $\vec{\varphi}$.

$$\mathcal{Z} = \int \mathcal{D}c_\alpha \mathcal{D}\vec{\varphi} \exp\left(-\mathcal{S}\right)$$

$$\mathcal{S} = \int d\tau \sum_{\mathbf{k}} c^\dagger_{\mathbf{k}\alpha} \left(\frac{\partial}{\partial \tau} - \varepsilon_{\mathbf{k}} \right) c_{\mathbf{k}\alpha}$$

$$+ \int d\tau d^2 r \left[\frac{1}{2} \left(\boldsymbol{\nabla}_r \vec{\varphi} \right)^2 + \frac{s}{2} \vec{\varphi}^2 + \ldots \right]$$

$$- \lambda \int d\tau \sum_i \vec{\varphi}_i \cdot (-1)^{\mathbf{r}_i} c^\dagger_{i\alpha} \vec{\sigma}_{\alpha\beta} c_{i\beta}$$

Coupling between fermions and antiferromagnetic order: $\lambda^2 \sim U$, the Hubbard repulsion

A technical aside.....

Hertz-Moriya-Millis theory

Integrate out fermions and obtain an effective action for the boson field $\vec{\varphi}$ alone. Because the fermions are gapless, this is potentially dangerous, and will lead to non-local terms in the $\vec{\varphi}$ effective action. Hertz focused on only the simplest such non-local term. However, there are an infinite number of non-local terms at higher order, and these lead to a breakdown of the Hertz theory in $d = 2$.

Ar. Abanov and A.V. Chubukov, *Phys. Rev. Lett.* **93**, 255702 (2004).

A technical aside.....

We need to perform an RG analysis on a local theory of both the fermions and the $\vec{\varphi}$. It appears that such a theory can be analyzed using a $1/N$ expansion, where N is the number of fermion flavors. At two-loop order, the $1/N$ expansion is well-behaved, and we can determine consistent RG flow equations. However, at higher loops we find corrections to the renormalizations which require summation of all planar graphs even at the leading order in $1/N$, and the $1/N$ expansion appears to be organized as a genus expansion of random surfaces. But even this genus expansion breaks down in the renormalization of a quartic coupling of $\vec{\varphi}$. In the following, I will describe some of the two loop results.

M. A. Metlitski and S. Sachdev, *Phys. Rev. B* **85**, 075127 (2010)

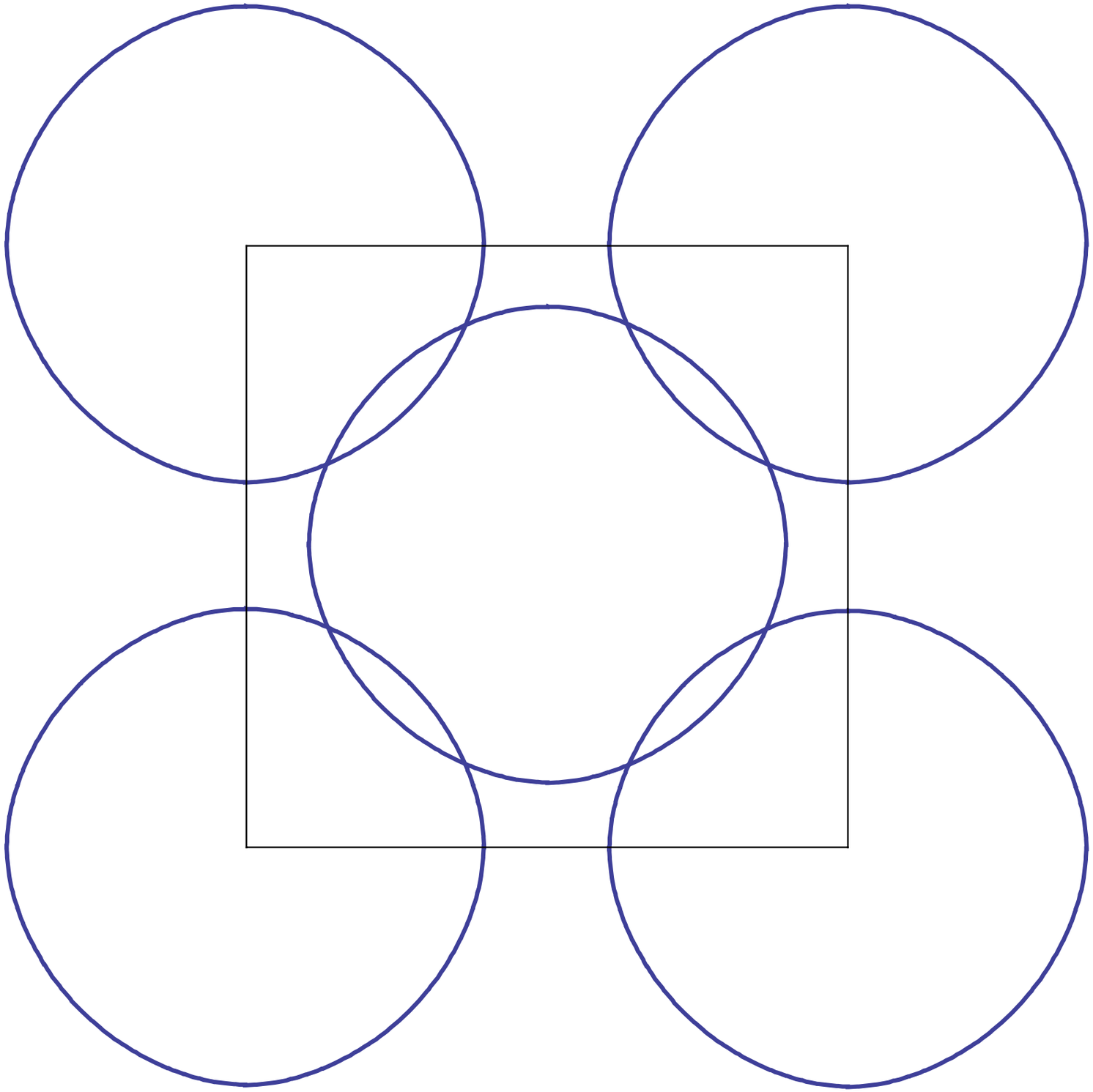

Fermi surfaces translated by $\mathbf{K} = (\pi, \pi)$.

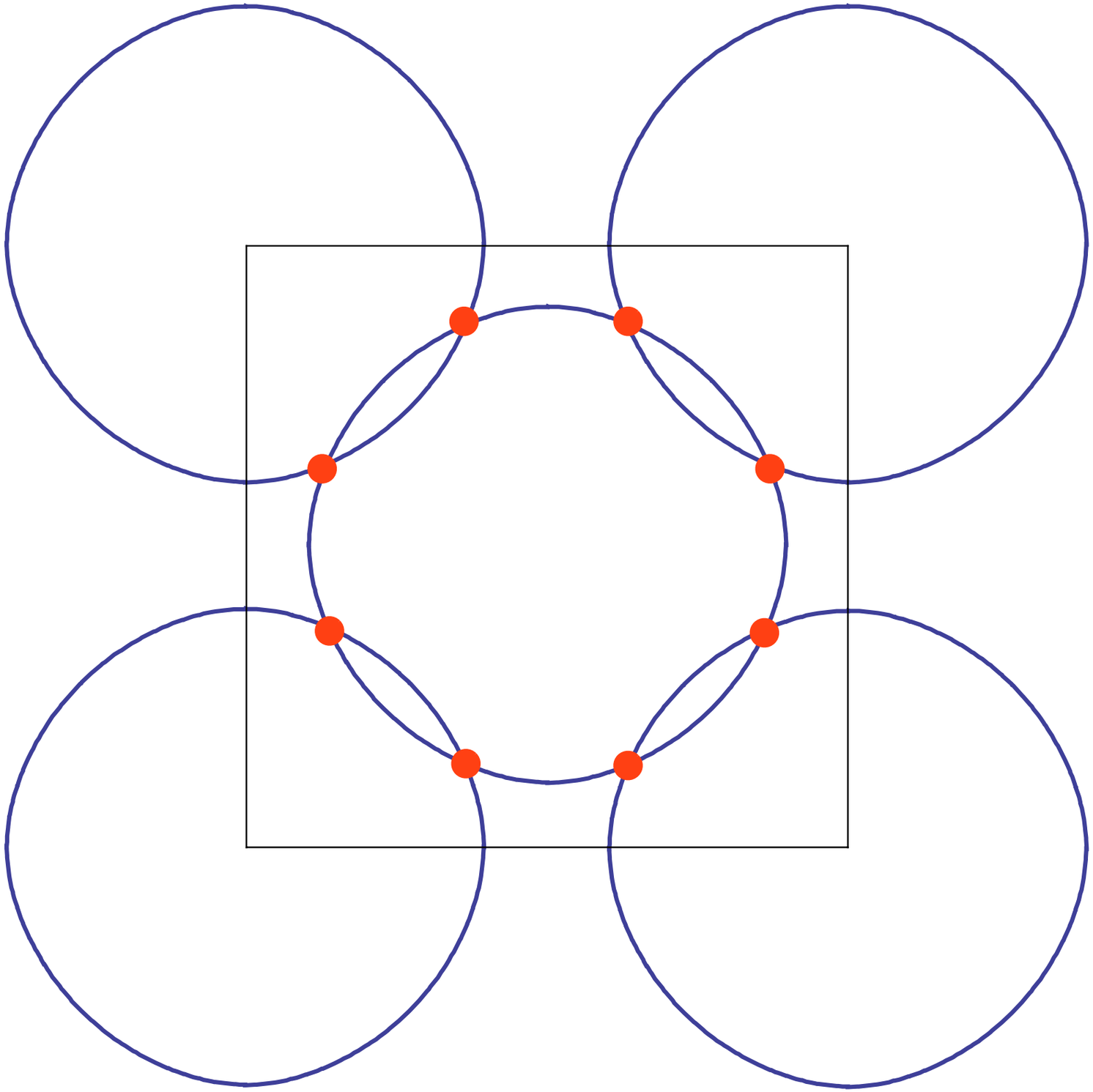

“Hot” spots

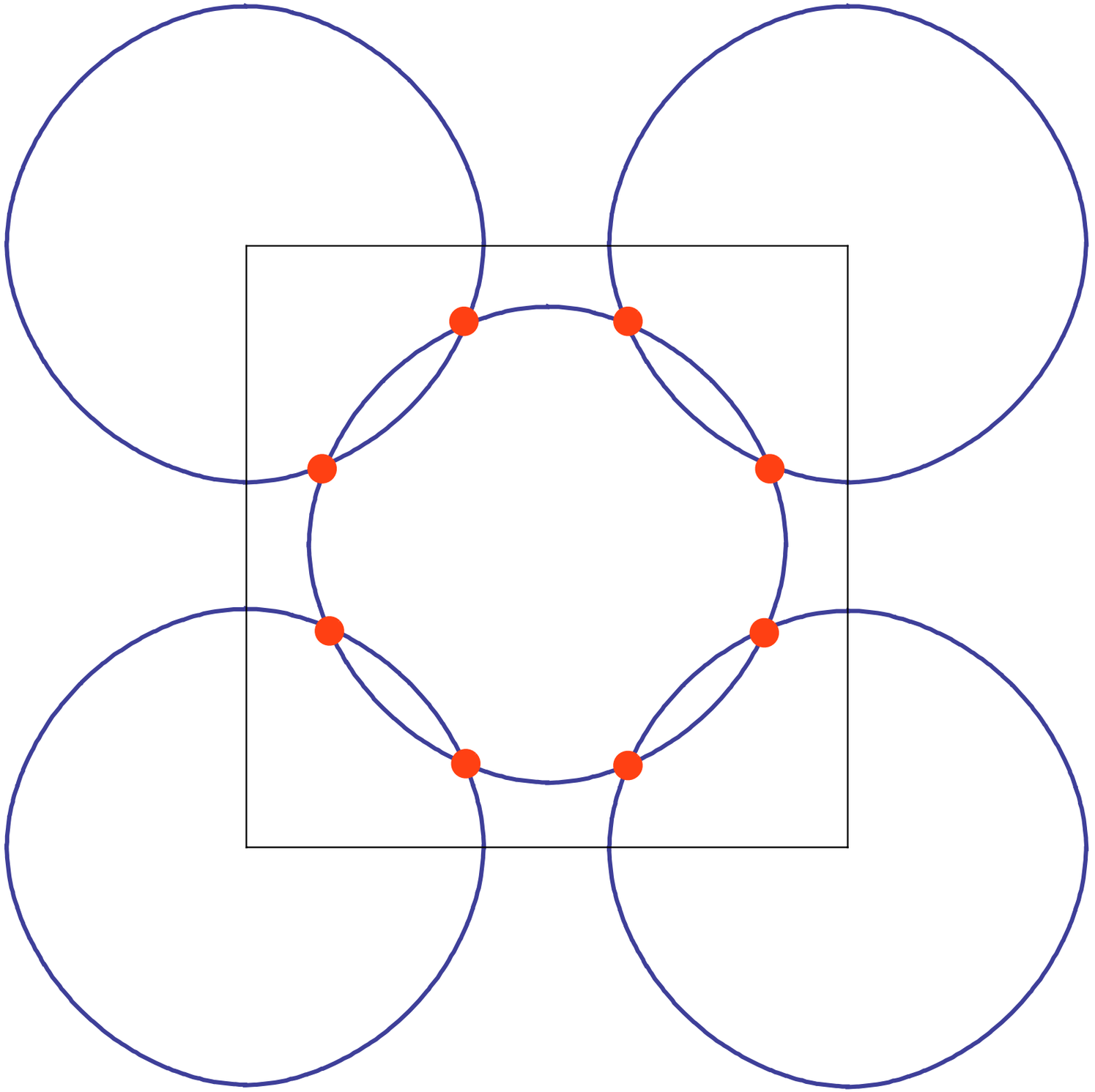

Low energy theory for critical point near hot spots

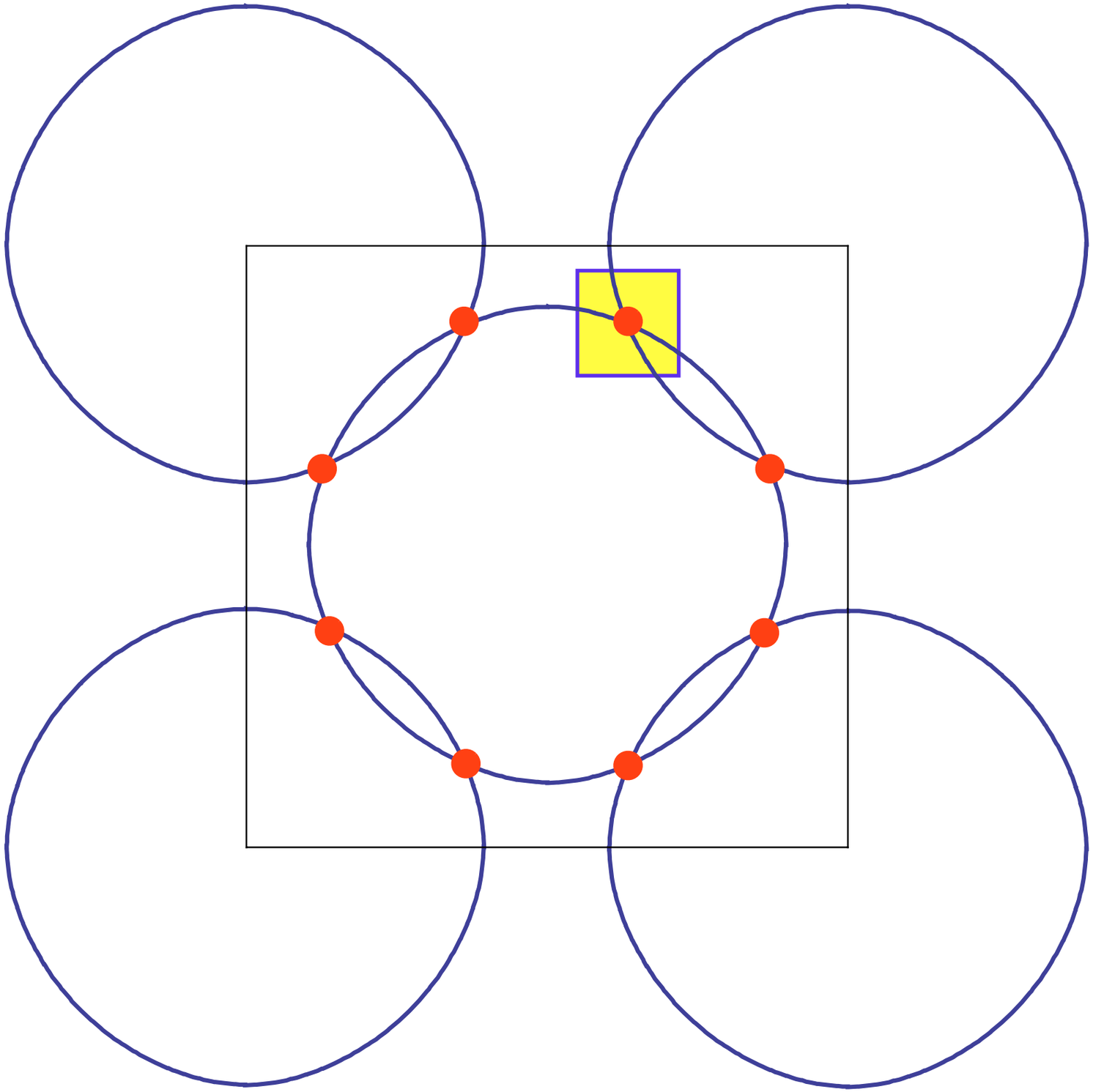

Low energy theory for critical point near hot spots

Theory has fermions $\psi_{1,2}$ (with Fermi velocities $\mathbf{v}_{1,2}$)
and boson order parameter $\vec{\varphi}$,
interacting with coupling λ

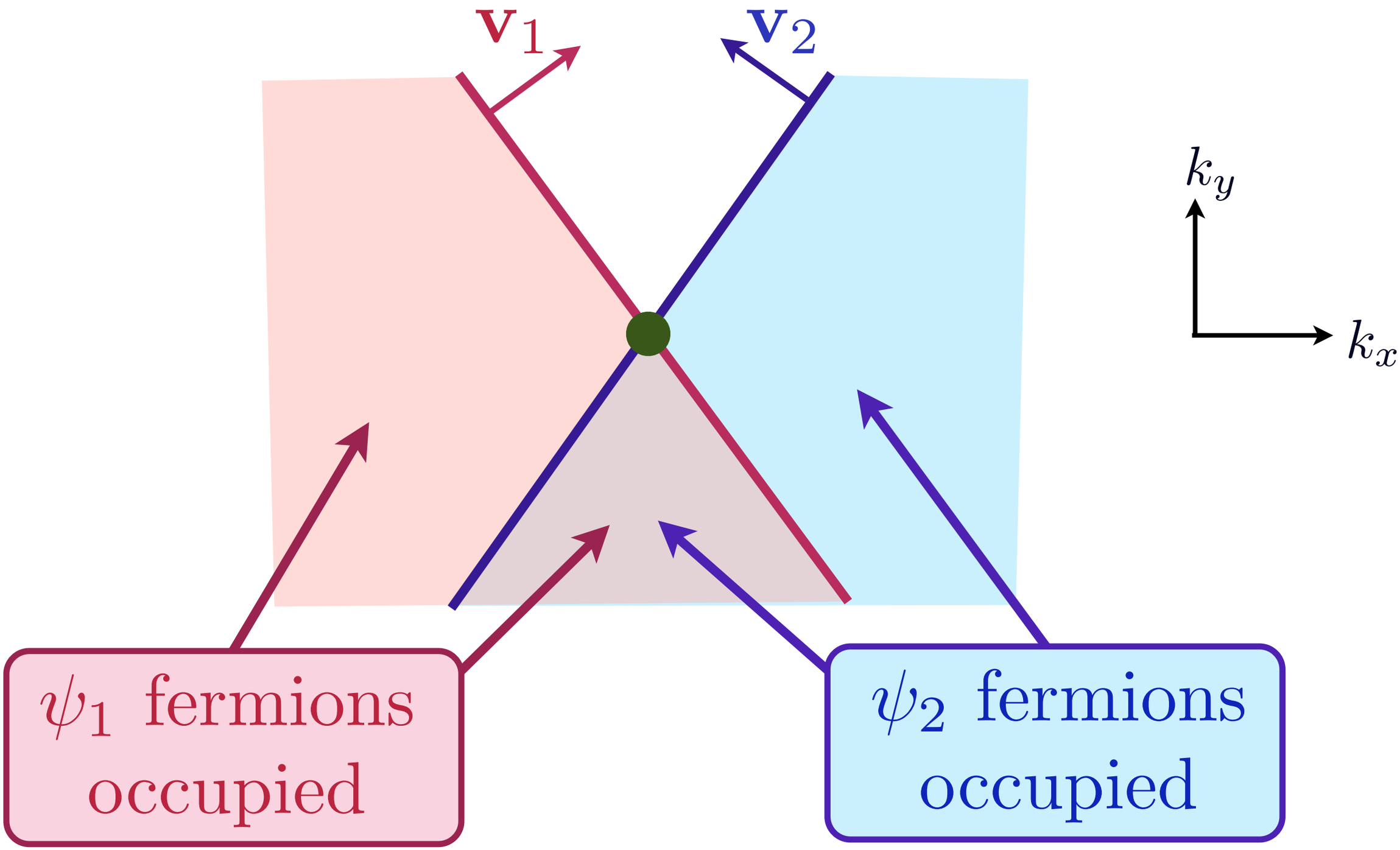

$$\mathcal{L}_f \quad = \quad \psi_{1\alpha}^{\ell\dagger}\left(\zeta\partial_\tau - i\mathbf{v}_1^\ell\cdot\boldsymbol{\nabla}_r\right)\psi_{1\alpha}^\ell + \psi_{2\alpha}^{\ell\dagger}\left(\zeta\partial_\tau - i\mathbf{v}_2^\ell\cdot\boldsymbol{\nabla}_r\right)\psi_{2\alpha}^\ell$$

Order parameter: $\mathcal{L}_\varphi = \frac{1}{2}\left(\boldsymbol{\nabla}_r\vec{\varphi}\right)^2 + \frac{\widetilde{\zeta}}{2}\left(\partial_\tau\vec{\varphi}\right)^2 + \frac{s}{2}\vec{\varphi}^2 + \frac{u}{4}\vec{\varphi}^4$

"Yukawa" coupling: $\mathcal{L}_c = -\lambda\vec{\varphi}\cdot\left(\psi_{1\alpha}^{\ell\dagger}\vec{\sigma}_{\alpha\beta}\psi_{2\beta}^\ell + \psi_{2\alpha}^{\ell\dagger}\vec{\sigma}_{\alpha\beta}\psi_{1\beta}^\ell\right)$

Ar. Abanov and A.V. Chubukov, *Phys. Rev. Lett.* **93**, 255702 (2004).

Theory has fermions $\psi_{1,2}$ (with Fermi velocities $\mathbf{v}_{1,2}$)
and boson order parameter $\vec{\varphi}$,
interacting with coupling λ

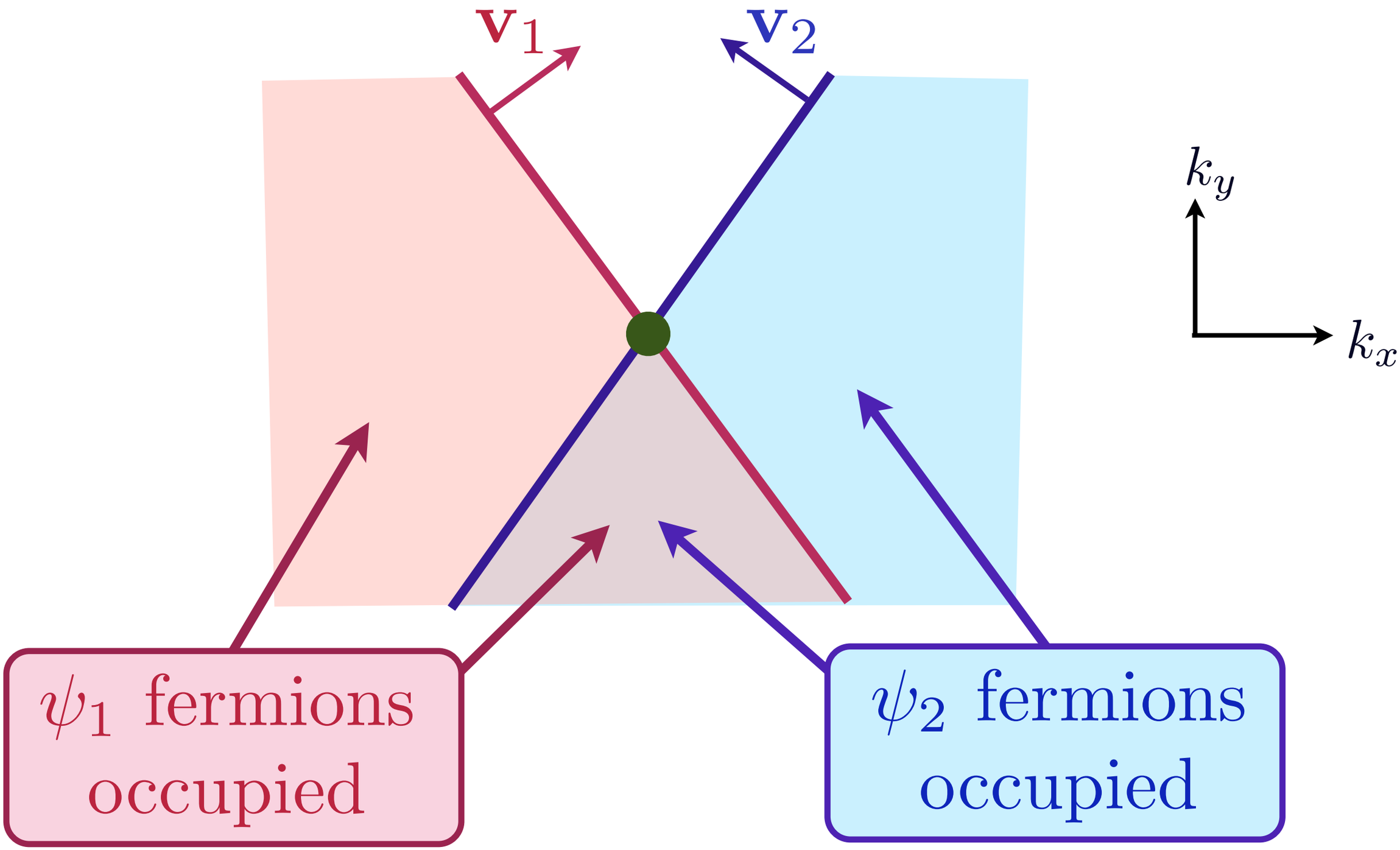

Critical point theory is strongly coupled in $d = 2$
Results are *independent* of coupling λ

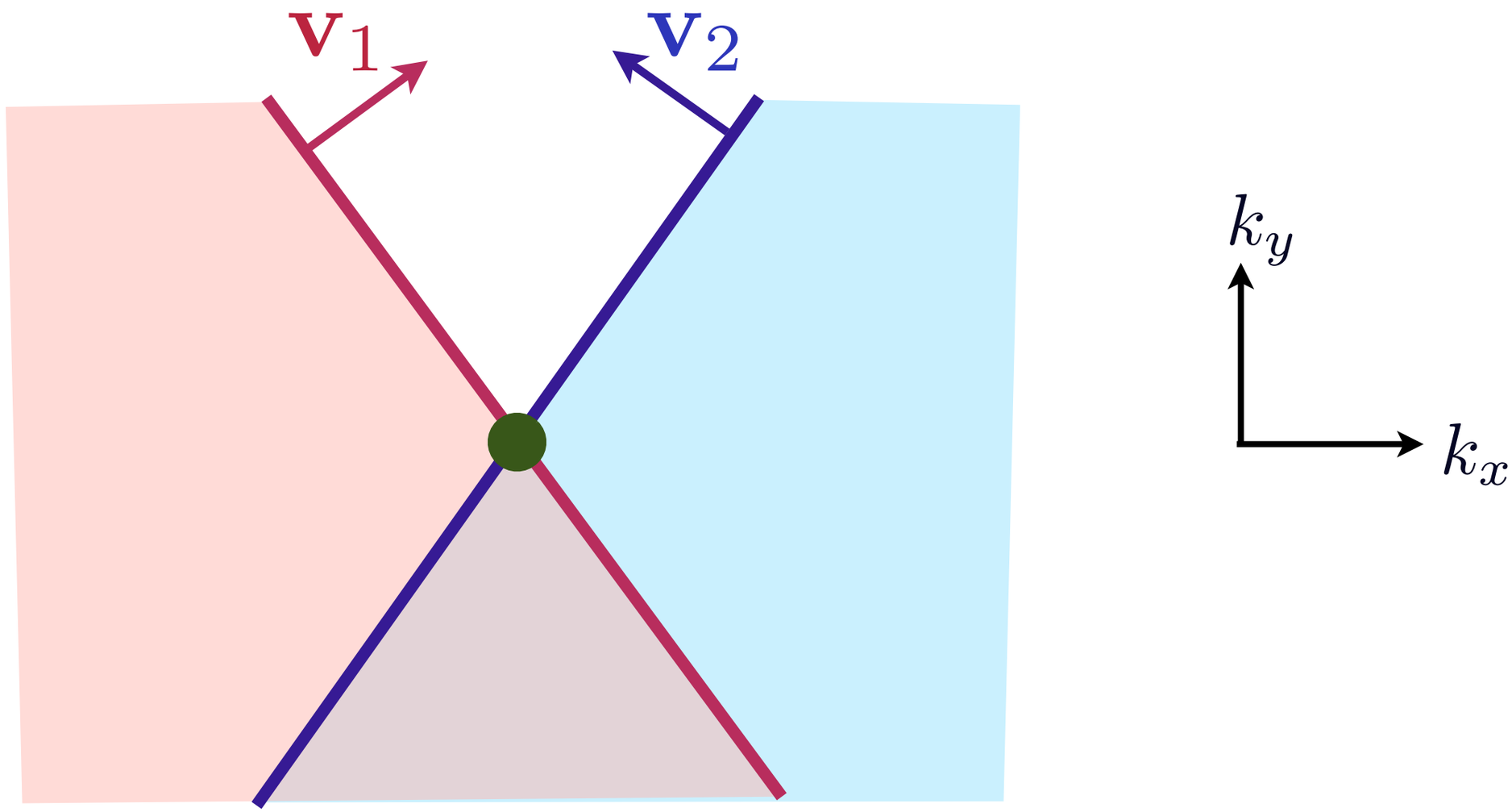

M. A. Metlitski and S. Sachdev, *Phys. Rev. B* **85**, 075127 (2010)

Critical point theory is strongly coupled in $d = 2$
Results are *independent* of coupling λ

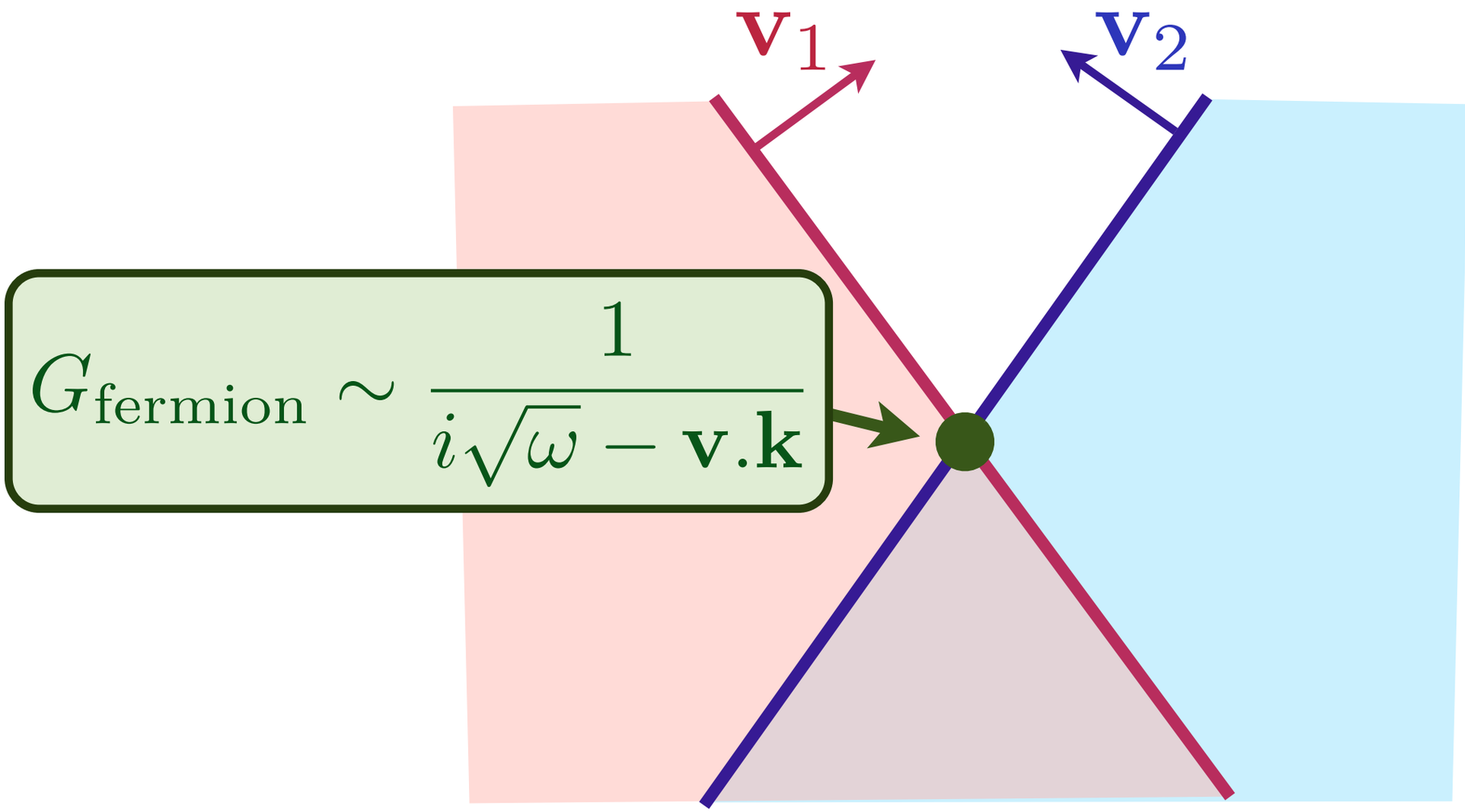

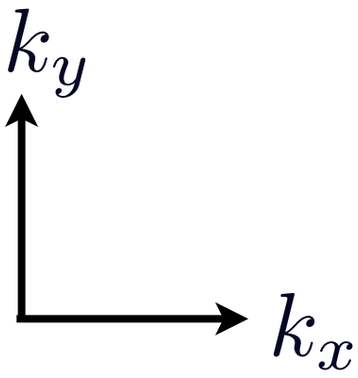

A. J. Millis, *Phys. Rev. B* **45**, 13047 (1992)

Ar. Abanov and A.V. Chubukov, *Phys. Rev. Lett.* **93**, 255702 (2004)

Critical point theory is strongly coupled in $d = 2$
Results are *independent* of coupling λ

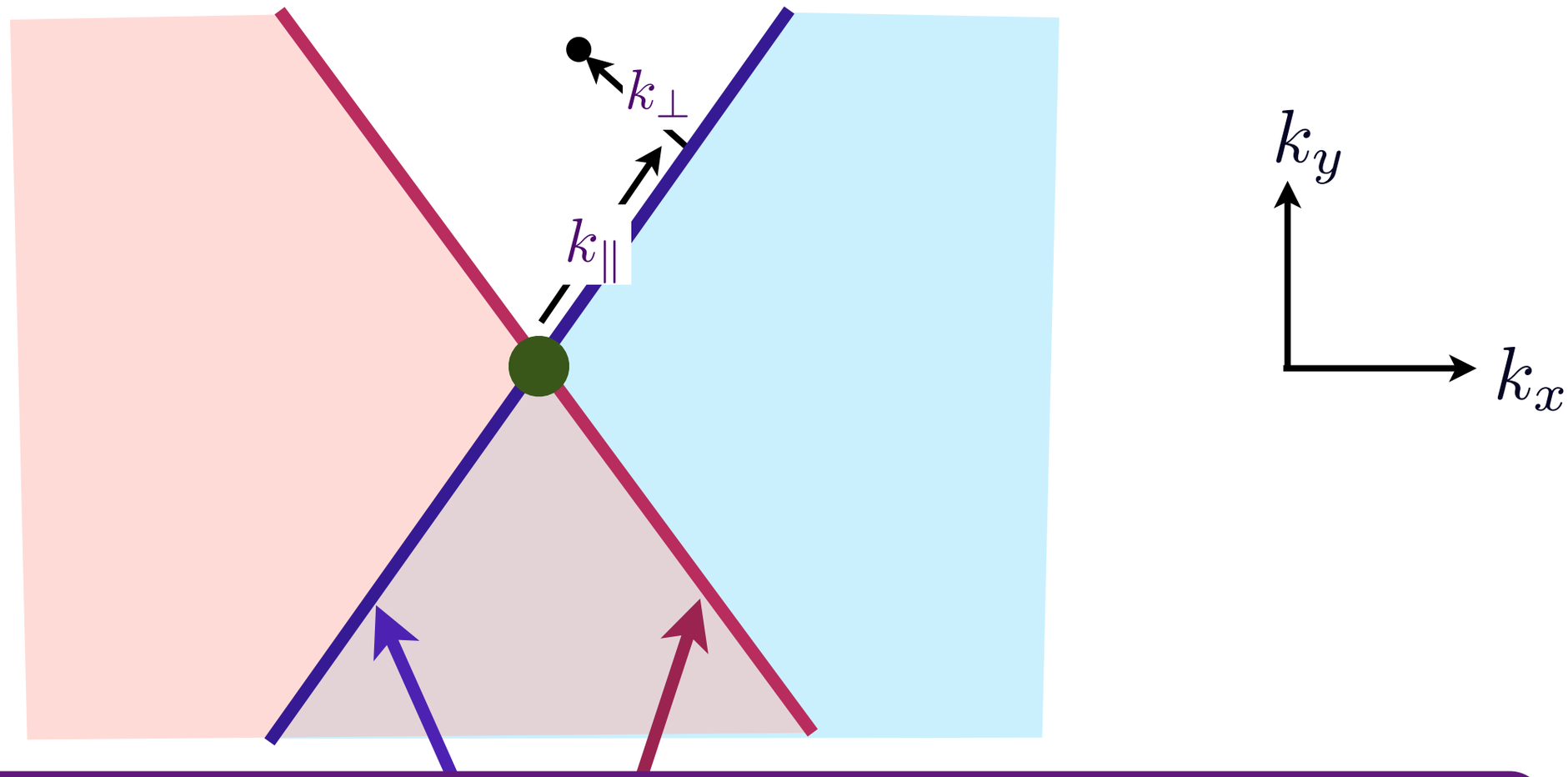

$$G_{\rm fermion} = \frac{Z(k_\parallel)}{i\omega - v_F(k_\parallel)k_\perp}, \qquad Z(k_\parallel) \sim v_F(k_\parallel) \sim k_\parallel$$

M. A. Metlitski and S. Sachdev, *Phys. Rev. B* **85**, 075127 (2010)

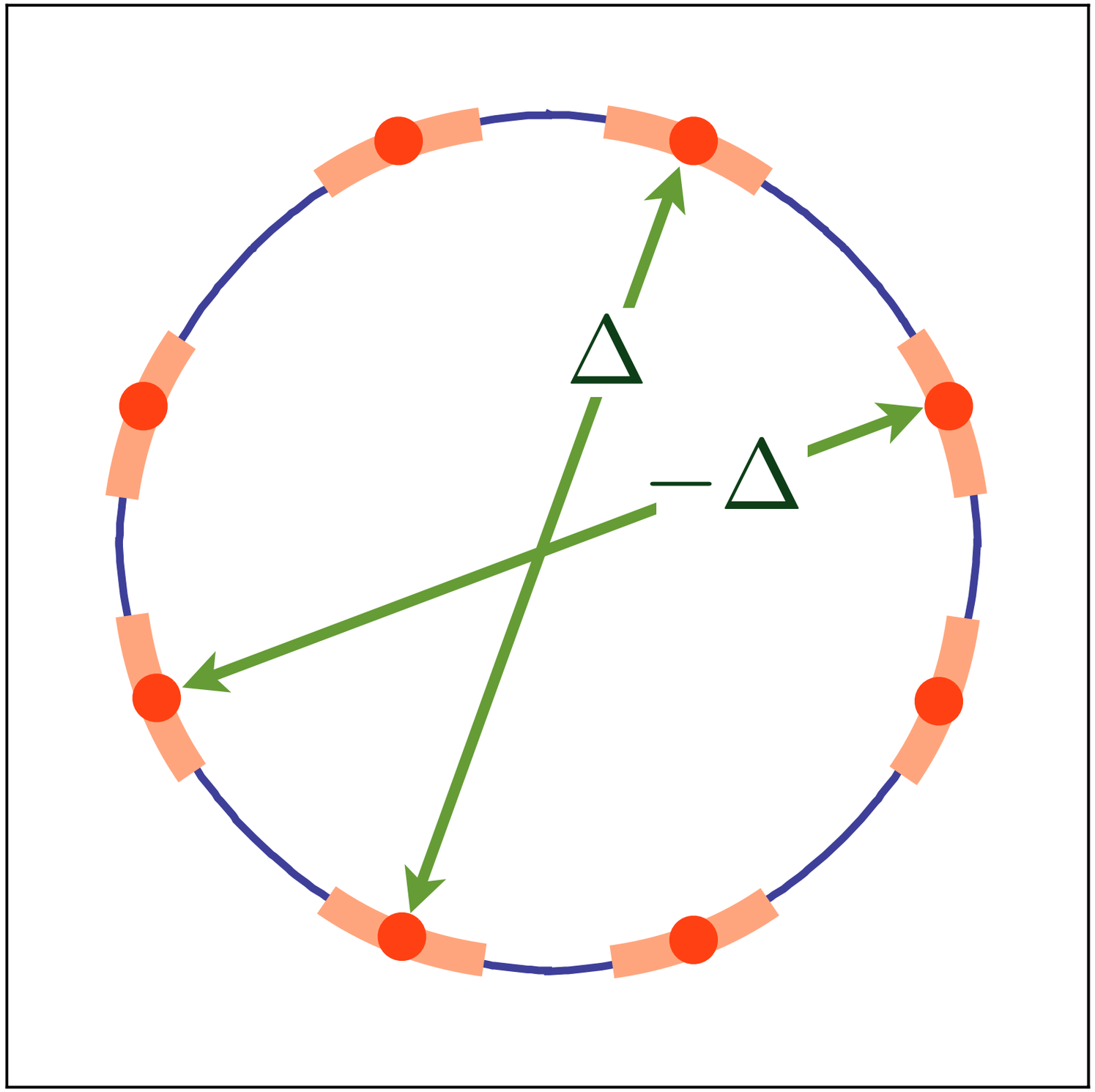

Unconventional pairing at *and near* hot spots

$$\left\langle c^{\dagger}_{\mathbf{k}\alpha} c^{\dagger}_{-\mathbf{k}\beta} \right\rangle = \varepsilon_{\alpha\beta}\Delta(\cos k_x - \cos k_y)$$

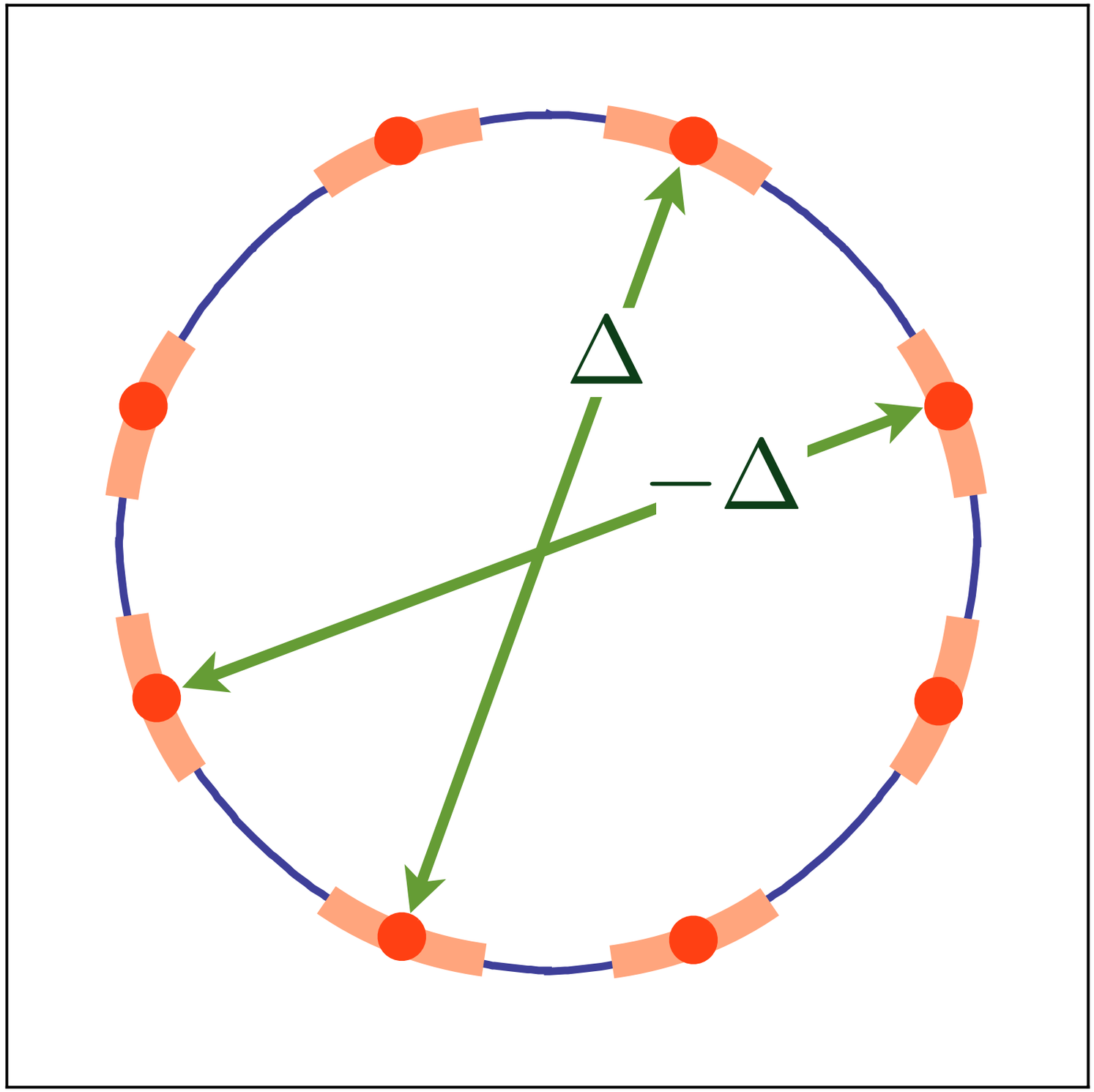

Unconventional pairing at *and near* hot spots

BCS theory

$$1 + \lambda_{\text{e-ph}} \underbrace{\log\left(\frac{\omega_D}{\omega}\right)}_{\text{Cooper logarithm}}$$

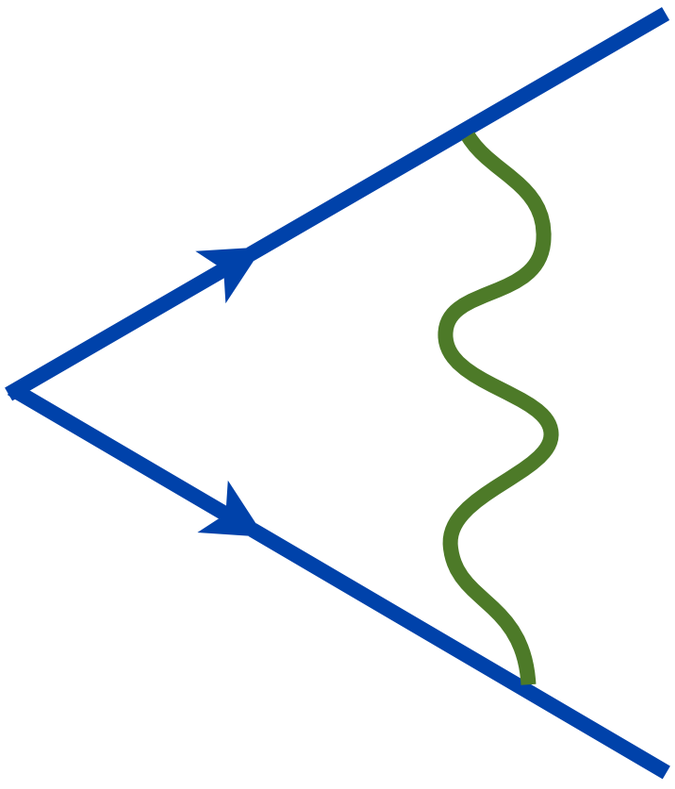

BCS theory

$$1 + \lambda_{\text{e-ph}} \log\left(\frac{\omega_D}{\omega}\right)$$

Electron-phonon coupling

BCS theory

$$1 + \lambda_{\text{e-ph}} \log\left(\frac{\omega_D}{\omega}\right)$$

Electron-phonon coupling

Debye frequency

BCS theory

$$1 + \lambda_{\text{e-ph}} \log\left(\frac{\omega_D}{\omega}\right)$$

Electron-phonon coupling

Debye frequency

Implies

$$T_c \sim \omega_D \exp\left(-1/\lambda\right)$$

Enhancement of pairing susceptibility by interactions

Antiferromagnetic fluctuations: weak-coupling

$$1 + \left(\frac{U}{t}\right)^2 \underbrace{\log\left(\frac{E_F}{\omega}\right)}$$

Cooper logarithm

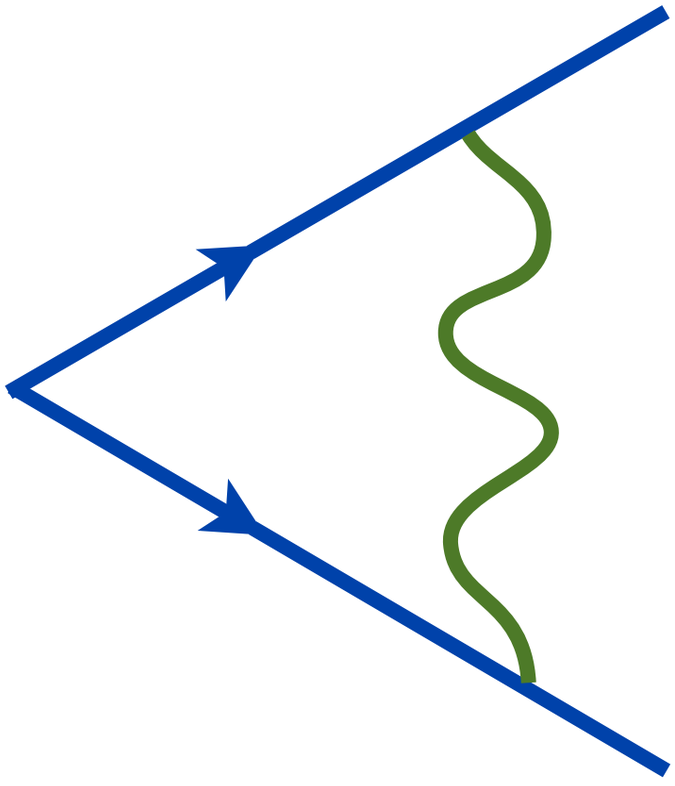

V. J. Emery, *J. Phys. (Paris) Colloq.* **44**, C3-977 (1983)
D.J. Scalapino, E. Loh, and J.E. Hirsch, *Phys. Rev. B* **34**, 8190 (1986)
K. Miyake, S. Schmitt-Rink, and C. M. Varma, *Phys. Rev. B* **34**, 6554 (1986)
S. Raghu, S.A. Kivelson, and D.J. Scalapino, *Phys. Rev. B* **81**, 224505 (2010)

Enhancement of pairing susceptibility by interactions

Antiferromagnetic fluctuations: weak-coupling

$$1 + \left(\frac{U}{t}\right)^2 \log\left(\frac{E_F}{\omega}\right)$$

Fermi energy

V. J. Emery, *J. Phys. (Paris) Colloq.* **44**, C3-977 (1983)
D.J. Scalapino, E. Loh, and J.E. Hirsch, *Phys. Rev. B* **34**, 8190 (1986)
K. Miyake, S. Schmitt-Rink, and C. M. Varma, *Phys. Rev. B* **34**, 6554 (1986)
S. Raghu, S.A. Kivelson, and D.J. Scalapino, *Phys. Rev. B* **81**, 224505 (2010)

Enhancement of pairing susceptibility by interactions

Antiferromagnetic fluctuations: weak-coupling

$$1 + \left(\frac{U}{t}\right)^2 \log\left(\frac{E_F}{\omega}\right)$$

Applies in a Fermi liquid as repulsive interaction $U \to 0$.

Fermi energy

V. J. Emery, *J. Phys. (Paris) Colloq.* **44**, C3-977 (1983)
D.J. Scalapino, E. Loh, and J.E. Hirsch, *Phys. Rev. B* **34**, 8190 (1986)
K. Miyake, S. Schmitt-Rink, and C. M. Varma, *Phys. Rev. B* **34**, 6554 (1986)
S. Raghu, S.A. Kivelson, and D.J. Scalapino, *Phys. Rev. B* **81**, 224505 (2010)

Enhancement of pairing susceptibility by interactions

Antiferromagnetic fluctuations: weak-coupling

$$1 + \left(\frac{U}{t}\right)^2 \log\left(\frac{E_F}{\omega}\right)$$

Applies in a Fermi liquid as repulsive interaction $U \to 0$.

Fermi energy

Implies

$$T_c \sim E_F \exp\left(-(t/U)^2\right)$$

V. J. Emery, *J. Phys. (Paris) Colloq.* **44**, C3-977 (1983)
D.J. Scalapino, E. Loh, and J.E. Hirsch, *Phys. Rev. B* **34**, 8190 (1986)
K. Miyake, S. Schmitt-Rink, and C. M. Varma, *Phys. Rev. B* **34**, 6554 (1986)
S. Raghu, S.A. Kivelson, and D.J. Scalapino, *Phys. Rev. B* **81**, 224505 (2010)

Enhancement of pairing susceptibility by interactions

Spin density wave quantum critical point

$$1 + \frac{\alpha}{\pi(1+\alpha^2)} \log^2\left(\frac{E_F}{\omega}\right)$$

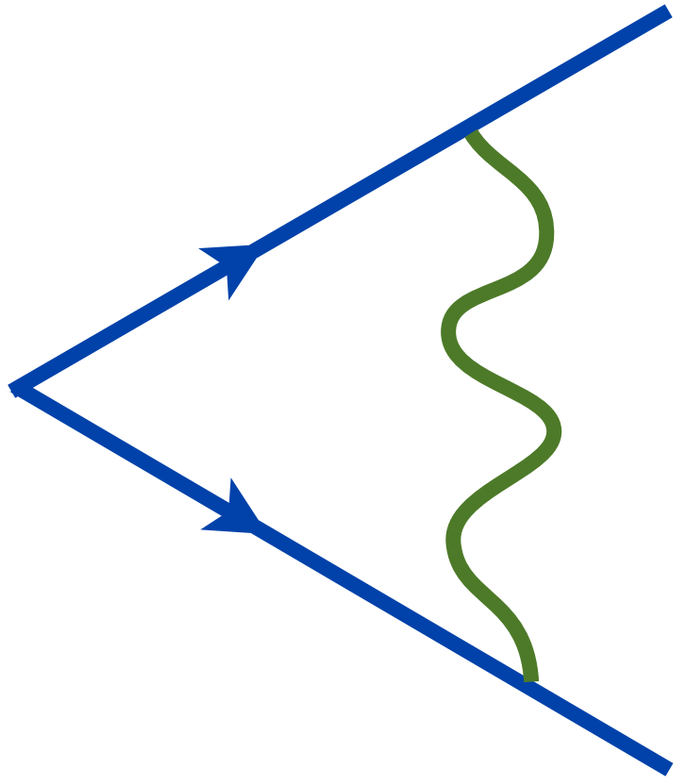

M. A. Metlitski and S. Sachdev, *Phys. Rev. B* **85**, 075127 (2010)

Enhancement of pairing susceptibility by interactions

Spin density wave quantum critical point

$$1 + \frac{\alpha}{\pi(1+\alpha^2)} \log^2\left(\frac{E_F}{\omega}\right)$$

M. A. Metlitski and S. Sachdev, *Phys. Rev. B* **85**, 075127 (2010)

Enhancement of pairing susceptibility by interactions

Spin density wave quantum critical point

$$1 + \frac{\alpha}{\pi(1+\alpha^2)} \log^2\left(\frac{E_F}{\omega}\right)$$

M. A. Metlitski and S. Sachdev, *Phys. Rev. B* **85**, 075127 (2010)

Enhancement of pairing susceptibility by interactions

Spin density wave quantum critical point

$$1 + \frac{\alpha}{\pi(1+\alpha^2)} \log^2\left(\frac{E_F}{\omega}\right)$$

Fermi energy

M. A. Metlitski and S. Sachdev, *Phys. Rev. B* **85**, 075127 (2010)

Enhancement of pairing susceptibility by interactions

Spin density wave quantum critical point

$$1 + \frac{\alpha}{\pi(1+\alpha^2)} \log^2\left(\frac{E_F}{\omega}\right)$$

Fermi energy

$\alpha = \tan\theta$, where 2θ is the angle between Fermi lines.

Independent of interaction strength U in 2 dimensions.

(see also Ar. Abanov, A.V. Chubukov, and A. M. Finkel'stein, *Europhys. Lett.* **54**, 488 (2001))
M. A. Metlitski and S. Sachdev, *Phys. Rev. B* **85**, 075127 (2010)

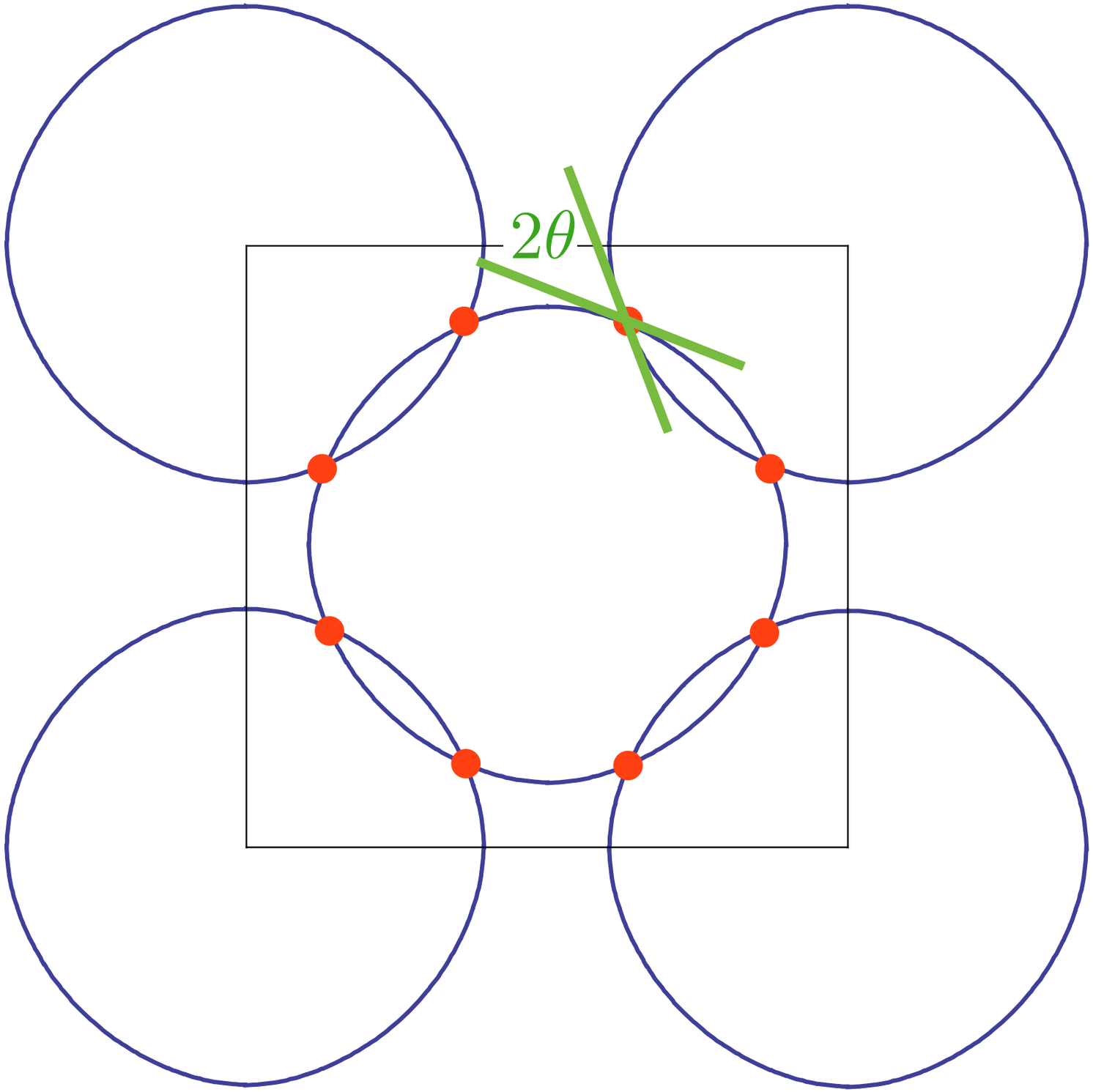
2θ

M. A. Metlitski and S. Sachdev, *Phys. Rev. B* **85**, 075127 (2010)

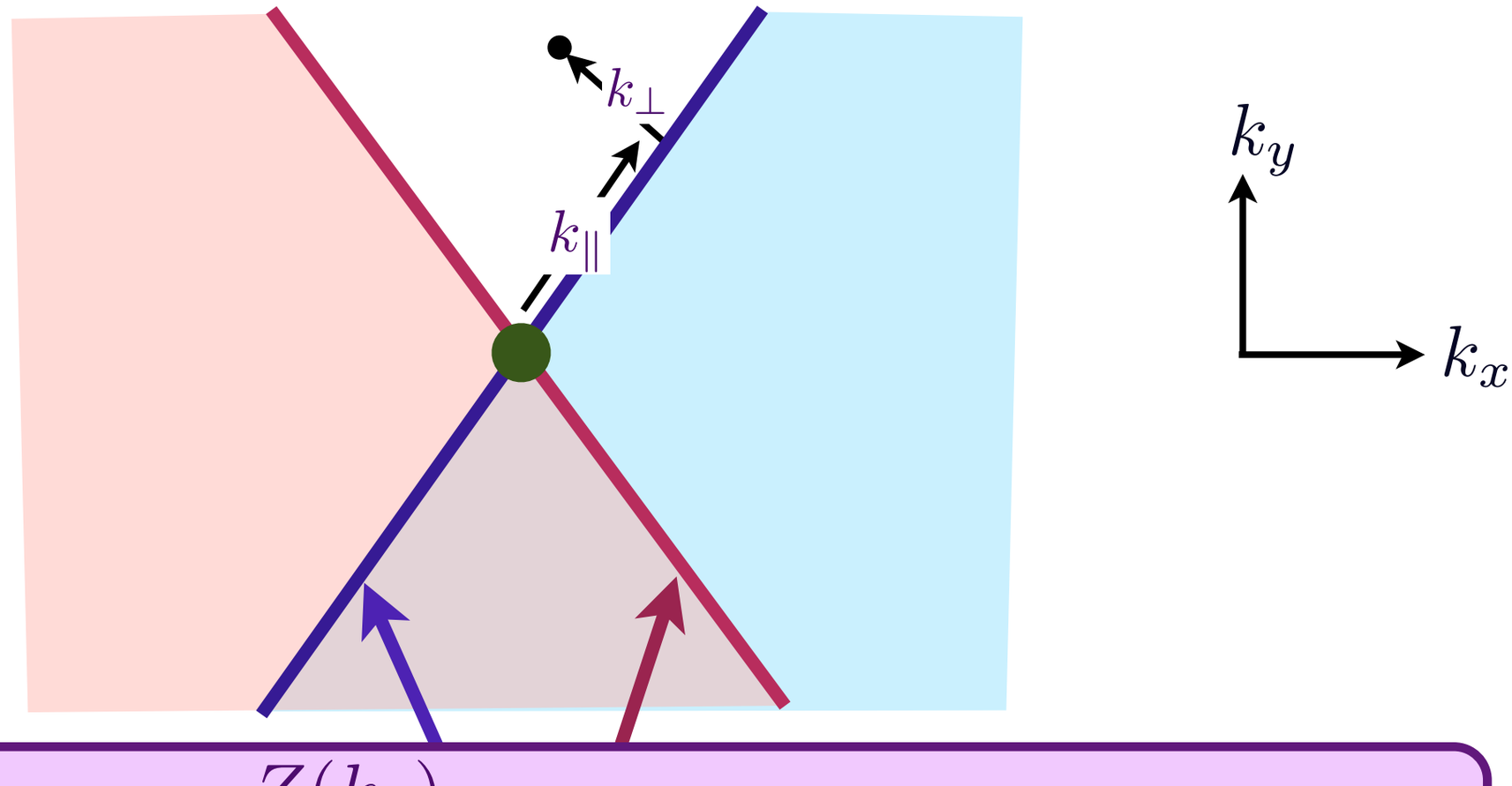

$$G_{\text{fermion}} = \frac{Z(k_\parallel)}{i\omega - v_F(k_\parallel)k_\perp}, \qquad Z(k_\parallel) \sim v_F(k_\parallel) \sim k_\parallel$$

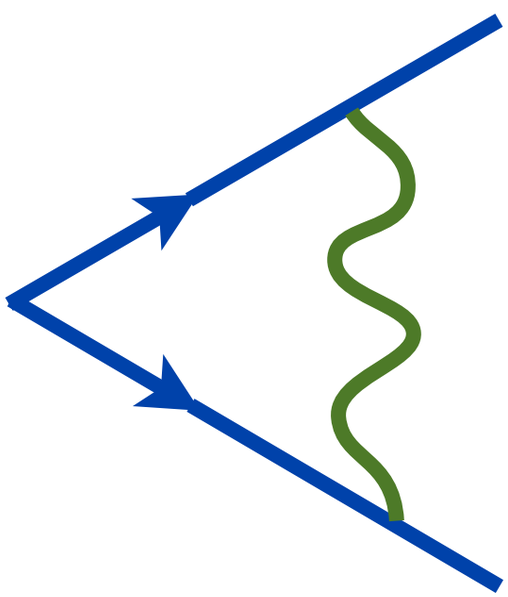

$$\int dk_\parallel \, \frac{1}{k_\parallel^2} \left(\frac{Z^2(k_\parallel)}{v_F(k_\parallel)} \right) \log \frac{k_\parallel^2}{\omega}$$

M. A. Metlitski and S. Sachdev, *Phys. Rev. B* **85**, 075127 (2010)

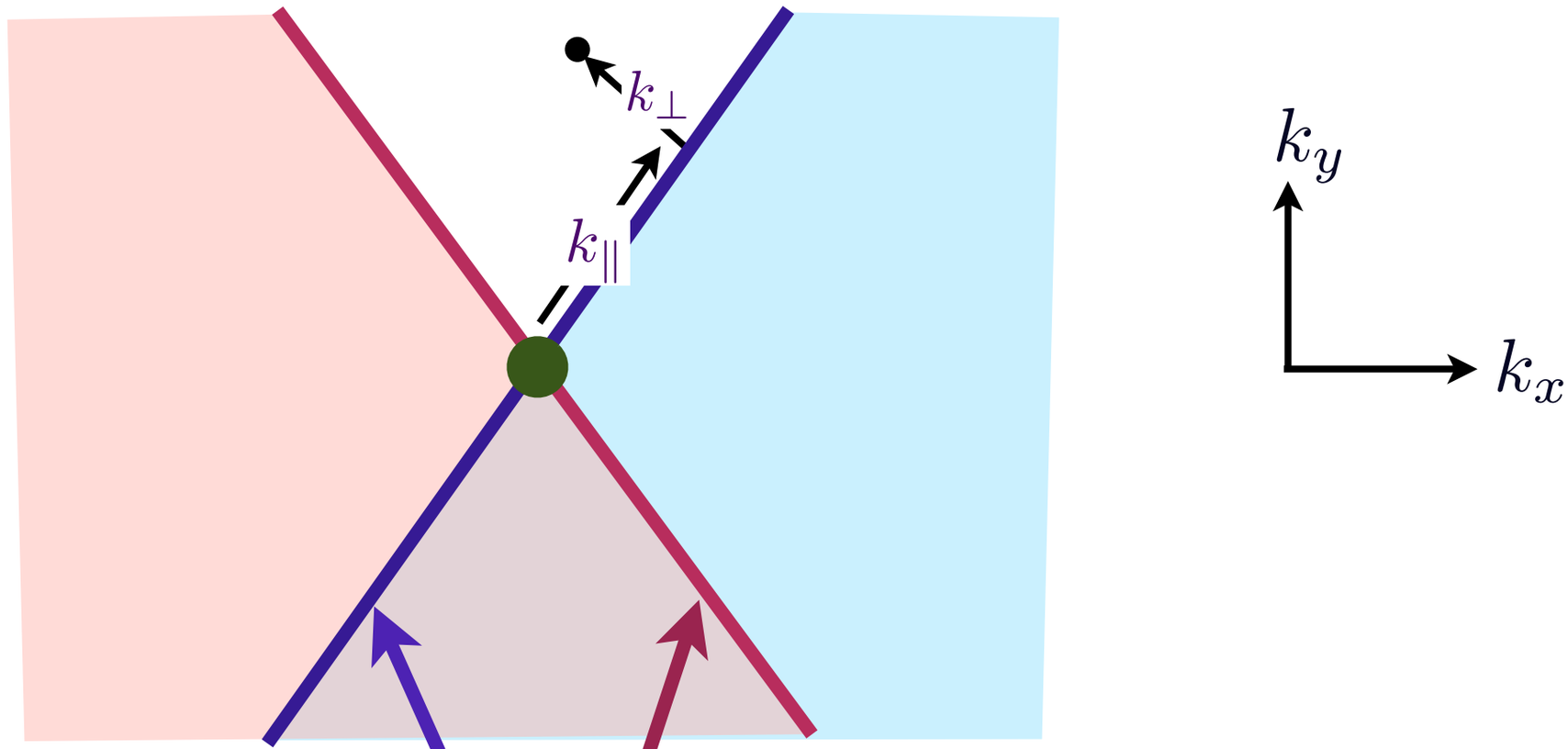

$$G_{\text{fermion}} = \frac{Z(k_\parallel)}{i\omega - v_F(k_\parallel)k_\perp}, \qquad Z(k_\parallel) \sim v_F(k_\parallel) \sim k_\parallel$$

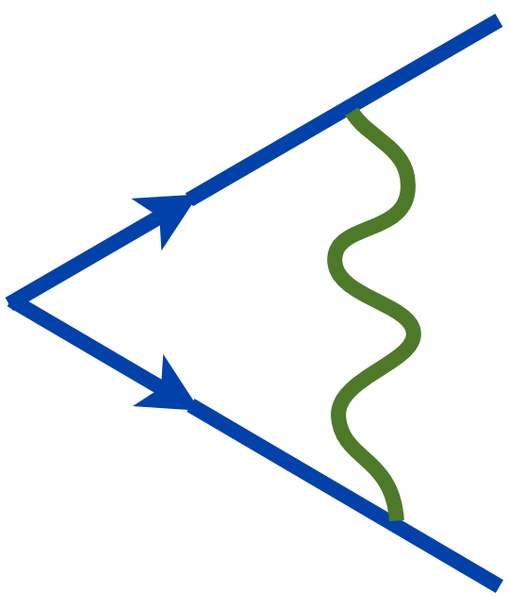

$$\int dk_\parallel \, \frac{1}{k_\parallel^2} \underbrace{\left(\frac{Z^2(k_\parallel)}{v_F(k_\parallel)}\right) \log \frac{k_\parallel^2}{\omega}}$$

Cooper logarithm

M. A. Metlitski and S. Sachdev, *Phys. Rev. B* **85**, 075127 (2010)

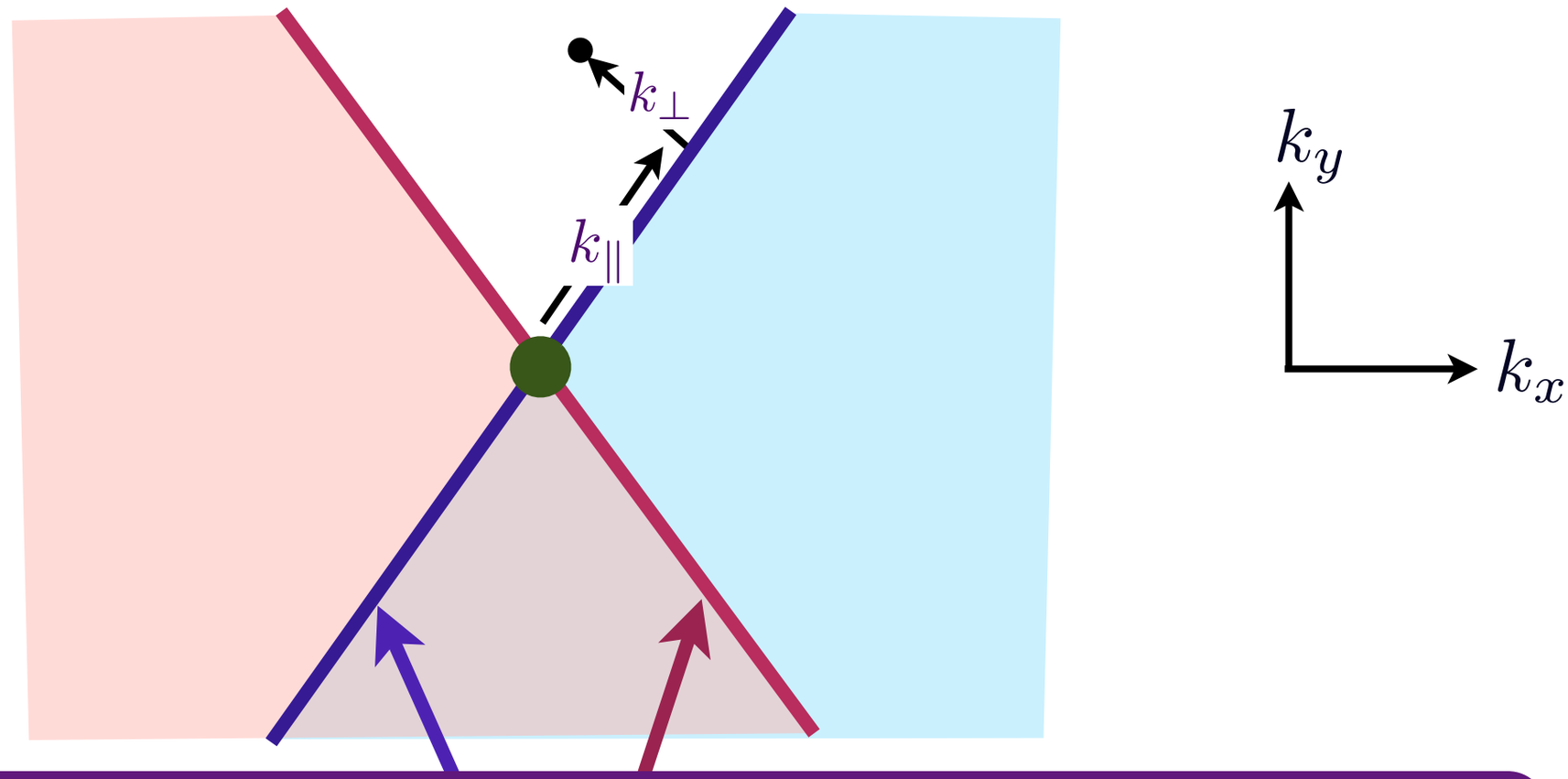

$$G_{\text{fermion}} = \frac{Z(k_\parallel)}{i\omega - v_F(k_\parallel)k_\perp}, \qquad Z(k_\parallel) \sim v_F(k_\parallel) \sim k_\parallel$$

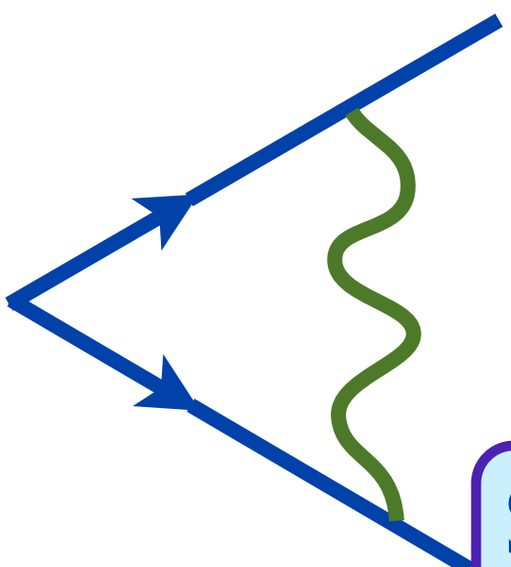

$$\int dk_\parallel \, \frac{1}{k_\parallel^2} \left(\frac{Z^2(k_\parallel)}{v_F(k_\parallel)} \right) \log \frac{k_\parallel^2}{\omega}$$

Spin fluctuation propagator

Cooper logarithm

Enhancement of pairing susceptibility by interactions

Spin density wave quantum critical point

$$1 + \frac{\alpha}{\pi(1+\alpha^2)} \log^2\left(\frac{E_F}{\omega}\right)$$

- $\log^2$ singularity arises from Fermi lines; singularity *at* hot spots is weaker.
- Interference between BCS and quantum-critical logs.
- Momentum dependence of self-energy is crucial.
- Not suppressed by $1/N$ factor in $1/N$ expansion.

Ar. Abanov, A.V. Chubukov, and A. M. Finkel'stein, *Europhys. Lett.* **54**, 488 (2001)
M. A. Metlitski and S. Sachdev, *Phys. Rev. B* **85**, 075127 (2010)

Numerical study of Fermi surface reconstructions

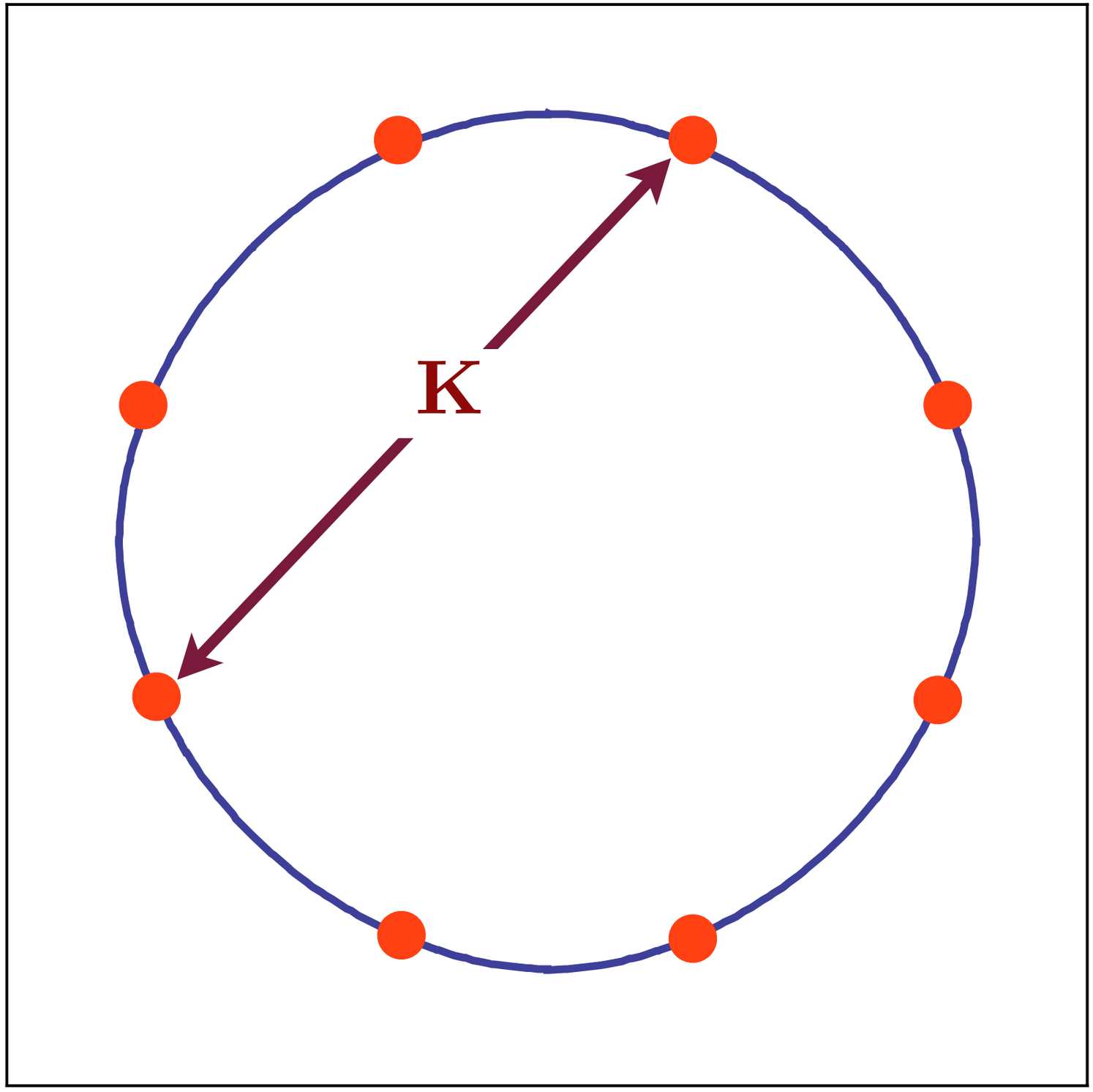

Hot spots in a single band model

Numerical study of Fermi surface reconstructions

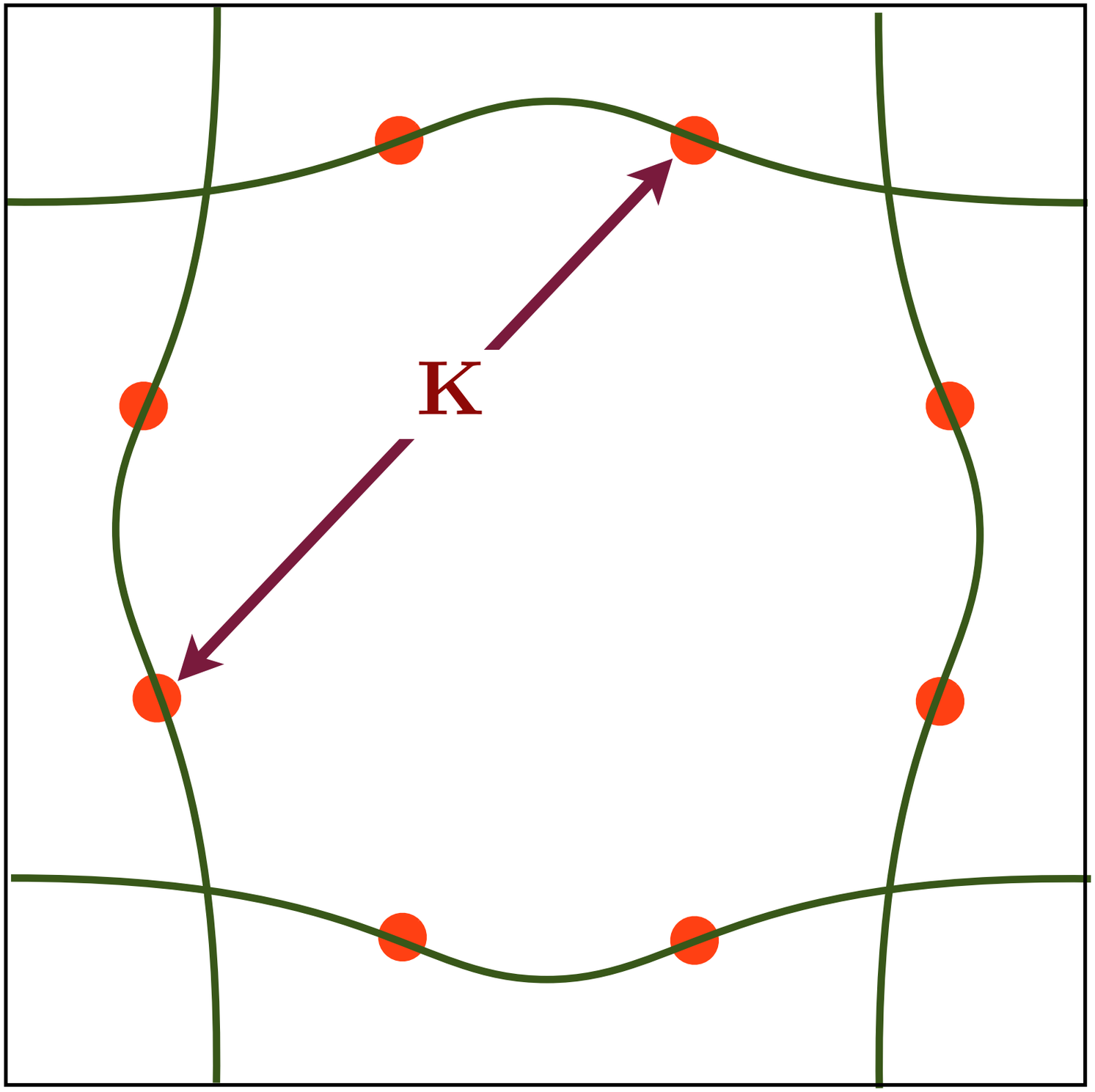

Hot spots in a two band model

E. Berg,
M. Metlitski, and
S. Sachdev, to
appear

Numerical study of Fermi surface reconstructions

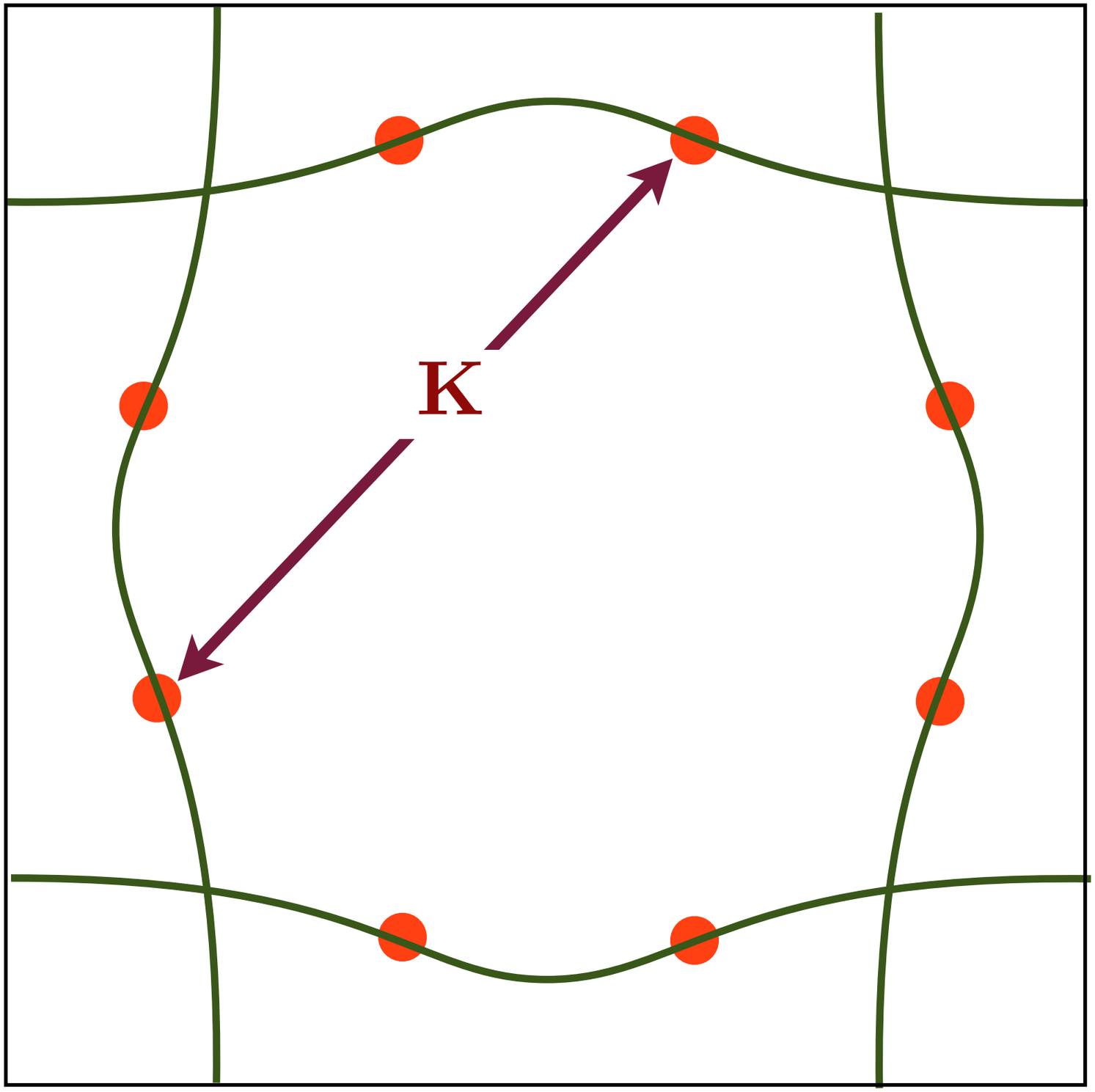

Hot spots in a two band model

E. Berg,
M. Metlitski, and
S. Sachdev, to
appear

Numerical study of Fermi surface reconstructions

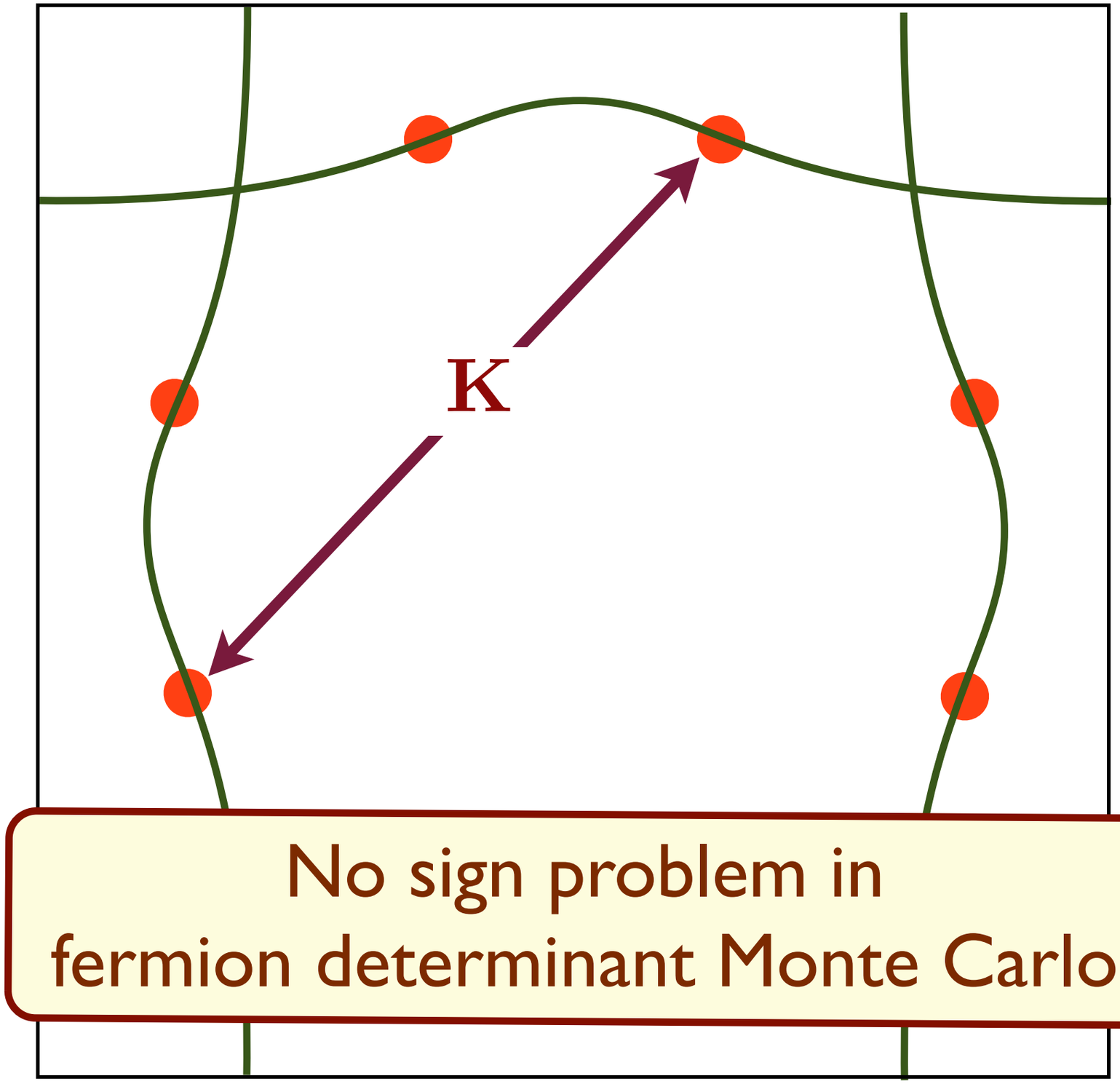

Hot spots in a two band model

E. Berg,
M. Metlitski, and
S. Sachdev, to
appear

Numerical study of Fermi surface reconstructions

Spin-fermion model: Electrons with dispersion $\varepsilon_{\mathbf{k}}$ interacting with fluctuations of the antiferromagnetic order parameter $\vec{\varphi}$.

$$\mathcal{Z} = \int \mathcal{D}c_\alpha \mathcal{D}\vec{\varphi} \exp\left(-\mathcal{S}\right)$$

$$\mathcal{S} = \int d\tau \sum_{\mathbf{k}} c^\dagger_{\mathbf{k}\alpha} \left(\frac{\partial}{\partial \tau} - \varepsilon_{\mathbf{k}} \right) c_{\mathbf{k}\alpha}$$

$$+ \int d\tau d^2 r \left[\frac{1}{2} \left(\boldsymbol{\nabla}_r \vec{\varphi} \right)^2 + \frac{s}{2} \vec{\varphi}^2 + \ldots \right]$$

$$- \lambda \int d\tau \sum_i \vec{\varphi}_i \cdot (-1)^{\mathbf{r}_i} c^\dagger_{i\alpha} \vec{\sigma}_{\alpha\beta} c_{i\beta}$$

Numerical study of Fermi surface reconstructions

Spin-fermion model: Electrons with dispersions $\varepsilon_{\mathbf{k}}^{(x)}$ and $\varepsilon_{\mathbf{k}}^{(y)}$ interacting with fluctuations of the antiferromagnetic order parameter $\vec{\varphi}$.

$$\mathcal{Z} = \int \mathcal{D}c_{\alpha}^{(x)} \mathcal{D}c_{\alpha}^{(y)} \mathcal{D}\vec{\varphi} \exp\left(-\mathcal{S}\right)$$

$$\mathcal{S} = \int d\tau \sum_{\mathbf{k}} c_{\mathbf{k}\alpha}^{(x)\dagger} \left(\frac{\partial}{\partial \tau} - \varepsilon_{\mathbf{k}}^{(x)} \right) c_{\mathbf{k}\alpha}^{(x)}$$

$$+ \int d\tau \sum_{\mathbf{k}} c_{\mathbf{k}\alpha}^{(y)\dagger} \left(\frac{\partial}{\partial \tau} - \varepsilon_{\mathbf{k}}^{(y)} \right) c_{\mathbf{k}\alpha}^{(y)}$$

$$+ \int d\tau d^2 r \left[\frac{1}{2} \left(\boldsymbol{\nabla}_r \vec{\varphi} \right)^2 + \frac{s}{2} \vec{\varphi}^2 + \ldots \right]$$

$$- \lambda \int d\tau \sum_i \vec{\varphi}_i \cdot (-1)^{\mathbf{r}_i} c_{i\alpha}^{(x)\dagger} \vec{\sigma}_{\alpha\beta} c_{i\beta}^{(y)} + \text{H.c.}$$

E. Berg, M. Metlitski, and S. Sachdev, to appear

T

SDW metal
with "small"
Fermi pockets

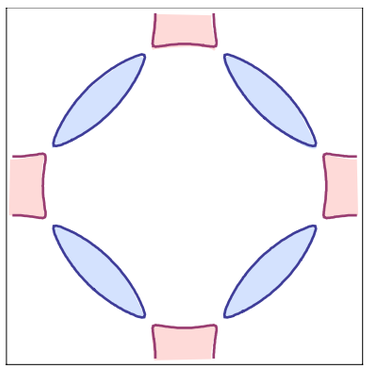

Fermi liquid
with "large"
Fermi surface

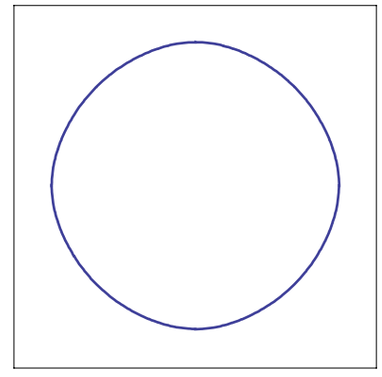

S

T

Strange metal ?

SDW metal with "small" Fermi pockets

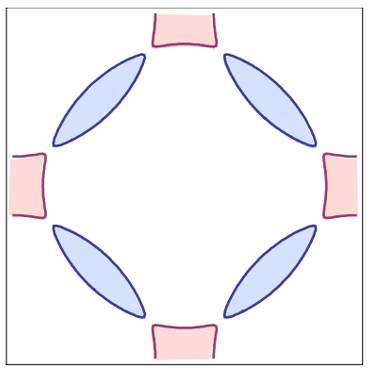

Superconductor ?

Fermi liquid with "large" Fermi surface

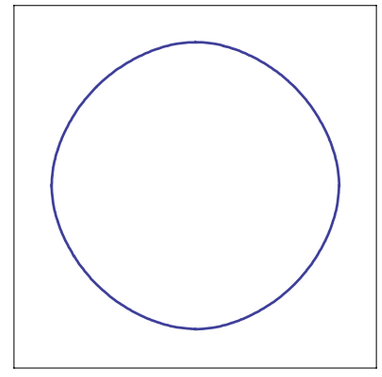

S

1. Dimerized antiferromagnets and the Wilson-Fisher CFT

2. J-Q model and deconfined criticality

3. Kagome lattice and Z_2 spin liquids

4. Spin liquids on the honeycomb lattice

5. Quantum critical points in metals: Fermi surface reconstruction